

AD-A111 551

OHIO STATE UNIV RESEARCH FOUNDATION COLUMBUS
LONG BONE AND JOINT RESPONSE TO MECHANICAL LOADING. (U)
NOV 81 A E ENGIN

F/6 6/16

F49620-79-C-0110

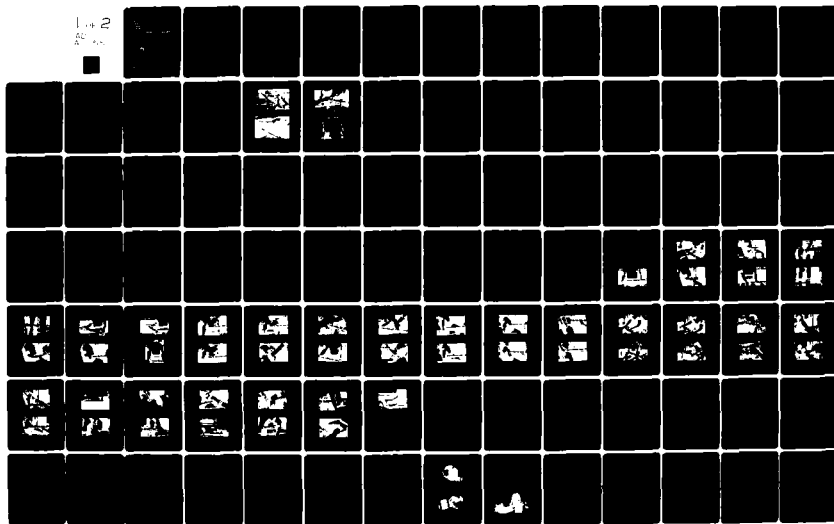
UNCLASSIFIED

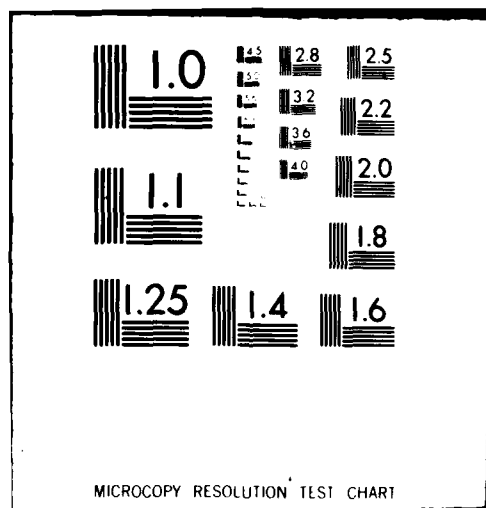
AFOSR-TR-82-0013

NL

1 + 2

82





AFOSR-TR- 82 - 0013

RF Project 761590/711899
FINAL REPORT

10

AD A111551

the
ohio
state
university

research foundation

1314 kinnear road
columbus, ohio
43212

LONG BONE AND JOINT RESPONSE
TO MECHANICAL LOADING

Ali Erkan Engin, Ph.D.
Professor
Department of Engineering Mechanics

For the Period
April 1, 1979 - September 30, 1981

Department of the Air Force
Air Force Office of Scientific Research (AFSC)
Bolling Air Force Base, D.C. 20332

Contract No. F49620-79-C-0110

November, 1981

82 08 02 060

Approved for public release;
distribution unlimited.

267360

DTIC
ESTER
MAR 3 1982
H

FILE COPY

YW

Unclassified

SECURITY CLASSIFICATION OF THIS PAGE (When Data Entered)

REPORT DOCUMENTATION PAGE		READ INSTRUCTIONS BEFORE COMPLETING FORM
1. REPORT NUMBER AFOSR-TR- 82 - 0013	2. GOVT ACCESSION NO. AD-A111551	3. RECIPIENT'S CATALOG NUMBER
4. TITLE (and Subtitle) LONG BONE AND JOINT RESPONSE TO MECHANICAL LOADING		5. TYPE OF REPORT & PERIOD COVERED FINAL REPORT
		6. PERFORMING ORG. REPORT NUMBER
7. AUTHOR(s) Ali Erkan Engin, Ph.D.		8. CONTRACT OR GRANT NUMBER(s) F49620-79-C-0110
9. PERFORMING ORGANIZATION NAME AND ADDRESS The Ohio State University Research Foundation, 1314 Kinnear Road Columbus, Ohio 43212		10. PROGRAM ELEMENT, PROJECT, TASK AREA & WORK UNIT NUMBERS 61102F 2312/A2
11. CONTROLLING OFFICE NAME AND ADDRESS Air Force Office of Scientific Research (AFSC) USAF-NL, Bolling Air Force Base D.C. 20332		12. REPORT DATE November 1981
		13. NUMBER OF PAGES 162
14. MONITORING AGENCY NAME & ADDRESS (if different from Controlling Office)		15. SECURITY CLASS. (of this report) Unclassified
		15a. DECLASSIFICATION, DOWNGRADING SCHEDULE
16. DISTRIBUTION STATEMENT (of this Report) Approved for public release; distribution unlimited.		
17. DISTRIBUTION STATEMENT (of the abstract entered in Block 20, if different from Report)		
18. SUPPLEMENTARY NOTES		
19. KEY WORDS (Continue on reverse side if necessary and identify by block number)		
Biomechanics	Force & Moment Transducer	Resistive Muscle Forces
Bioengineering	Force Applicator with Sonic Emitters	Resistive Muscle Moments
Human Joints	Kinematics with Sonic Emitters	Sonic Digitizing
20. ABSTRACT (Continue on reverse side if necessary and identify by block number)		
<p>→ The research program presented in this report is concerned with collection of active muscle force and moment response data of the human upper and lower extremities when the extremities are subjected to various external forces. The major components of the specially designed and built experimental apparatus are a subject restraint system, a force application device which employs three sonic emitters, and an upper arm (or upper leg) cuff with four sonic emitters. The sonic emitters are utilized to determine the three-dimensional direction and the location of the force application on the limbs and the orientation of the limbs.</p>		

Unclassified

SECURITY CLASSIFICATION OF THIS PAGE (When Data Entered)

20. (Continued)

with respect to the torso. Kinematics of relative motion between two body segments is presented in a format suitable for utilization of four sonic emitters on the moving body segment. The necessary computer software for PDP 11/34A is also developed to collect both kinematic and force data on human subjects.

The numerical results are presented from a set of experiments conducted on three male and three female subjects to determine their active muscle resistance against the external forces to dislodge their limbs from the initial or so-called stowed position. From a second set of experiments, extensive numerical results on determination of the active muscle force capabilities of the subjects, when their limbs are dislodged from the initial configuration, are also presented for various orientations of the limbs with respect to the torso. In addition to these two sets of experiments, some representative results of a special set of experiments dealing with the forced kinematic motion of the shoulder complex are included in the report.

It is concluded that although there are intra- and inter-subject variations for the maximum values of the resistive muscle force and moment data for the limbs, there are some trends one can establish for the behavior of their magnitudes. It is expected that incorporation of the results of the present research into the multi-segmented mathematical models of the human body should improve the long-time response capabilities of these models so that they can simulate more realistically the biodynamic events which take place prior to flail injuries.

Unclassified

PREFACE

This is the final report for the research project entitled "Long Bone and Joint Response to Mechanical Loading" sponsored by Air Force Office of Scientific Research (AFSC) at Bolling Air Force Base under Contract Number F49620-79-C-0110. The research has been monitored by Lt Col George W. Irving, III, Program Manager of Life Sciences Directorate of AFOSR and it has been administered by the Ohio State University Research Foundation under Project Number 711899. Dr. Leon Kazarian of the Aerospace Medical Research Laboratory of Wright-Patterson Air Force Base has also provided some comments and suggestions on the technical direction of the research program.

The principal investigator acknowledges the able assistance provided by the graduate research associates Richard D. Peindl and James L. Fry on various aspects of the research.

The investigation was conducted in conformance with the Human Subject Program Guidelines established by the Ohio State University Human Subject Review Committee.

AIR FORCE OFFICE OF SCIENTIFIC RESEARCH (AFSC)
NOTICE OF TRANSMITTAL TO DTIC
This technical report has been reviewed and is
approved for public release IAW AFR 120-12.
Distribution is unlimited.
MATTHEW J. KERPER
Chief, Technical Information Division

DTIC
SERIALIZED
MAY 1980

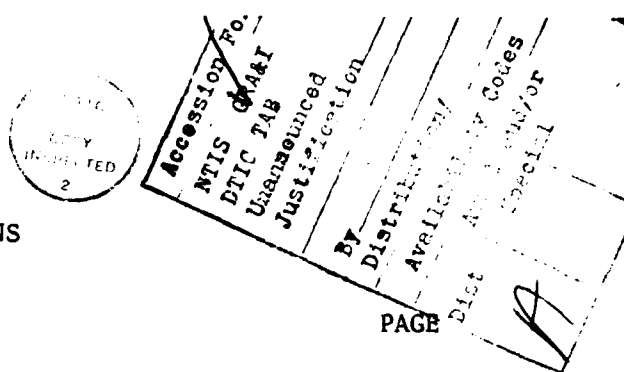
TABLE OF CONTENTS

	PAGE
INTRODUCTION	12
DESCRIPTION OF THE MAJOR COMPONENTS OF THE EXPERIMENTAL SETUP	18
The Force and Moment Transducer and Its Calibration	18
The Principles of Sonic Digitizing and a Force Applicator with Sonic Emitters	24
KINEMATICS BY MEANS OF SONIC EMITTERS	29
DESCRIPTION OF SOFTWARE DEVELOPMENT	35
System Generation	35
Transducer Calibration Program	36
Data Acquisition Program	37
Data Analysis Program	38
DATA COLLECTION ON HUMAN SUBJECTS	41
Anthropometry of Subjects	41
Description of Experiments	46
ACTIVE MUSCLE FORCE AND MOMENT RESULTS FOR THE UPPER EXTREMITIES	73
ACTIVE MUSCLE FORCE AND MOMENT RESULTS FOR THE LOWER EXTREMITIES	81
RESULTS ON THE FORCED KINEMATIC MOTION OF THE SHOULDER COMPLEX	83
CONCLUDING REMARKS	92
APPENDIX A. TRANSDUCER CALIBRATION PROGRAM	98
APPENDIX B. DATA ACQUISITION PROGRAM	105
APPENDIX C. DATA PROCESSING PROGRAM	111
APPENDIX D. TABULATED ACTIVE MUSCLE FORCE AND MOMENT RESULTS FOR THE UPPER EXTREMITIES	130
APPENDIX E. TABULATED ACTIVE MUSCLE FORCE AND MOMENT RESULTS FOR THE LOWER EXTREMITIES	145
REFERENCES	160
PUBLICATIONS ARISING FROM THIS RESEARCH CONTRACT	162

LIST OF ILLUSTRATIONS

FIGURE

1	Overall view of the subject restraint system and data collection equipment. Subject is prepared for the shoulder force and moment data collection, [7]	14
2	Force is being applied by means of the global force applicator (GFA) on the subject's arm, [7]	14
3	Close-up view of the force transducer and the force cuff, [7]	15
4	Close-up view of the exoskeletal device (ESD), [7]	15
5	Schematic drawing of the force and moment transducer	19
6	Loading of the transducer for the shear and moment calibration	24
7	a) Loading of the transducer for the axial force calibration b) Torque application on the transducer for the torque calibration	25
8	The 2-dimensional microphone/sensor assembly	26
9	The force applicator	28
10	Motion of body segment B with respect to body segment A in three dimensional space. Displacement of body segment B from position 1 to position 2 is illustrated	30
11	Representation of the motion of body segment B from position 1 to position 2 in terms of a rotation α about and translation s along the screw axis. A pure rotation of magnitude α of a point Q about an axis parallel to the screw axis is also displayed	33
12	Schematic drawing of experimental setup	47
13	Definition of θ and ϕ angles with respect to the coordinate system attached to the fixed-body segment	48
14	Force application on the wrist along the negative y direction by one of the male subjects (MS1)	48
15	Force application on the wrist along the negative y direction by one of the female subjects (FS2)	49



LIST OF ILLUSTRATIONS (CONTINUED)

FIGURE		PAGE
16	Force application along the positive z direction by one of the male subjects (MS1)--Seat armrest initiation force . .	49
17	Force application along the positive z direction by one of the female subjects (FS3)--Seat armrest initiation force .	50
18	Force application along the negative y direction by one of the male subjects (MS1)--D-ring force simulation	50
19	Force application along the negative y direction by one of the female subjects (FS2)--D-ring force simulation	51
20	Force application on the ankle along the positive y direction by one of the male subjects (MS1)	51
21	Force application on the ankle along the positive y direction by one of the female subjects (FS2)	52
22	Force application on the wrist by one of the male subjects (MS1) when forearm is 30° laterally rotated	52
23	Force application on the wrist by one of the female subjects (FS3) when forearm is 30° laterally rotated	53
24	Force application on the wrist by one of the male subjects (MS1) when forearm is 60° laterally rotated	53
25	Force application on the wrist by one of the female subjects (FS3) when forearm is 60° laterally rotated	54
26	Force application on the wrist by one of the male subjects (MS1) with fully extended elbow and arm orientation at $\phi = 0^\circ$ & $\theta = 30^\circ$	54
27	Force application on the elbow by one of the male subjects (MS1) with fully extended elbow and arm orientation at $\phi = 0^\circ$ & $\theta = 30^\circ$	55
28	Force application on the wrist by one of the male subjects (MS1) with fully extended elbow and arm orientation at $\phi = 0^\circ$ & $\theta = 60^\circ$	55
29	Force application on the elbow by one of the male subjects (MS1) with fully extended elbow and arm orientation at $\phi = 0^\circ$ & $\theta = 60^\circ$	56

LIST OF ILLUSTRATIONS (CONTINUED)

FIGURE		PAGE
30	Force application on the wrist by one of the male subjects (MS1) with fully extended elbow and arm orientation at $\phi = 0^\circ$ & $\theta = 120^\circ$	56
31	Force application on the elbow by one of the male subjects (MS1) with fully extended elbow and arm orientation at $\phi = 0^\circ$ & $\theta = 120^\circ$	57
32	Force application on the wrist by one of the male subjects (MS1) with fully extended elbow and arm orientation at $\phi = 30^\circ$ & $\theta = 30^\circ$	57
33	Force application on the wrist by one of the male subjects (MS1) with fully extended elbow and arm orientation at $\phi = 60^\circ$ & $\theta = 60^\circ$	58
34	Force application on the wrist by one of the male subjects (MS1) with fully extended elbow and arm orientation at $\phi = 60^\circ$ & $\theta = 120^\circ$	58
35	Force application on the wrist by one of the male subjects (MS1) with fully extended elbow and arm orientation at $\phi = 90^\circ$ & $\theta = 30^\circ$	59
36	Force application on the wrist by one of the male subjects (MS1) with fully extended elbow and arm orientation at $\phi = 90^\circ$ & $\theta = 60^\circ$	59
37	Force application on the elbow by one of the male subjects (MS1) with fully extended elbow and arm orientation at $\phi = 90^\circ$ & $\theta = 60^\circ$	60
38	Force application on the wrist by one of the male subjects (MS1) with fully extended elbow and arm orientation at $\phi = 90^\circ$ & $\theta = 90^\circ$	60
39	Force application on the wrist by one of the male subjects (MS1) with fully extended elbow and arm at $\phi = 90^\circ$ & $\theta = 120^\circ$	61
40	Force application on the elbow by one of the male subjects (MS1) with fully extended elbow and arm at $\phi = 90^\circ$ & $\theta = 120^\circ$	61

LIST OF ILLUSTRATIONS (CONTINUED)

FIGURE		PAGE
41	Force application on the wrist by one of the female subjects (FS2) with fully extended elbow and arm orientation at $\phi = 0^\circ$ & $\theta = 30^\circ$	62
42	Force application on the elbow by one of the female subjects (FS2) with fully extended elbow and arm orientation at $\phi = 0^\circ$ & $\theta = 30^\circ$	62
43	Force application on the wrist by one of the female subjects (FS2) with fully extended elbow and arm orientation at $\phi = 0^\circ$ & $\theta = 60^\circ$	63
44	Force application on the wrist by one of the female subjects (FS2) with fully extended elbow and arm orientation at $\phi = 0^\circ$ & $\theta = 90^\circ$	63
45	Force application on the elbow by one of the female subjects (FS2) with fully extended elbow and arm orientation at $\phi = 0^\circ$ & $\theta = 90^\circ$	64
46	Force application on the wrist by one of the female subjects (FS2) with fully extended elbow and arm orientation at $\phi = 0^\circ$ & $\theta = 120^\circ$	64
47	Force application on the wrist by one of the female subjects (FS2) with fully extended elbow and arm orientation at $\phi = 30^\circ$ & $\theta = 30^\circ$	65
48	Force application on the elbow by one of the female subjects (FS2) with fully extended elbow and arm orientation at $\phi = 30^\circ$ & $\theta = 30^\circ$	65
49	Force application on the wrist by one of the female subjects (FS2) with fully extended elbow and arm orientation at $\phi = 90^\circ$ & $\theta = 30^\circ$	66
50	Force application on the wrist by one of the female subjects (FS2) with fully extended elbow and arm orientation at $\phi = 90^\circ$ & $\theta = 60^\circ$	66
51	Force application on the wrist by one of the female subjects (FS2) with fully extended elbow and arm orientation at $\phi = 90^\circ$ & $\theta = 90^\circ$	67

LIST OF ILLUSTRATIONS (CONTINUED)

FIGURE		PAGE
52	Force application on the ankle by one of the male subjects (MS1) with knee at 90° flexion and upper leg is 30° abducted .	67
53	Force application on the knee by one of the male subjects (MS1) with knee at 90° flexion and upper leg is 30° abducted .	68
54	Force application on the ankle by one of the male subjects (MS1) with fully extended knee and leg is along A-P direction.	68
55	Force application on the knee by one of the male subjects (MS1) with fully extended knee and leg is 30° abducted	69
56	Force application on the ankle by one of the male subjects (MS1) with fully extended knee and leg is 60° abducted	69
57	Force application on the ankle by one of the female subjects (FS3) with knee at 90° flexion and upper leg is 30° abducted .	70
58	Force application on the knee by one of the female subjects (FS3) with knee at 90° flexion and upper leg is 30° abducted .	70
59	Force application on the ankle by one of the female subjects (FS3) with fully extended knee and leg is along A-P direction.	71
60	Force application on the knee by one of the female subjects (FS3) with fully extended knee and leg is 30° abducted	71
61	Force application on the ankle by one of the female subjects (FS3) with fully extended knee and leg is 60° abducted	72
62	Resistive muscle force vs. time curves for the force F_1 by the male (MS1, MS2, MS3) and the female (FS1, FS2, FS3) subjects	74
63	Maximum values of resistive muscle force by the male (MS1, MS2, MS3) and the female (FS1, FS2, FS3) subjects at various lower arm positions while the upper arm is rotated by keeping its orientation along the torso	76
64	Maximum values of resistive muscle force by the male (MS1, MS2, MS3) and the female (FS1, FS2, FS3) subjects at various arm positions in $\phi = 0^\circ$ plane	76
65	Maximum values of resistive muscle force by the male subjects against the external force applications on the elbow and the wrist at various arm positions in $\phi = 0^\circ$ plane	77

LIST OF ILLUSTRATIONS (CONTINUED)

FIGURE		PAGE
66	Maximum values of resistive muscle force by the female subjects against the external force applications on the elbow and the wrist at various arm positions in $\phi = 0^\circ$ plane .	77
67	Maximum values of resistive muscle force by the male (MS1, MS2, MS3) and the female (FS1, FS2, FS3) subjects against the external force applications on the elbow at various arm positions in $\phi = 30^\circ, 60^\circ, 90^\circ$, and 120° planes	78
68	Maximum values of resistive muscle force by the male subjects against the external force applications on the elbow and the wrist at various arm positions in $\phi = 30^\circ, 60^\circ, 90^\circ$, and 120° planes	79
69	Maximum values of resistive muscle force by the female subjects against the external force applications on the elbow and the wrist at various arm positions in $\phi = 30^\circ, 60^\circ, 90^\circ$, and 120° planes	80
70	Maximum values of resistive muscle force by the male (MS1, MS2, MS3) and the female (FS1, FS2, FS3) subjects for the knee flexed and the knee locked configurations for various lateral positions of the upper leg at $\theta = 90^\circ$	82
71	Maximum values of resistive muscle force by the male (MS1, MS2, MS3) and the female (FS1, FS2, FS3) subjects for the knee flexed and the knee locked configurations for various lateral positions of the upper leg at $\theta = 120^\circ$	84
72	Maximum values of resistive muscle force by the male (MS1, MS2, MS3) and the female (FS1, FS2, FS3) subjects for the knee flexed and the knee locked configurations for various lateral positions of the upper leg with $\theta = 40^\circ$	85
73	Maximum values of resistive muscle force by the male (MS1, MS2, MS3) and the female (FS1, FS2, FS3) subjects for the locked knee configurations and for two lateral positions of the upper leg with $\theta = 0^\circ$	86
74	Relative axes locator device (RALD)	87
75	Upper arm cuff fitted with six sonic emitters	87
76	Subject in position for superior-inferior drawer tests	88

LIST OF ILLUSTRATIONS (CONTINUED)

FIGURE		PAGE
77	Resistive force versus drawer displacement for $\theta = 90^\circ$, $\phi = 0^\circ$ upper arm orientation	89
78	Resistive force versus drawer displacement for $\theta = 90^\circ$, $\phi = 30^\circ$ upper arm orientation	89
79	Resistive force versus drawer displacement for a) $\theta = 90^\circ$, $\phi = 60^\circ$, b) $\theta = 90^\circ$, $\phi = 90^\circ$, and c) $\theta = 90^\circ$, $\phi = 115^\circ$ upper arm orientation	90
80	Resistive force versus drawer displacement for the superior- inferior drawer ($\theta = 0^\circ$)	91

LIST OF TABLES

TABLE		PAGE
1	Calibration crosstalk matrix [C]	22
2	Selected anthropometry of male subjects 1, 2, 3	43
3	Selected anthropometry of female subjects 1, 2, 3	44
I	Maximum magnitudes of the active muscle force & moment vectors at the shoulder joints of three male subjects during dislodging of the arm from the indicated positions	131
II	Maximum magnitudes of the active muscle force & moment vectors at the shoulder joints of three female subjects during dislodging of the arm from the indicated positions	132
III	Maximum magnitudes of the active muscle force & moment vectors at the shoulder joints of three male subjects at the dislodged positions of the lower arm from the seat armrest	133
IV	Maximum magnitudes of the active muscle force & moment vectors at the shoulder joints of three female subjects at the dislodged positions of the lower arm from the seat armrest	134
V	Maximum magnitudes of the active muscle force & moment vectors at the shoulder joints of three male subjects for the indicated positions of the arm with $\phi = 0^\circ$	135

LIST OF TABLES (CONTINUED)

TABLE		PAGE
VI	Maximum magnitudes of the active muscle force & moment vectors at the shoulder joints of three female subjects for the indicated positions of the arm with $\phi = 0^\circ$	136
VII	Maximum magnitudes of the active muscle force & moment vectors at the shoulder joints of three male subjects for the dislodged positions of the arm with $\phi = 30^\circ$	137
VIII	Maximum magnitudes of the active muscle force & moment vectors at the shoulder joints of three female subjects for the dislodged positions of the arm with $\phi = 30^\circ$	138
IX	Maximum magnitudes of the active muscle force & moment vectors at the shoulder joints of three male subjects for the dislodged positions of the arm with $\phi = 60^\circ$	139
X	Maximum magnitudes of the active muscle force & moment vectors at the shoulder joints of three female subjects for the dislodged positions of the arm with $\phi = 60^\circ$	140
XI	Maximum magnitudes of the active muscle force & moment vectors at the shoulder joints of three male subjects for the dislodged positions of the arm with $\phi = 90^\circ$	141
XII	Maximum magnitudes of the active muscle force & moment vectors at the shoulder joints of three female subjects for the dislodged positions of the arm with $\phi = 90^\circ$	142
XIII	Maximum magnitudes of the active muscle force & moment vectors at the shoulder joints of three male subjects for the dislodged positions of the arm with $\phi = 120^\circ$	143
XIV	Maximum magnitudes of the active muscle force & moment vectors at the shoulder joints of three female subjects for the dislodged positions of the arm with $\phi = 120^\circ$	144
XV	Maximum magnitudes of the active muscle force & moment vectors at the hip joints of three male subjects for the indicated positions of the leg with $\theta = 0$, knee locked	146
XVI	Maximum magnitudes of the active muscle force & moment vectors at the hip joints of three female subjects for the indicated positions of the leg with $\theta = 0$, knee locked	147

LIST OF TABLES (CONTINUED)

TABLE		PAGE
XVII	Maximum magnitudes of the active muscle force & moment vectors at the hip joints of three male subjects for the indicated positions of the leg with $\theta = 40^\circ$, knee locked . . .	148
XVIII	Maximum magnitudes of the active muscle force & moment vectors at the hip joints of three male subjects for the indicated positions of the leg with $\theta = 40^\circ$, knee flexed . . .	149
XIX	Maximum magnitudes of the active muscle force & moment vectors at the hip joints of three female subjects for the indicated positions of the leg with $\theta = 40^\circ$, knee locked . . .	150
XX	Maximum magnitudes of the active muscle force & moment vectors at the hip joints of three female subjects for the indicated positions of the leg with $\theta = 40^\circ$, knee flexed . . .	151
XXI	Maximum magnitudes of the active muscle force & moment vectors at the hip joints of three male subjects for the indicated positions of the leg with $\theta = 90^\circ$, knee locked . . .	152
XXII	Maximum magnitudes of the active muscle force & moment vectors at the hip joints of three male subjects for the indicated positions of the leg with $\theta = 90^\circ$, knee flexed . . .	153
XXIII	Maximum magnitudes of the active muscle force & moment vectors at the hip joints of three female subjects for the indicated positions of the leg with $\theta = 90^\circ$, knee locked . . .	154
XXIV	Maximum magnitudes of the active muscle force & moment vectors at the hip joints of three female subjects for the indicated positions of the leg with $\theta = 90^\circ$, knee flexed . . .	155
XXV	Maximum magnitudes of the active muscle force & moment vectors at the hip joints of three male subjects for the indicated positions of the leg with $\theta = 120^\circ$, knee locked . . .	156
XXVI	Maximum magnitudes of the active muscle force & moment vectors at the hip joints of three male subjects for the indicated positions of the leg with $\theta = 120^\circ$, knee flexed . . .	157
XXVII	Maximum magnitudes of the active muscle force & moment vectors at the hip joints of three female subjects for the indicated positions of the leg with $\theta = 120^\circ$, knee locked . . .	158
XXVIII	Maximum magnitudes of the active muscle force & moment vectors at the hip joints of three female subjects for the indicated positions of the leg with $\theta = 120^\circ$, knee flexed . . .	159

INTRODUCTION

Abandoning disabled aircraft which can not be flown may be accomplished by either bailing out via seat ejection, or by the ejection of the encapsulated crew station containing one or more aircraft personnel. If the separation from the disabled aircraft occurs by seat ejection, the body of the ejected crew member is subjected to a high-speed air stream (the windblast) generating large magnitudes of aerodynamic forces on the higher and lower extremities of the body. Despite the design improvements on the seats with provision for the limbs to be lodged in a favorable position during ejection, dislodging of the limbs occur frequently when the body is ejected into the windblast.

Primary cause of the dislodging of the limbs is the difference between the magnitudes of the deceleration forces acting on the limbs and the torso. Note that immediately after ejection, the seat and its occupant have the same speed as the aircraft; however, due to shape (frontal area) and mass differences between the limbs and the torso to which the mass of the ejection seat is also attached the aerodynamic drag forces acting on these parts will be different, higher on the limbs than on the torso. Thus, there is a strong tendency of dislodging of the limbs from their so-called stowed position. The dislodged limbs swing freely and without control and they are stopped only by some part of the seat structure or by collision with another part of the body. The resulting, so-called "flail injuries" are the dislocations of the major articulating joints and various types of long bone injuries. The probability of these injuries increase significantly with increasing aircraft speed [1]. It was also estimated that [2] almost half of all ejections taking place under combat conditions result in flail injury or death to the pilot.

Several years ago recognizing the seriousness of the flail injury problem, the Aerospace Medical Research Laboratory (AMRL) of the Air Force Systems Command has initiated both experimental and analytical programs. Some experimental wind tunnel measurements have been already conducted [3,4,5] and a theoretical effort has been started by Schneck [6]. In Reference [6] a potential flow solution is presented for estimating the

pressure distribution around the lower arm when the seated body is subjected to windblast. In this theoretical study by inclusion of the effects of the flow separation it was also possible to predict the presence of a pressure drag force which acts to throw the lower arm outward, away from the torso. Results of this study can provide some input data in regard to prescribing time-dependent forces on the body segments of the Articulated Total Body Model (ATBM) of the AMRL. The ATBM is particularly a useful model to study the pilot ejection problem provided appropriate joint torques and segmental loading data to simulate windblast forces are known and incorporated into the model.

Approximately five years ago, a research program under co-sponsorship of the Mathematics and Analysis Branch of the AMRL and the National Highway Traffic Safety Administration (NHTSA) was initiated at the Engineering Mechanics Department of The Ohio State University to collect passive resistive force, moment and torque data at the five major joints of the human body. The research was conducted with some obvious limitations on live human subjects. The joints which were studied, in order of descending priority, were the shoulder, knee, hip, elbow and ankle. The final report [7] of this forementioned research program along with a series of papers [8-15] illustrate various aspects of the research and present experimental results on both passive and active resistive force, moment and torque data at the major articulating joints of the human body. We will next present very briefly some of the highlights of the experimental phase of this previous research program [7]. The primary purpose of this brief background presentation is to illustrate the substantial changes and improvements that were made on the experimental apparatus in order to accomplish tasks of the present research program sponsored by the Air Force Office of Scientific Research.

The major components of the experimental apparatus developed for the previous research program were a subject restraint system (Fig. 1), a global force applicator, GFA (Fig. 2) and the exoskeletal device, ESD (Figs. 1 & 4). The subject restraint system with its pitch, and yaw capabilities allowed orientation of the subject to various selected positions. This was an important feature of the subject restraint system

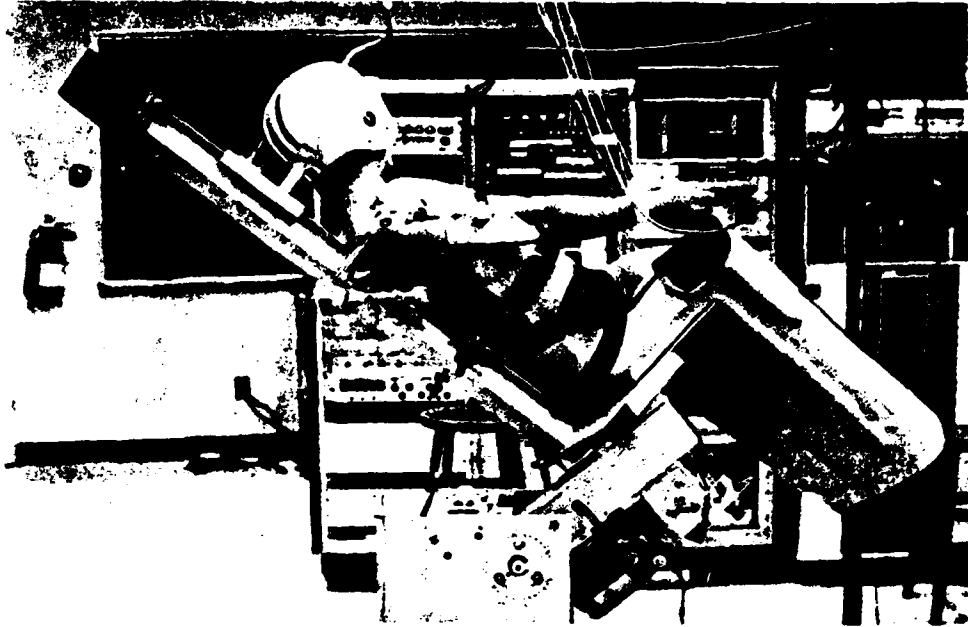


Fig. 1. Overall view of the subject restraint system and data collection equipment. Subject is prepared for the shoulder force and moment data collection, [7].



Fig. 2. Force is being applied by means of the global force applicator (GFA) on the subject's arm, [7].

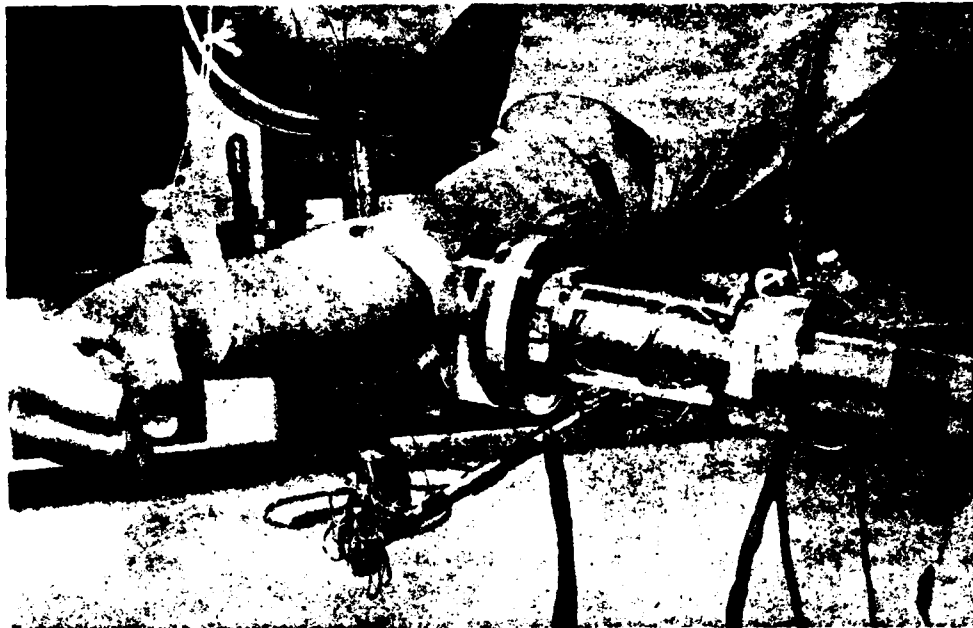


Fig. 3. Close-up view of the force transducer and the force cuff, [7].

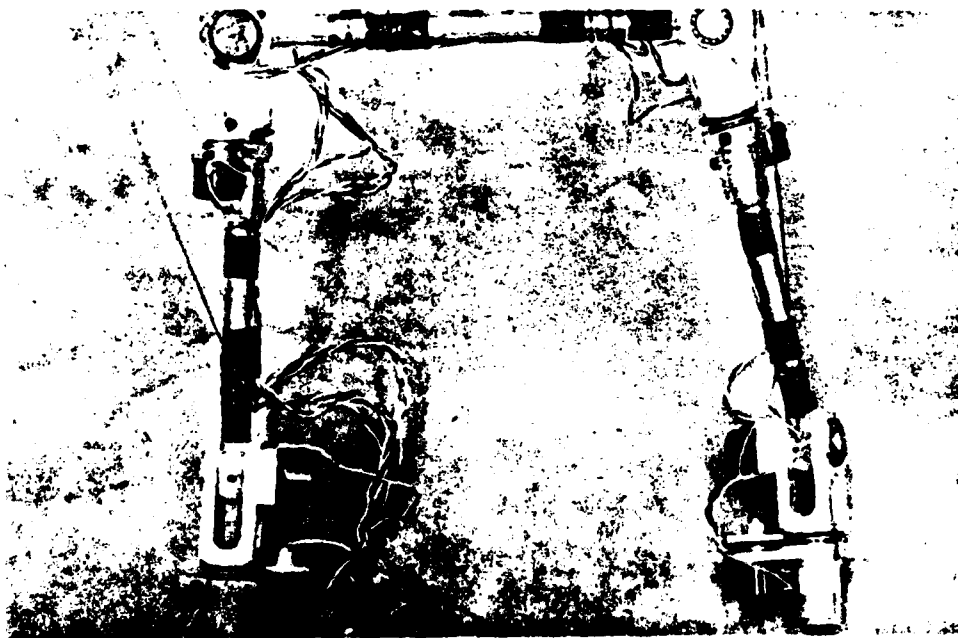


Fig. 4. Close-up view of the exoskeletal device (ESD), [7].

which assisted in the mobilization of subject's appropriate body segment at a constant elevation while the experimenter moved the adjacent body segment by means of the GFA throughout its entire range of motion as shown for the shoulder in Figs. 2 & 3. To eliminate the gravitational component of the moment values at the joint, the force application to the moving body segment was made in a horizontal plane while the elevation of the moving body segment was maintained by a support line in such a way that in the direction of the force application a relaxed floating type of motion of the moving body segment was achieved. Both the security and the support characteristics of the restraint system allowed total relaxation, thus minimizing active muscle effects during the experiment.

Forces were applied to the moving body segments of the subject by means of the GFA (Fig. 2) which consists of four links and eight revolute joints containing high precision potentiometers. The outputs of the potentiometers and the length dimensions of the links were utilized to obtain the direction as well as the point of application of the force vector. Note that in Fig. 2 the last two links of the GFA are shown. The GFA is terminated by a force transducer and a force cuff which is free to rotate about its axis. The force transducer was designed and built to measure all three components of the force and moment vectors. Of course, the predominant force component was the one along the direction of the last link of the GFA and all the other force as well as the moment components were relatively small in magnitude if one maintained approximately perpendicular force application on the moving body segment.

The third major component of the experimental apparatus was the ESD as shown in Fig. 4. The ESD also consists of eight revolute joints whose rotations are monitored by means of high precision potentiometers. Although there were major design differences between the ESD and the GFA, from the kinematics point of view the ESD can be considered as a miniaturized version of the GFA. Fundamental design requirements of the ESD were (a) capability of providing complete freedom of motion between two adjacent body segments, and (b) capability of providing sufficient data to determine kinematics of the relative motion between two body segments which are connected with a complex anatomical joint. Principles of

orthopedic bracing were utilized in attaching the ends of the ESD to the moving and fixed body segments. For example, for the shoulder an upper arm shell and the back rail of the chair, where the torso support shell is attached, were used for the ESD connections as shown in Figs. 1 & 2. For the fitting of the upper arm shell, special care was given to locate the bony landmarks such as the medial and lateral epicondyles of the humerus so that contacts can be maintained between these landmarks and the shell. In addition, the relative soft tissue motion between the upper arm and the shell was kept minimal because of the following reasons: a) light weight and very low friction construction of the ESD, b) balancing of the weight of the ESD by means of pulleys and small weights in such a way that the subjects did not feel its presence, and c) application of the GFA force on a portion of the arm away from the shell segment to which the moving end of the ESD was attached.

The development of the ESD, the GFA, the subject restraint system, and the associated theoretical concepts were made to achieve at least three major tasks. The first one was the quantitative determination of the range of motion in the joints; the second one was quantitative determination of passive resistive force and moments at the joints; the third task was quantitative determination of passive resistive torques associated with the rotational motion of the body segments about their long bone axes. In this research program three male subjects were tested and the tests were repeated at least three times.

In this report, first, a detailed description of the major components of the experimental apparatus is presented. This is followed by a presentation of kinematics of relative motion between two body segments which is cast into a format suitable for employment of four sonic emitters on the moving body segment. Next, a description of the computer software for the collection of both kinematic and force data on human subjects is provided.

The numerical results are presented from experiments in which three male and three female subjects were tested. Two sets of experiments were conducted for the collection of active muscle force and moment data. The first set of experiments was designed to determine the active muscle

resistance of subjects when there is a strong tendency of dislodging of the limbs from their stowed position. The second set of experiments was designed to determine the active muscle resistance of subjects when the limbs are dislodged from their stowed position. In this set of experiments various combinations of θ and ϕ angles for the moving body segments were considered. The angles θ and ϕ define the orientation of the moving body segment with respect to the fixed body segment. In addition to these two sets of experiments, numerical results of a set of experiments dealing with the forced kinematic motion of the shoulder complex are presented. We will next supply a description of the major components of the experimental setup developed for the tasks of the present research program.

DESCRIPTION OF THE MAJOR COMPONENTS OF THE EXPERIMENTAL SETUP

Major changes were made in almost every aspect of the previous program in order to improve the accuracy, repeatability and reliability of the data. These changes are: a) design, manufacturing and calibration of a new force and moment transducer, b) replacement of the GFA with a new force applicator which utilizes three sonic emitters, c) replacement of the ESD with an elastic cuff which holds four sonic emitters, d) purchase of sonic digitizing equipment manufactured by Science Accessories Corp. (Model 6P6-3D-3), e) replacement of the previous obsolete data collection system with the purchase of a PDP 11/34 mini-computer with floating point processor manufactured by Digital Equipment Corp., and f) interfacing a 14-bit, 32-channel analog-digital converter manufactured by Data Translation Corp. (Model DT1712/5714-64) with PDP 11/34 computer. Further details about the items, listed above and developed by us during the research program will next be presented.

THE FORCE AND MOMENT TRANSDUCER AND ITS CALIBRATION

The force and moment transducer, which is referred to as the force transducer in the introduction section of this report, is physically similar to the force transducer utilized in previous research program [7] on the measurement of resistive torques in major human joints. The transducer which was designed, built and calibrated for the present research

program, however, employs a number of significant improvements over its predecessor. These improvements are basically of two types: 1) modifications to the physical design, and 2) a significantly altered calibration approach. The subsequent discussion will describe these changes in some detail and indicate the benefits derived from their implementation.

As before the transducer is essentially a cylindrical shell with strain gages located on the shell surface to sense force and moment in three orthogonal directions as shown in Fig. 5. However certain physical design alterations have been made to increase the transducer sensitivity. Since the predominant force component which occur in use is in the axial or z-direction, design changes were made specifically to increase the load sensing capability in the axial force measurement circuit. This was accomplished in two ways: 1) by decreasing the shell wall thickness

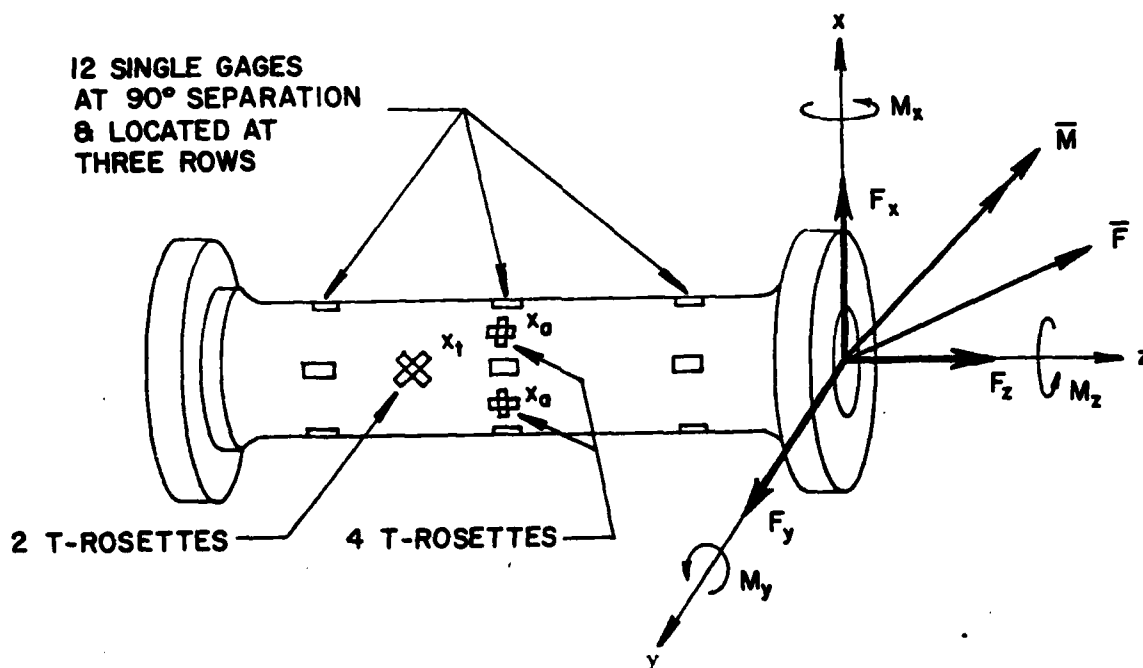


Fig. 5 Schematic drawing of the force and moment transducer

(from .100" in the previous design to .032" in the current transducer), and 2) by increasing the number of T rosettes used to sense axial strain from two to four. The choice of shell wall thickness was based, primarily, on a consideration of the transducer's ability to withstand predicted load configurations while maintaining an adequate safety factor against buckling. Of course, cost and machining capability were also considered. The addition of two more T rosettes naturally increases the sensitivity by increasing the change in resistivity and hence the change in bridge voltage for a given applied load. In this way, an approximate 150% increase in axial sensitivity over the previous transducer was achieved. The change in wall thickness also served to increase the sensitivity of all the other load measuring circuits.

The force transducer currently in use is also greater in length than the previous one. This was done primarily to accommodate more gages (12 single gages and 6 rosettes as opposed to 8 single gages and 4 rosettes previously) and also to improve the shear force measurement capabilities. The shear load measuring circuits have been changed from half bridges to full bridges, and their calibration techniques have been significantly altered. The calibration techniques will now be discussed in some detail.

One of the basic problems encountered in transducers which measure force and moment in multiple directions is cross-talk among the measuring circuits. The cross-talk is due to erroneous output of the circuits belonging to the other directions when a force or moment is applied in a particular direction. This effect can result from slight deviations in gage alignments, imperfections occurring in the gage application, or imperfections which occur due to machining tolerances which make ideal load applications impossible. While reasonable care in the construction of the transducer has kept the cross-talk to a minimum we also account for their effects in the subsequent load analysis.

Calibration was performed by applying known loads to each channel in turn and recording the six outputs of the transducer. Ideally, only the channel corresponding with the applied load should register the load. Here a channel designates quantities observed on the strain gage bridges corresponding to F_x , F_y , F_z , M_x , M_y , and M_z . Considering primary and

cross-talk signals of the transducer behave linearly with applied forces and moments throughout the working range of the transducer, it is then possible to characterize the behavior of the transducer by the relationship

$$[S] = [C][L] \quad (1)$$

where the matrices $[S]$ and $[L]$ are the column vectors representing the bridge output voltages (signals) and the input loads, respectively. The elements of matrix $[C]$ are determined from the calibration data. The diagonal elements represent the primary signals and the non-diagonal elements represent the cross-talk effects.

For example, consider that we are calibrating the axial mode of the transducer and that the axial bridge is our first measuring circuit. Then the signals, s_i , that we observe as the bridge outputs are as follows

$$\left. \begin{aligned} s_1 &= C_{11}L_1 && \text{(the primary signal)} \\ s_2 &= C_{21}L_1 \\ s_3 &= C_{31}L_1 \\ s_4 &= C_{41}L_1 \\ s_5 &= C_{51}L_1 \\ s_6 &= C_{61}L_1 \end{aligned} \right\} \begin{aligned} & \text{cross-talk} \\ & \text{(ideally, these should be zero)} \end{aligned} \quad (2)$$

If we perform calibrations of the subsequent modes we obtain:

	<u>mode 2</u>		<u>mode 3</u>	
	$s_1 = C_{12}L_2$		$s_1 = C_{13}L_3$	
(primary signal)	$s_2 = C_{22}L_2$		$s_2 = C_{23}L_3$	etc.
	$s_3 = C_{32}L_2$	(primary signal)	$s_3 = C_{33}L_3$	
	.		.	
	.		.	
	.		.	
	$s_6 = C_{62}L_2$		$s_6 = C_{63}L_3$	

Note here that the C_{ij} 's are the slopes of best fit lines of voltages obtained at a variety of loads. Therefore for any arbitrary loading, the

total observed signals for the transducer channels, S_i , arise as a result of:

$$\begin{aligned} S_1 &= C_{11}L_1 + C_{12}L_2 + C_{13}L_3 + C_{14}L_4 + C_{15}L_5 + C_{16}L_6 \\ &\vdots \\ S_6 &= C_{61}L_1 + C_{62}L_2 + C_{63}L_3 + C_{64}L_4 + C_{65}L_5 + C_{66}L_6 \end{aligned} \quad (3)$$

or,

$$[S] = [C][L]$$

The coefficient matrix obtained as a result of the transducer calibration is shown in Table 1.

With these mathematical concepts of the load analysis in mind, let us consider some of the subtle physical aspects of the transducer calibration that were employed. The calibration of the axial force (F_z) and torque

Table 1

Calibration Crosstalk Matrix [C]

(Units are Volts/lb or Volts/lb-in)

0.01532	0.00023	0.00000	-0.00016	0.00090	0.00108
-0.00090	0.03986	0.00000	0.00097	-0.00020	-0.00390
0.00037	0.00012	0.02987	-0.00009	0.00229	0.00028
0.00045	-0.00003	-0.00028	0.02924	0.00033	0.00707
0.00047	-0.00011	0.00094	-0.00030	-0.10616	0.00164
-0.00001	0.00008	-0.00021	-0.00149	-0.00106	0.10876

(M_z) modes are relatively simple due to the relative ease with which we can apply these types of loads. The application of pure shears (F_x and F_y) and pure moments (M_x and M_y), is very difficult, however, in the absence of highly specialized equipment. These modes were calibrated in the following manner.

The transducer was fixed at one end so as to perform as a cantilevered beam and steadily increasing loads were applied in two specific locations as shown in Fig. 6. Of course these types of loading involve both a shear load, $L_1 = F$, and a bending moment with respect to the moment bridge location, $L_2 = d_1 \times F$ and $L_2 = d_2 \times F$. Therefore, we have two sets of signals: As a result of $L_1 = F$ and $L_2 = d_1 \times F$:

$$\begin{aligned} s_1 &= C_{11}L_1 + C_{12}L_2 \\ &\vdots \\ &\vdots \end{aligned} \tag{4}$$

$$s_6 = C_{61}L_1 + C_{62}L_2,$$

and as a result of $L_1 = F$ and $L_2 = d_2 \times F$:

$$\begin{aligned} s'_1 &= C_{11}L_1 + C_{12}L_2 \\ &\vdots \\ &\vdots \end{aligned} \tag{5}$$

$$s'_6 = C_{61}L_1 + C_{62}L_2$$

If we denote b_1, b_2, \dots, b_6 as the slopes of the best fit voltage vs. load lines, then we see that:

$$\begin{aligned} \frac{s_1}{F} &= C_{11} + d_1 C_{12} = b_1 & \text{and} & & \frac{s'_1}{F} &= C_{11} + d_2 C_{12} = b'_1 \\ &\vdots & & & &\vdots \\ &\vdots & & & &\vdots \\ \frac{s_6}{F} &= C_{61} + d_1 C_{62} = b_6 & & & \frac{s'_6}{F} &= C_{61} + d_2 C_{62} = b'_6 \end{aligned} \tag{6}$$

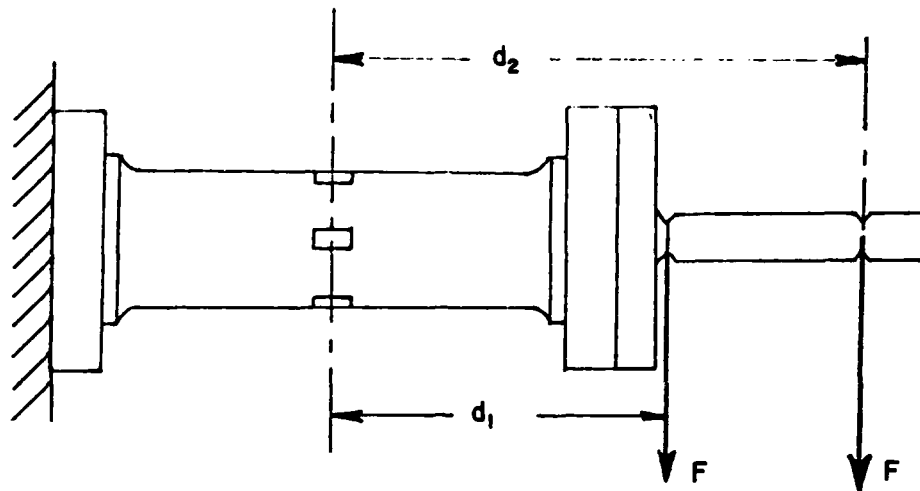


Fig. 6 Loading of the transducer for the shear and moment calibration.

In Eq. (6) there are 12 equations in 12 unknowns; we solve for the unknowns, however, two at a time, e.g.

$$\begin{aligned} C_{11} + d_1 C_{12} &= b_1 \\ C_{11} + d_2 C_{12} &= b_1' \end{aligned} \quad (7)$$

This process gives us two column vectors of $[C]$ for the corresponding moment and shear applications. A subsequent repeat of this procedure in a direction orthogonal to the one just performed yields the next two column vectors of $[C]$. The fifth and sixth columns of $[C]$ corresponding to the axial and torque applications completes the calibration matrix.

We have shown how the loads were applied for the shear and bending moment calibrations in Fig. 6. Finally, the axial load and torque calibration configurations are included as Figs. 7a and b respectively for the sake of completeness.

PRINCIPLES OF SONIC DIGITIZING AND A FORCE APPLICATOR WITH SONIC EMITTERS

Before we discuss some details of the force applicator we will introduce the principles of sonic digitizing. In the current research, the kinematics of both the moving body segment and the force applicator are

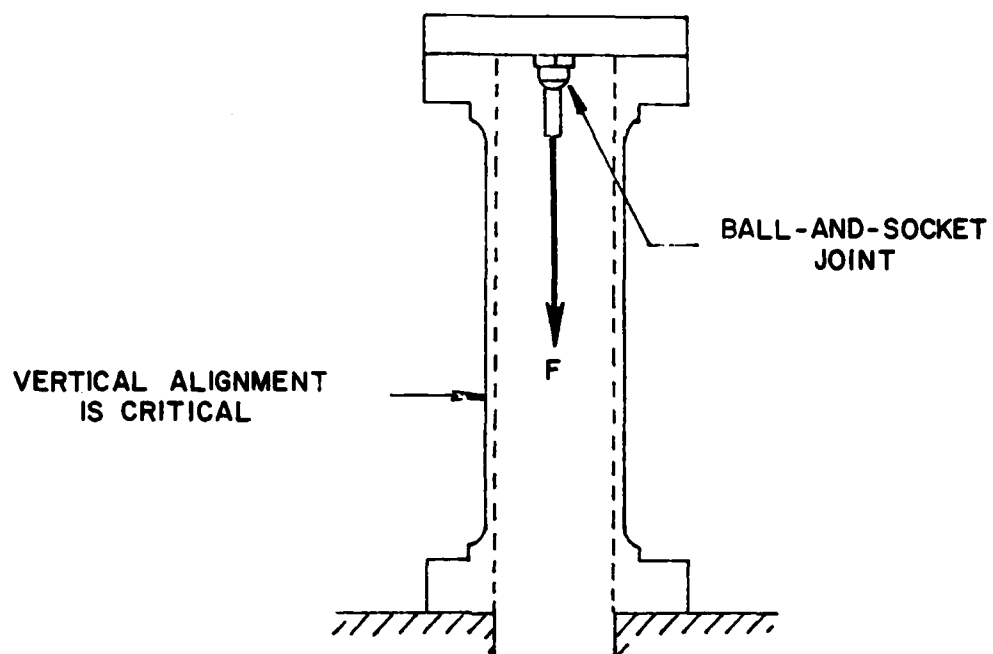


Fig. 7a Loading of the transducer for the axial force calibration.

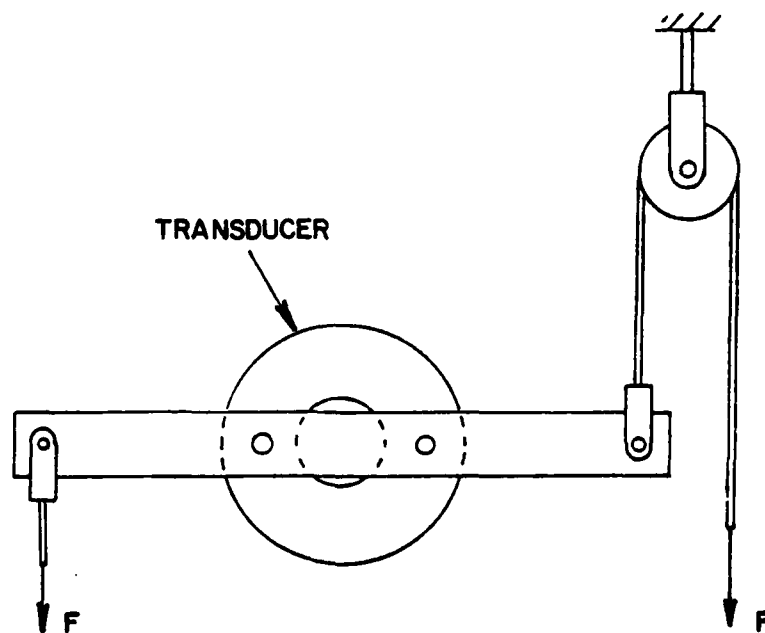


Fig. 7b Torque application on the transducer for the torque calibration.

monitored by a Graf/Pen Sonic Digitizer manufactured by Science Accessories Corporation. Sonic digitizing is the process of converting information on location or position in one, two, or three dimensions to digital values in a form suitable for data transmission, storage, and processing. The system used to accomplish this conversion consists of two or three microphone/sensor assemblies (for 2-D and 3-D data conversions, respectively), an electronic control unit and a generator/multiplexer unit which is used to select and power eight sonic impulse emitters. To explain the digitizer's operation, let us first consider the 2-D mode of operation.

The two-dimensional microphone/sensor assembly consists of two perpendicular linear microphones as shown in Fig. 8. These sensors define a planar effective working area of approximately 35 cm x 35 cm. The Graf/Pen uses impulses generated at the tip of the emitter to calculate its position in the working area. The times required for the sound waves to reach the two microphone/sensors are converted into distance measurements (x and y coordinates). The measurements are then transmitted to the computer in BCD Cartesian form. The 2-D mode is primarily used to digitize joint surface curves which are obtained either from X-ray projections or

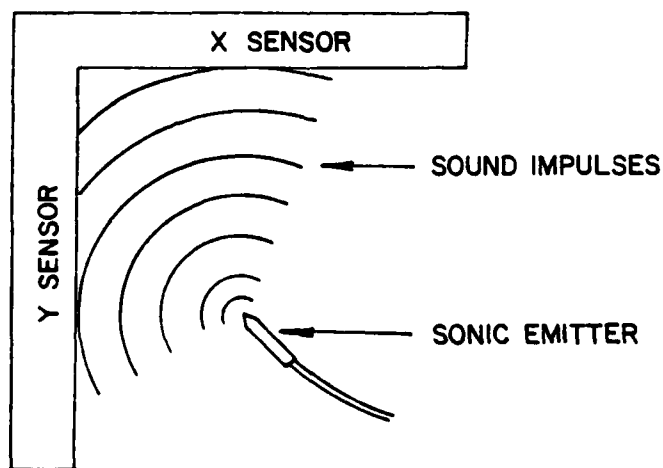


Fig. 8 The 2-dimensional microphone/sensor assembly.

physical cross-sections of the articulating joints. These coordinate curves are subsequently used in the joint model analysis. Note that concurrent with this present work a research program on dynamic modeling of human articulating joints has been conducted for the AMRL [16,17]. The 2-D microphone/sensor assembly also has a menu capability which provides the ability of simultaneous alphanumeric data entry to the computer by the digitizer.

Of course, one advantage of using sound as a ranging device is that digitation need not be confined to a plane. The 3-D microphone/sensor unit used for the kinematic data acquisition, consists of four linear microphones arranged in a planar, rectangular manner. These microphones, in turn, define a 3-dimensional effective working volume of approximately 150 cm x 75 cm x 180 cm along the x, y, and z directions respectively. The 3-D mode of operation is similar to that of the 2-D mode. In the 3-D set up, however, the distances measured are the slant ranges to each of the four coplanar sensors. Thus the information generated by each sensor represents the radius of a circular arc which includes the impulse source (the tip of the sonic emitter) and is in a plane perpendicular to the sensor. Four sensors are used merely for the purpose of accuracy. In actual operation, the digitizer examines the signal from all four sensors, selects the three smallest signals, and disregards the fourth. The location of the sonic emitter is then calculated as being at the intersection of the three smallest arcs. The three slant ranges are easily converted into Cartesian x, y, and z coordinates by a microprocessor in the control unit and converted for transmission. In the 3-D mode of operation, the sonic digitizer will monitor up to seven sonic emitters and output their positional information in serial form. One additional sonic emitter is always reserved for 2-D data or alphanumeric input.

As stated previously, one of the purposes of the sonic digitizer is to monitor the kinematics of the force applicator used in this research. Fig. 9 shows the picture of the present force applicator, which is a significant improvement over the multiple-linkage force applicator (GFA) used in the previously conducted research [7]. The force transducer which is used has already been described in a previous section of this report.

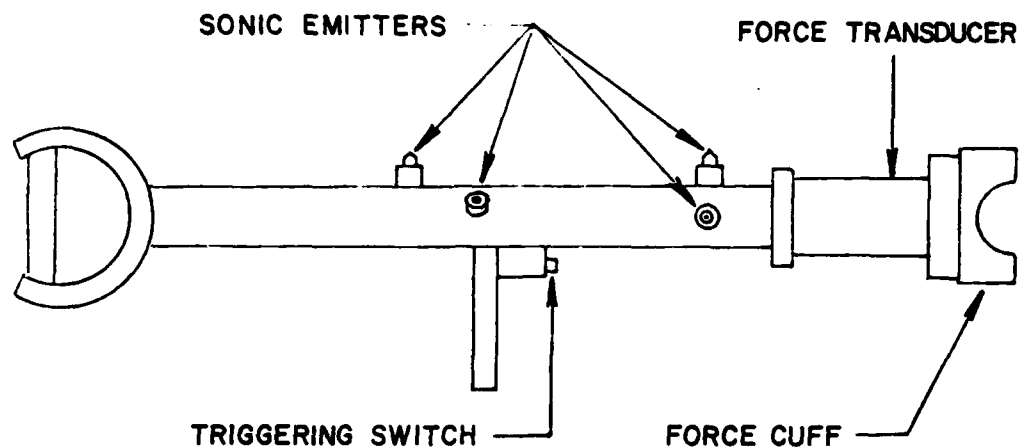


Fig. 9 The force applicator.

The position and direction of force application are obtained by a vector analysis which proceeds from the position information of three sonic emitters located on the force applicator. Note that there are more than three sonic emitters on the force applicator. However, the coordinate information obtained from three sonic emitters is sufficient for determination of the position and direction of force application.

Aside from the improvements in the force transducer itself, this force applicator has several advantages over the previously used multiple linkage system. It has significantly improved our mobility, and its ease of handling allows better control of the magnitude and direction of force application. In addition, data acquisition is now controlled by the force applicator operator. An on-off switch has been installed on the front handle of the force applicator which controls the firing of the sonic emitters located on both the force applicator and on the moving body segment. The signals transmitted from the sonic digitizer to the computer are then, in turn, used to trigger A to D conversions of the signals originating from the force transducer. The digital readings from the transducer are synchronized with the coordinate data from the sonic emitters for input into data files. This process continues until it is terminated by the person controlling the force applicator.

KINEMATICS BY MEANS OF SONIC EMITTERS

In this section theoretical aspects of the kinematics of the relative motion in three dimensional space will be presented by considering the motion of the upper arm with respect to the torso and casting the equations into a format suitable for the utilization of sonic emitters.

The quantitative determination of the nature of the relative motion between two body segments (e.g. the upper arm and the torso), which are connected by a complex anatomical joint, is of prime importance to the biomechanician as well as to those in medicine. The simple hinge joint with one degree of freedom and the ball and socket joint with three degrees of freedom are the most popular joints employed in multisegmented mathematical models of the human body. Under both physiological and external loads, each articulating human joint can be considered as a general joint which can display up to six degrees of freedom, to some extent. A good example of a general joint is the shoulder complex, which exhibits four independent articulations among the humerus, scapula, clavicle, and thorax. Of course at the shoulder complex, the six degrees of freedom refers to the motion of the humerus relative to the torso. If one considers the total number of degrees of freedom for the motions executed by the various bones of the shoulder complex one can easily get a number much higher than six even with the proper consideration of various constraints present in the joint complex.

The basic concept for the study of the relative motion between two body segments is quite fundamental and takes its impetus from the study of the general motion of two rigid bodies, say A and B, in three-dimensional space. The relative motion of body B with respect to body A can be characterized by a unique axis called the screw axis. The relative displacement of body B from one position to another can be defined in terms of a rotation α about, the translation s along the screw axis. For each incremental displacement of body B with respect to body A, a new screw axis is defined. In fact, if the displacements taken by body B are made infinitesimal in size, the collection of the screw axes will form a ruled surface called an axode. There are two unique axodes, one associated

with the motion of body B with respect to body A, and another one associated with the motion of A with respect to B. During the relative motion, the two axodes roll and slide relative to each other along a generator which is momentarily common to both axode surfaces [18]. For a ball and socket joint, the axodes become two rolling cones with common apexes at the center of the sphere; for a hinge joint, they simply degenerate to a single axis, i.e. the axis of the joint. Of course, in each one of these specialized cases the translation s along the screw axis becomes zero.

Let us consider the relative motion of arm designated as body segment B in Fig. 10 with respect to the torso which is designated as body segment A. For the intention of studying the relative motion between these two

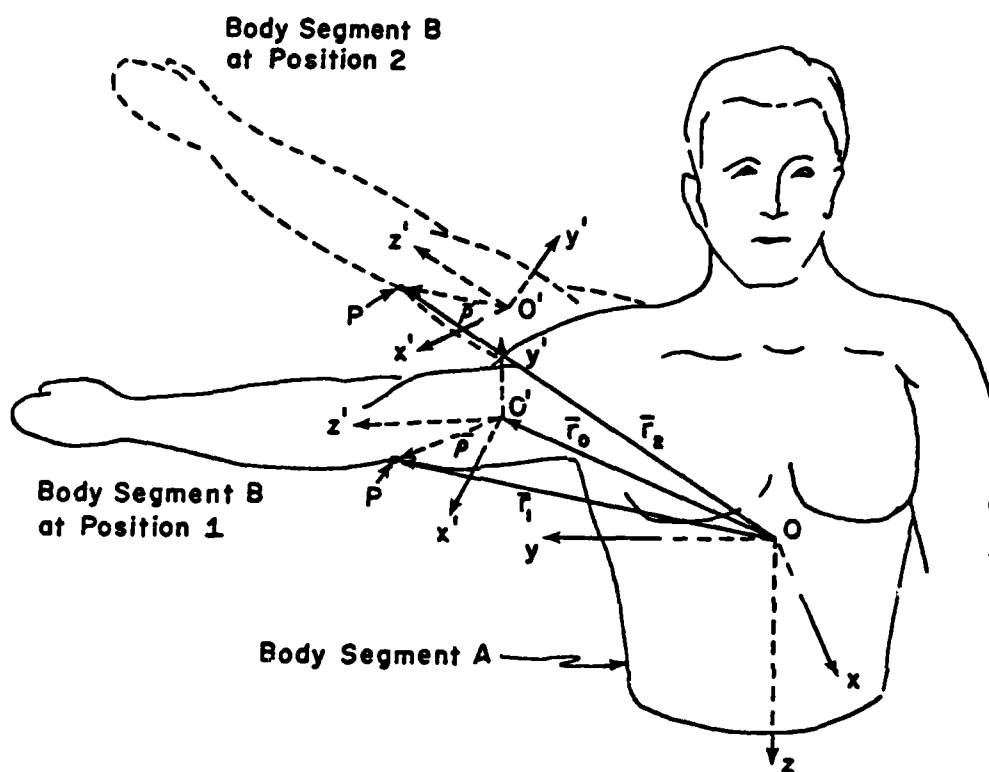


Fig. 10 Motion of body segment B with respect to body segment A in three dimensional space. Displacement of body segment B from position 1 to position 2 is illustrated.

body segments, let us assume that one of them e.g., body segment A, be fixed and the other one, body segment B, is moving relative to body segment A. Note that the range of motion between body segments A and B is controlled by the joint anatomy and ligamentous as well as muscle forces present during motion. It is very essential to point out before we proceed further that no human body segment is a rigid body in the sense defined in mechanics. However, for the purposes of studying the nature of motion in a given anatomical joint the adjacent body segments to this joint can be assumed to be rigid bodies if certain precautions are observed. Let the unprimed xyz and the primed x'y'z' cartesian coordinate systems be attached to the body segments A and B, respectively. These coordinate systems can be also referred to as fixed and moving coordinate systems since body segment A is assumed to be fixed and body segment B is considered to be moving.

Let P be the point designating one of the sonic emitters attached to the body segment B whose position is indicated by vectors $\bar{\rho}$ and \bar{r}_1 (\bar{r}_1 @ position 1; \bar{r}_2 @ position 2) in references x'y'z' and xyz, respectively. Since point P is fixed in a moving body segment, the components of vector $\bar{\rho}$ in reference x'y'z' will remain constant, whereas the components of vector \bar{r}_1 will change as the body segment B moves relative to body segment A. In fact, the relative position of the moving segment is considered completely determined with respect to the fixed segment if for every point in the moving segment and its associated local position vector $\bar{\rho}$, the corresponding \bar{r}_1 can be found. From Fig. 10 the relationship between vectors \bar{r}_1 , \bar{r}_0 and $\bar{\rho}$ can be written in compact matrix form

$$[r_1] = [r_0] + [T][\rho] \quad (8)$$

where the elements of matrix T, t_{ij} are the direction cosines of the O'x', O'y' and O'z' axes relative to the axes of the xyz reference. Thus, matrix T represents rotational orientation of x'y'z', whereas matrix $[r_0]$ represents separation of x'y'z' with respect to the fixed xyz reference. It is more convenient to express Eq. (8) in terms of augmented vectors \bar{r}_{1a} , $\bar{\rho}_a$ whose first component is 1, and a single 4 x 4 matrix T_a by adding the equation $1 = 1$ to the system of equations contained in Eq. (8).

Thus, Eq. (8) takes the following expanded and compact forms:

$$\begin{bmatrix} 1 \\ x_1 \\ y_1 \\ z_1 \end{bmatrix} = \begin{bmatrix} 1 & 0 & 0 & 0 \\ x_0 & t_{11} & t_{12} & t_{13} \\ y_0 & t_{21} & t_{22} & t_{23} \\ z_0 & t_{31} & t_{32} & t_{33} \end{bmatrix} \begin{bmatrix} 1 \\ x'_1 \\ y'_1 \\ z'_1 \end{bmatrix} \quad \text{or} \quad [r_{1a}] = [T_a][p_a] \quad (9)$$

Note that there is a new matrix T_a for each position of body segment B, however, at a given position the matrix T_a is the same for all points of body segment B. Hence, determination of the matrix T_a is sufficient to know the position of the moving body segment relative to the fixed one.

For the total description of the relative motion between two body segments, besides the knowledge of the instantaneous positions of the one body segment relative to another, we must have a description of the nature of the displacement during the motion of the moving segment from position 1 to position 2. Needless to say, instantaneous positions and displacements are very closely related. Displacement analysis results in determination of the set of screw axes; thus, it is essential for the accurate determination of the locations of the joint centers (i.e. centers of rotation). As explained at the beginning part of this section, displacement of body segment B from position 1 to position 2 can be defined in terms of a rotation α about, the translation s along the screw axis, Fig. 11. If the two positions considered are close enough, then the displacements are incremental and refer to a new screw axis each time.

Let us again consider the point P which defines the location of one of the sonic emitters fixed to the body segment B. As the body segment B moves from position 1 to position 2, we can define the position vectors \bar{r}_1 and \bar{r}_2 which are expressed in terms of components in xyz references:

$$\bar{r}_1 = x_1\hat{i} + y_1\hat{j} + z_1\hat{k} \quad \text{and} \quad \bar{r}_2 = x_2\hat{i} + y_2\hat{j} + z_2\hat{k} \quad (10)$$

The components of \bar{r}_2 will be related to the components of \bar{r}_1 by the following special case of an affine transformation:

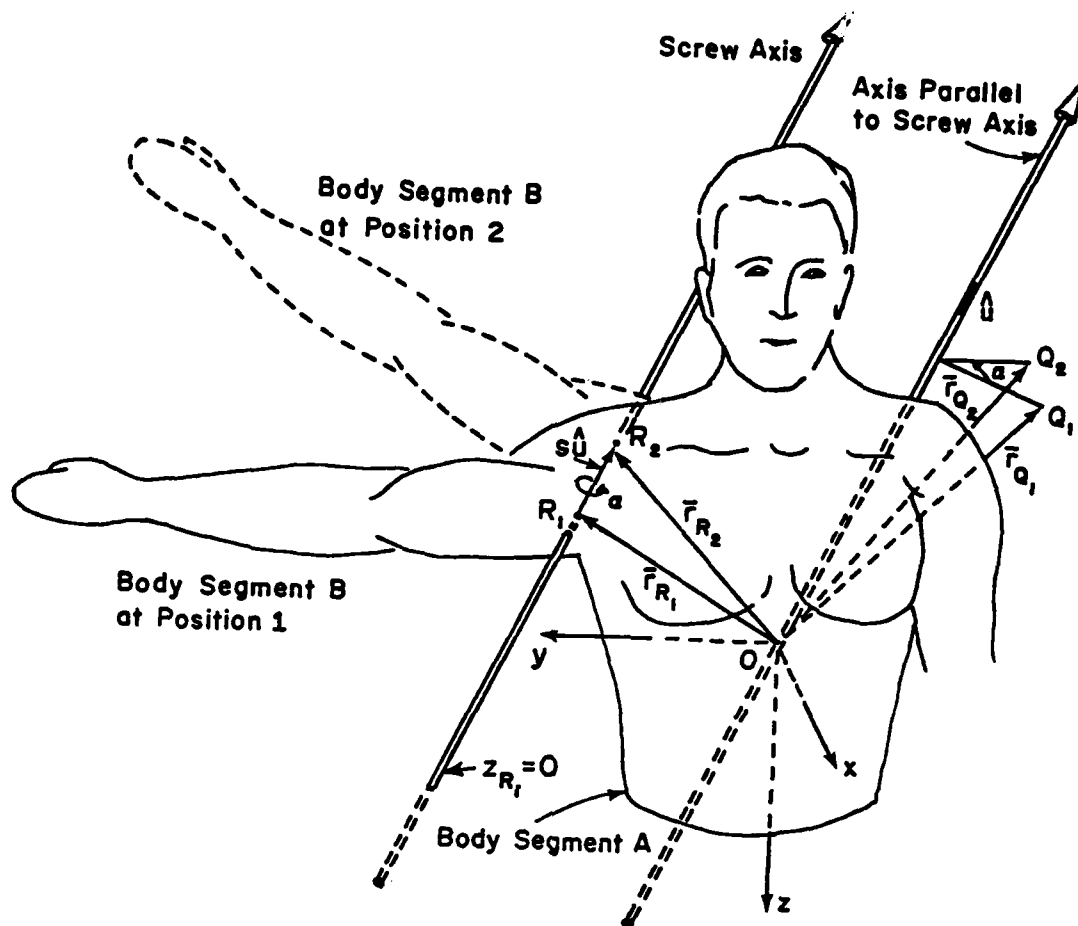


Fig. 11 Representation of the motion of body segment B from position 1 to position 2 in terms of a rotation α about and translation s along the screw axis. A pure rotation of magnitude α of a point Q about an axis parallel to the screw axis is also displayed.

$$\begin{bmatrix} x_2 \\ y_2 \\ z_2 \end{bmatrix} = \begin{bmatrix} m_{11} & m_{12} & m_{13} \\ m_{21} & m_{22} & m_{23} \\ m_{31} & m_{32} & m_{33} \end{bmatrix} \begin{bmatrix} x_1 \\ y_1 \\ z_1 \end{bmatrix} + \begin{bmatrix} a_x \\ a_y \\ a_z \end{bmatrix} \quad (11)$$

Eq. (11) can be written in augmented form as

$$\begin{bmatrix} 1 \\ x_2 \\ y_2 \\ z_2 \end{bmatrix} = \begin{bmatrix} 1 & 0 & 0 & 0 \\ a_x & m_{11} & m_{12} & m_{13} \\ a_y & m_{21} & m_{22} & m_{23} \\ a_z & m_{31} & m_{32} & m_{33} \end{bmatrix} \begin{bmatrix} 1 \\ x_1 \\ y_1 \\ z_1 \end{bmatrix} \quad (12)$$

Eqs. (11) and (12) can be expressed in a more compact form as

$$[r_2] = [M][r_1] + [a] \quad \text{and} \quad [r_{2a}] = [M_a][r_{1a}], \quad (13a,b)$$

respectively. From a mathematical point of view, the augmented form describes the motion of a three-dimensional set of points contained within body segment B relative to a hyperplane [19]. In Eq. (13a) matrix M represents a pure rotation about the screw axis and also contains direction cosines information for the screw axis. The augmented matrix M_a in Eqs. (12) and (13b) has the total information for determination of the displacement of the moving body.

To determine the matrix M_a , it is sufficient to know the coordinates of four non-coplanar points P_1, P_2, P_3 and P_4 in the moving body segment (or on the extension of the moving body segment) in both positions 1 and 2. Four sonic emitters attached to the moving body segment represent these points whose coordinates can be monitored continuously. Let us designate the position vectors of these four sonic emitters by \bar{p}_{ij} and \bar{r}_{ij} relative to the moving $x'y'z'$ and the fixed xyz references, respectively. In this subscripted notation, the first subscript i ($i = 1,2,3,4$) is used to designate an emitter and the second subscript j ($j = 1,2$) is used for the designation of positions 1 and 2. The augmented vectors \bar{r}_{ija} for each emitter can be related via Eq. (13b),

$$[r_{i2a}] = [M_a][r_{i1a}] \quad (i = 1,2,3,4) \quad (14)$$

Eq. (14) represents four matrix equations which can be written in one equation by defining a new matrix A whose columns are the augmented vectors, \bar{r}_{ija} ,

$$[A_j] \triangleq \begin{bmatrix} 1 & 1 & 1 & 1 \\ x_{1j} & x_{2j} & x_{3j} & x_{4j} \\ y_{1j} & y_{2j} & y_{3j} & y_{4j} \\ z_{1j} & z_{2j} & z_{3j} & z_{4j} \end{bmatrix} \quad (j = 1, 2) \quad (15)$$

With the definition given by Eq. (15), Eq. (14) becomes

$$[A_2] = [M_a][A_1] \quad (16)$$

The matrix A has a non-vanishing determinant since it is formed by the position vectors of non-coplanar points (sonic emitters); thus, it has an inverse and the desired matrix M_a is easily obtained from Eq. (16),

$$[M_a] = [A_2][A_1]^{-1} \quad (17)$$

When the matrix M_a is determined by means of Eq. (17) and data obtained from four sonic emitters attached to the moving body segment, information such as direction cosines of the screw axis, rotation α about and translations along the screw axis, and the coordinates of the piercing point of the screw axis with one of the reference planes can be obtained according to the theory presented previously, [7,10].

DESCRIPTION OF SOFTWARE DEVELOPMENT

Software is dependent, to various extents, upon the architecture of the particular computer on which it is to run. A Digital Equipment Corporation PDP 11/34A was selected for this research project. The software for this machine included an RSX-11M operating system, a Fortran-IV compiler, a scientific subroutine package and interface and applications programs. In this section we will discuss in some detail, the system generation process, the force transducer calibration software, and the data acquisition and analysis programs.

SYSTEM GENERATION

Generation of the operating system required considerable planning and consultation with Digital representatives in order to tailor the system to the project's needs. An important and troublesome component of the system

software is the set of routines to manage the operation of peripherals, including the Data Translation model DT 1712/5714-64, 14-bit analog-digital converter and the Science Accessories Corporation model GP6-3D-3 sonic digitizer. These major components of the experimental apparatus are considered "foreign" equipment and could not be installed with the system by the Digital Equipment Corporation representatives. This necessitated considerable time and study to become familiar with the entire operating system and hardware. Provided with a basic outline of a software interface for an A-D board, a subprogram was developed to address the A-D board, to identify the channel to be read, to supply any "software" gain to the signal and to check if the A-D conversion was successful.

Because of a foreign hardware interface involvement, the subprogram had to be written in MACRO-11, the assembly language of the PDP-11. This necessitated the learning of an entirely new programming language since we had prior experience only in Fortran. The final requirement was that this subprogram be callable from a Fortran program. The result of this effort is the subprogram entitled (OSUATD), a listing of which is included in both the transducer calibration program (CHNCAL), and the data acquisition program (BIGQIO), found in Appendices A and B.

TRANSDUCER CALIBRATION PROGRAM

The transducer calibration program (CHNCAL), a listing of which is contained in Appendix A, is short and straightforward. (CHNCAL) computes the total, mean, standard deviation and the minimum and maximum values of 1000 samples read from each channel of the A-D board. All non-zero values are analyzed, totals are accumulated and the minimum and maximum values are found. Following this, the mean and standard deviation are calculated. The divisor for the standard deviation calculation is one less than the number of samples taken.

Output includes the channel number being sampled, the mean, the minimum and maximum values read, and a status code. If errors are encountered, appropriate descriptive messages are displayed. The program may be run stand-alone for single sweeps of the A-D channel(s), or it may be run from an indirect command file. The indirect command file, a separate, monitor control routine, provides prompts for test identification

and executes (CHNCAL) each time a calibration test is set up, thus eliminating the need for manually installing and executing the program for each test set-up. The command file (TRNCAL) prompts for the name of the calibration test being performed, displays the date and time of the test, prompts for the amount of the load applied to the transducer and executes (CHNCAL), repeating the date, time and applied load prompts until the testing sequence is completed. A listing of (TRNCAL) is included in Appendix A.

Two subroutines are called in (CHNCAL). The subroutine (OSUATD), described briefly above, obtains the A-D readings, checks for successful conversion, and applies gain if desired. It is called 1000 times for each channel tested. (TALLY) is the statistical subroutine which takes the 1000 readings for a channel and calculates the total, mean, the minimum and maximum values and checks for null or single-value input. It is called once for each channel tested. The program tests channels 32 to 37 of the A-D board, but may be easily edited for other sampling configurations.

DATA ACQUISITION PROGRAM

The data acquisition program, (BIGQIO), is designed to create an unformatted data file containing digitized points in space and concurrent transducer readings. A complete listing of this program is contained in Appendix B. The program queues from the Science Accessories sonic digitizer. Each point is described by a set of three coordinates, relating the position to the origin of the 3-D sonic tablet. Seven individual points are monitored throughout the testing. The first three points are obtained from sonic emitters mounted on the force applicator. The remaining four points are mounted, by use of an elastic cuff, on the moving body segment of the subject. Thus, each scan of the digitizer monitors the positions of these seven points.

The sonic digitizer can scan its seven channels up to eight times each second. Since this is, in computer reference, a long time, the sonic digitizer is considered to be the limiting factor in the rate of data acquisition. It is for this reason that the data acquisition program queues from the digitizer. During the time between the sampling of the

digitized points, the computer scans each of the six transducer channels 100 times and takes the mean of each channel's readings, where each channel of the A-D board represents a separate strain gage bridge of the force transducer.

(BIGQIO) prompts for a name to be given to the data file. The format for the file name is [SIX CHARACTER STRING], [THREE CHARACTER STRING], [SINGLE DIGIT], (e.g.: SHOLD.DAT;1). The file name is used later to identify a particular test configuration from the test log, which is kept separately and contains a description of the test position, the subject's identification, the 3-D sonic tablet position relative to the body coordinate system and the data file name.

The file structure is currently set for one file per test. Each file may contain a variable number of records. Each record contains a complete set of digitized points and transducer readings. (BIGQIO) prompts for the number of records to be allocated for each test. The number entered in response to this prompt should be approximately five times the duration of the test (in seconds). For an average ten second test, 50 should be entered for the number of records, where each record contains one sweep of the seven sonic emitters and the mean of 700 readings for each of the six transducer channels.

The program begins data collection whenever the first sonic emitter coordinates are received. (BIGQIO) will halt if the number of records allocated is exceeded, if the A-D board fails to convert a signal or if the digitizer sends a series of zeros. Since the number of records should be generously estimated, the collection of data should be completed before the record allocation is exceeded.

Two subroutines are utilized in (BIGQIO). The system library routine (ASSIGN) is used to identify the data file, assigning a logical unit number and name to the file. The second subroutine (OSUATD) has been described above.

DATA ANALYSIS PROGRAM

The program (TABLE) is designed to read data from disk storage and analyze it, printing the results for each position during a particular test. The program is interactive, requiring manual input from the

terminal. The prompts for input are self-explanatory. Each prompt includes the number of permissible characters for each entry. Since a series of tests may be performed for a given chair position, prompts are divided into general position and identification prompts, and test specific prompts. The position and identification prompts are:

- (a) (Enter the name of joint tested [S-9]:) Enter up to nine alphanumeric characters for use in the output heading.
- (b) (Enter subject name or number [S-25]:) Enter up to 25 alphanumeric characters for identification on the output heading.
- (c) (Enter the coordinates of the 3-D board origin, with respect to the fixed body segment origin:) Enter the X, Y and Z coordinates in decimal numbers.
- (d) (Enter, in degrees, the rotation of the 3-D board from the vertical [N-8]:) Enter the appropriate decimal number.
- (e) (Enter, in degrees, the rotation of the 3-D board from the X-Y plane [N-8]:) Enter a decimal number.
- (f) (Enter the coordinates of the fixed joint center with respect to the fixed body segment origin:) Enter the appropriate coordinates as decimal numbers.
- (g) (Enter the length to the JOINT CENTER [N-8]:) Enter a decimal number.
- (h) (Enter the tilt of the chair, in degrees [N-8]:) Enter a decimal number.
- (i) (Enter the rotation of the chair, in degrees [N-8]:) Enter a decimal number.

For each test under the above board and chair positions for the specified joint and subject, the following prompts are issued:

- (a) (Enter any messages (Maximum - 80 characters):) Enter up to 80 characters which describe the specific test.
- (b) (Enter data file name [S-13]:) Enter up to 13 characters which identify the file containing the data for the test (e.g.: SHOLD.DAT; 1).

- (c) (Enter the number of records to be read [N-5]:) Enter the number of records contained in the data file (this information was output from (BIGQIO).)

Data analysis program outputs to the hardcopy terminal and includes: a header identifying the test and subject; the calculated spherical coordinates, θ and ϕ , of the moving body segment; the force and moment components and magnitudes; the calculated fixed joint center and the distances between various fixed sonic emitters. The distances between fixed sonic emitters, such as those on the force applicator, should remain constant and thus serve as a check on the validity of the data.

All calculations are performed with respect to the 3-D board coordinate system. The results are then transformed to the fixed body coordinate system. Therefore, the transformation matrix will be dealt with last. We next provide a brief description of the subroutines of data analysis program.

Point of Force Application [SUBROUTINE FORPT]

The first calculations are to determine the point of application of the force. This subroutine is called once for every set of data points. It uses the coordinates of the first three sonic emitters to determine the direction and position of the point of force application.

Moving Body Segment Position [SUBROUTINE POSITN]

The position of the moving body segment is necessary for calculation of the joint center. This subroutine calculates the position from the four sonic emitters located on the moving body segment. The process is similar to locating the point of force application.

Spherical Coordinates, θ , ϕ [SUBROUTINE SPHERE]

The location of the moving body segment is located by the spherical coordinates, θ and ϕ . This subroutine calculates these angles when called from (SUBROUTINE JTCNT). The vector between the positions of the moving body segment toward the joint center is first transformed to the fixed body segment coordinate system and θ and ϕ are calculated directly.

Fixed Joint Center [SUBROUTINE FJTCNT]

Given the input of the coordinates of a fixed position at the joint center, this subroutine calculates a relatively fixed joint center located at the end of the long bone axis of the moving body segment.

Matrix Inversion [SUBROUTINE MINV]

This subroutine inverts a matrix using the standard Gauss-Jordan method. The determinant is also calculated. A determinant of zero indicates that the matrix is singular.

Matrix Multiplication [SUBROUTINE GMPRD]

This subroutine multiplies two matrices to form a resultant general matrix.

Transformation Matrix [SUBROUTINE MATRIX]

When all the positions, locations and values have been calculated, the reference coordinate system (3-D board), must be related to the fixed body coordinate system. This subroutine rotates and translates the 3-D coordinate system into the fixed body segment coordinate system, using the angles of the 3-D board (tilt and rotation), the position of the respective origins and the angles of the chair (tilt and rotation).

DATA COLLECTION ON HUMAN SUBJECTS

The main thrust of the research program reported here is the collection of the active muscle force and moment data on the higher and lower extremities of the human body. In this section of the report, first, anthropometry of the subjects and later a detailed description of the experiments are presented.

ANTHROPOMETRY OF SUBJECTS

In this research program, six healthy subjects (3 male, 3 female) between the ages of 20-22 were tested. Subjects were university students with no special training in athletics. Selected anthropometric measurements of these six subjects are given in Table 2 for male subjects and in Table 3 for female subjects. The body segment circumferences given in these two tables were obtained according to the following definitions [20]:

- (a) Shoulder Circumference: maximum horizontal circumference over the deltoid muscle.
- (b) Chest Circumference: horizontal circumference at nipple level during normal breathing.
- (c) Waist Circumference: horizontal circumference at level of the greatest lateral indentation of trunk.
- (d) Wrist Circumference: minimum circumference above the wrist bones (styloid processes of radius and ulna).
- (e) Lower Arm Circumference: maximum circumference wherever found, with the upper arm horizontal, forearm vertical, and the elbow 90°, muscles tensed.
- (f) Elbow Circumference: circumference encompassing the elbow tip and the elbow crotch, with the upper arm horizontal, forearm vertical, and the elbow at 90°, muscles tensed.
- (g) Biceps Circumference: maximum circumference with elbow bent at 90° and biceps maximally flexed.
- (h) Arm, Axillary Circumference: horizontal circumference at the armpit, arms hanging loosely at the side.
- (i) Arm, Scye Circumference: circumference encompassing the highest skeletal point on the lateral edge of the acromion process and the highest point in the axilla (armpit).
- (j) Thigh, Upper Circumference: horizontal circumference just below the gluteal furrow.
- (k) Thigh, Lower Circumference: horizontal circumference just above the knee.
- (l) Calf Circumference: maximum horizontal circumference, wherever found.
- (m) Ankle Circumference: minimum horizontal circumference above the projections of the ankle bones (external and internal malleoli).

The following definitions were used for the linear dimensions given in Tables 2 and 3:

- (a) Forearm-Wrist Length: distance from tip of elbow to the styloid process of radius.

Table 2

SELECTED ANTHROPOMETRY OF MALE SUBJECTS 1, 2, 3.

(All length dimensions are in cm)

	1	2	3
Weight (Newtons)	663	756	757
Stature	170	171.2	185.5
Shoulder Circumference	113	112.5	111.2
Chest Circumference	94.3	100.2	97.0
Waist Circumference	75.0	87.4	81.1
Wrist Circumference	16.6	17.5	16.0
Lower Arm Circumference	30.5	29.5	28.6
Elbow Circumference	31.6	32.5	31.4
Biceps Circumference	32.1	33.5	31.5
Arm, Axillary Circumference	31.4	33.8	29.8
Arm, Scye Circumference	42.1	48.6	45.6
Thigh, Upper Circumference	54.6	57.2	57.8
Thigh, Lower Circumference	39.0	42.5	39.5
Calf Circumference	35.4	39.6	38.5
Ankle Circumference	21.5	24.0	22.5
Forearm - wrist length	25.2	26.5	28.5
Shoulder - elbow length	34.2	34.4	39.4
Shoulder - height, sitting	58.0	58.8	60.5
Sitting height	90.1	89.6	92.0
Shoulder breadth	46.7	48.5	47.1
Chest breadth	28.8	32.0	30.5
Chest depth	19.0	21.0	20.6
Waist depth	18.9	21.5	19.6
Buttock - knee length	57.1	59.8	62.1
Buttock - popliteal length	41.1	48.2	52.0
Knee height, sitting	51.8	51.2	57.9
Elbow - to - elbow breadth	46.5	49.5	47.2
Hip breadth, sitting	35.0	36.5	35.6
Knee - to - knee breadth, sitting	19.1	22.5	19.9
Leg length (tibial point - Malleo.)	37.8	37.5	45.0
Trochanterion height	87.0	88.0	98.0

Table 3

SELECTED ANTHROPOMETRY OF FEMALE SUBJECTS 1, 2, 3.

(All length dimensions are in cm)

	1	2	3
Weight (Newtons)	578	592	645
Stature	163.2	174	169.5
Shoulder Circumference	101.3	101.5	107.6
Chest Circumference	84.5	88.5	98.0
Waist Circumference	74.3	70.5	78.1
Wrist Circumference	15.5	15.6	16.4
Lower Arm Circumference	25.5	24.3	26.4
Elbow Circumference	26.7	27.8	28.0
Biceps Circumference	29.3	27.6	29.4
Arm, Axillary Circumference	28.7	28.5	31.6
Arm, Scye Circumference	39.1	39.4	39.8
Thigh, Upper Circumference	60.0	56.5	62.2
Thigh, Lower Circumference	42.1	38.5	43.1
Calf Circumference	38.2	37.8	37.9
Ankle Circumference	22.9	22.6	22.6
Forearm - wrist length	25.0	27.5	25.9
Shoulder - elbow length	32.2	35.3	34.9
Shoulder - height, sitting	61.8	58.6	61.5
Sitting height	89.2	90.2	90.4
Shoulder breadth	43.7	43.2	44.5
Chest breadth	27.2	28.0	28.6
Chest depth	19.0	19.0	20.2
Waist depth	17.4	17.3	18.2
Buttock - knee length	57.1	60.1	57.6
Buttock - popliteal length	48.3	48.8	48.0
Knee height, sitting	49.8	52.0	52.1
Elbow - to - elbow breadth	41.0	39.6	42.2
Hip breadth, sitting	41.6	40.2	41.5
Knee - to - knee breadth, sitting	17.0	15.0	16.8
Leg length (tibial point - Malleo.)	36.4	39.6	39.0
Trochanterion height	85.0	90.0	85.5

- (b) Shoulder-Elbow Length: distance from the top of the acromion process to the bottom of the elbow when subject sits erect, upper arm vertical at side and the forearm making a right angle with upper arm.
- (c) Shoulder Height, Sitting: vertical distance from the sitting surface to the most lateral point on the superior surface of the acromion process of the scapula.
- (d) Sitting Height: vertical distance from the sitting surface to the top of the head.
- (e) Shoulder Breadth: maximum horizontal distance across the deltoid muscles when subject sits erect, upper arms vertical at sides and forearms extended horizontally.
- (f) Chest Breadth: horizontal distance across the chest at nipple level when subject stands erect and breathing normally.
- (g) Chest Depth: horizontal distance from front to back of chest at nipple level when subject stands erect and breathing normally.
- (h) Waist Depth: horizontal distance between the back and abdomen at the level of the greatest lateral indentation at the waist when subject stands erect with relaxed abdomen.
- (i) Buttock-Knee Length: horizontal distance from the plane of the rearmost point on the buttocks to the front of the knee when subject sits erect with knees and ankles at right angles.
- (j) Buttock-Popliteal Length: horizontal distance from the plane of the rearmost point on the buttocks to the back of the lower leg at the knee when subject sits erect with knees and ankles at right angles.
- (k) Knee Height, Sitting: vertical distance from the floor to the uppermost point on the knee when subject sits erect with knees and ankles at right angles.
- (l) Elbow-to-elbow Breadth: maximum horizontal distance across the lateral surface of the elbows when subject sits erect with upper arms vertical and touching the sides, and forearms extended horizontally.

- (m) Hip Breadth, Sitting: maximum horizontal distance across the hips when subject sits erect with knees and ankles at right angles.
- (n) Knee-to-knee Breadth, Sitting: maximum horizontal distance across the lateral surfaces of the knee when subject sits erect with knees at right angles and pressed together lightly.
- (o) Leg Length: distance between the tibial point and malleolar point.
- (p) Trochanteric Height: vertical distance between the trochanteric point and floor when subject stands erect.

During anthropometric measurements and subsequent experiments male subjects wore swimming trunks, female subjects wore gymnast's leotards.

DESCRIPTION OF EXPERIMENTS

Two sets of experiments on the collection of active force and moment data were considered. The first set of experiments was designed to determine the active muscle resistances and corresponding moment values at the shoulder and hip joints of subjects when there is a strong tendency of dislodging of the upper and lower extremities from their initial (stowed) positions. These experiments included seat armrest initiation force simulation, D-ring force simulation, and face curtain force simulation. Brief description of these force applications are given next by the aid of a coordinate system for which positive x-direction refers to anterior direction, positive y-direction to right lateral and, naturally, positive z-direction refers to inferior direction if the origin of the cartesian coordinate system is fixed in the mid-torso location. In Fig. 12 this coordinate system is shown as (x_t, y_t, z_t) . The angles θ_1, ϕ_1 and θ_2, ϕ_2 shown in Fig. 12 define the angular orientation of the subject restraint system and the microphone assembly, respectively, with respect to the laboratory coordinate system (X, Y, Z) .

In the experiment entitled "seat armrest initiation force simulation" we determined the magnitudes of forces necessary to separate the lower arm from the initial seat armrest position. For the first part of the experiment the force cuff of the force applicator was placed along the

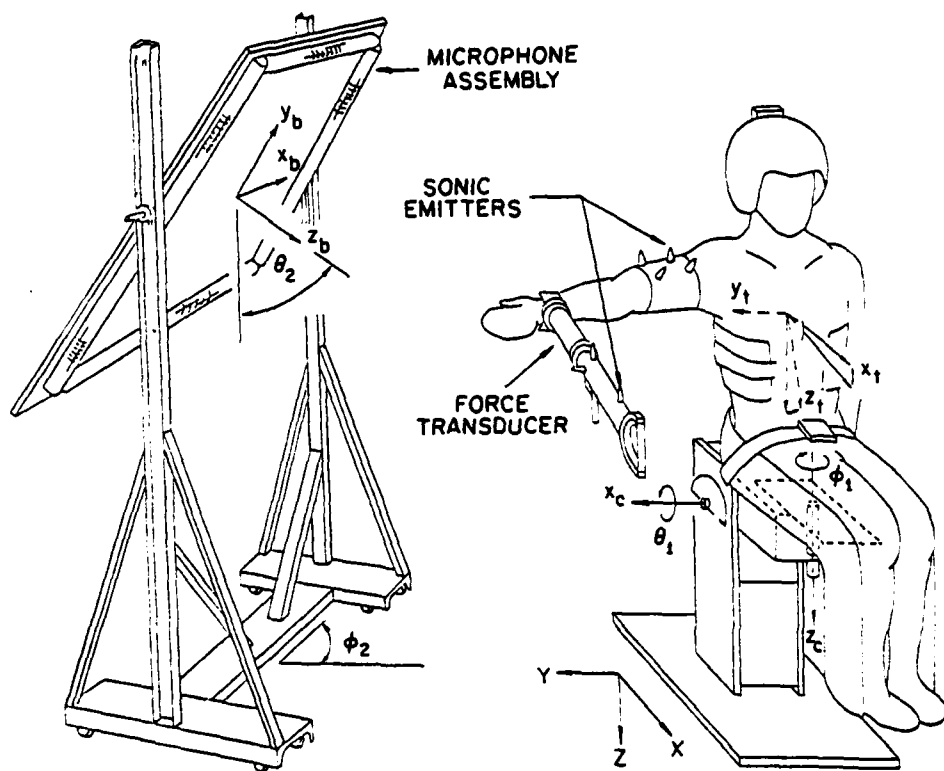


Fig. 12 Schematic drawing of experimental setup.

y-direction on the lower arm and on the wrist, as shown in Figs. 14 & 15, thus, subjects applied an isometric force, F_1 , along the negative y-direction, i.e. medially, on the force transducer. In the second part of the experiment the force application by the subjects was along the positive z-direction as shown in Figs. 16 & 17, and these forces are tabulated as F_2 in results section. In the "D-ring force simulation" experiment the subjects as shown in Figs. 18 & 19, with extended arm and hand near the crotch applied an isometric force along the negative y-direction on the force transducer. In the "face curtain force simulation" experiment the subjects with a flexed elbow brought their hands toward the lateral side of their face and at this position they applied an isometric force along the negative y-direction on the force cuff

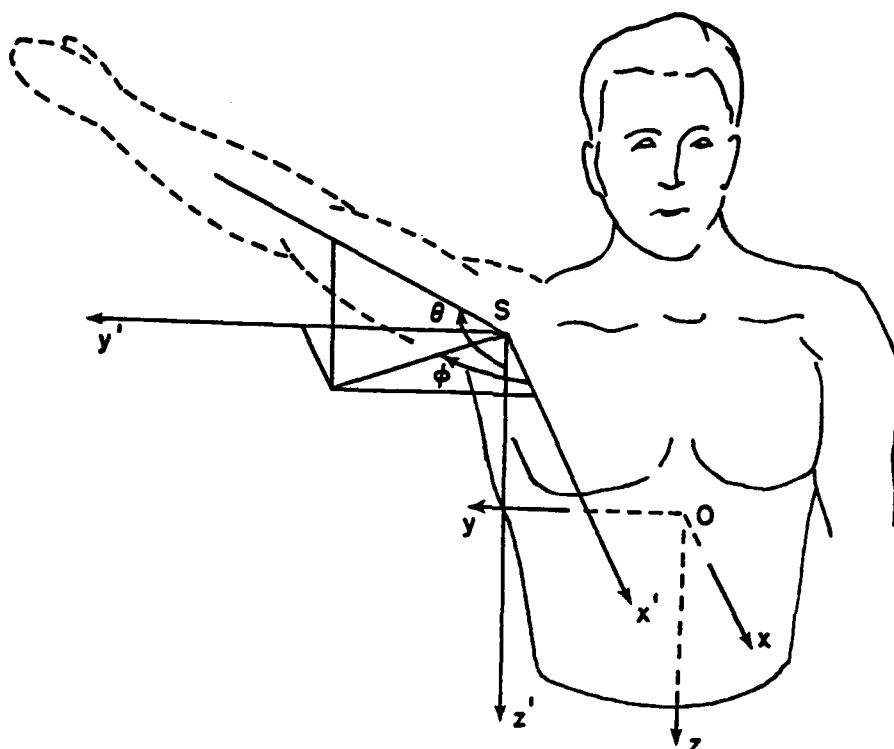


Fig. 13. Definition of θ and ϕ angles with respect to the coordinate system attached to the fixed-body segment.

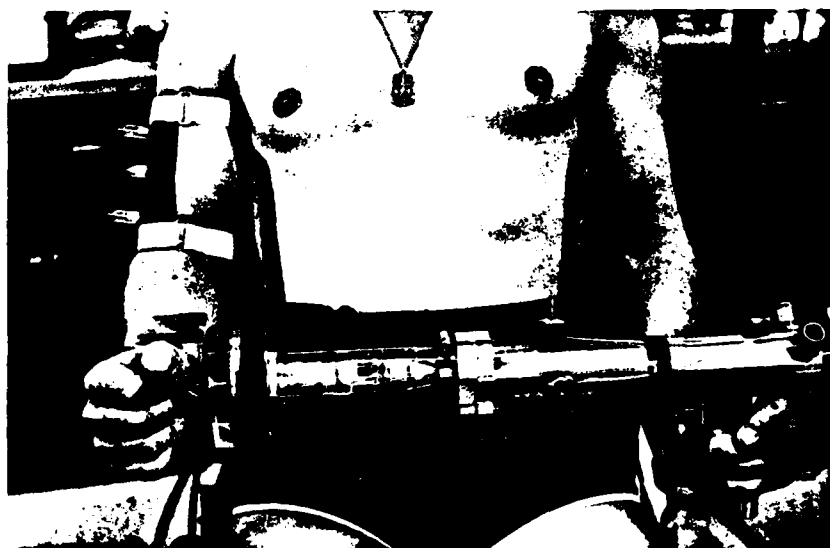


Fig. 14. Force application on the wrist along the negative y direction by one of the male subjects (MS1).



Fig. 15. Force application on the wrist along the negative y direction by one of the female subjects (FS2).



Fig. 16. Force application along the positive z direction by one of the male subjects (MS1)--Seat armrest initiation force.

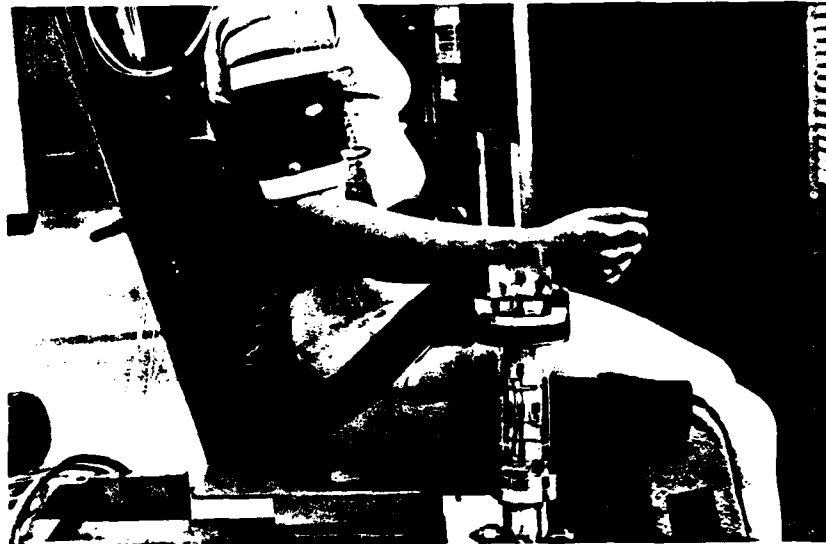


Fig. 17. Force application along the positive z direction by one of the female subjects (FS3)--Seat armrest initiation force.

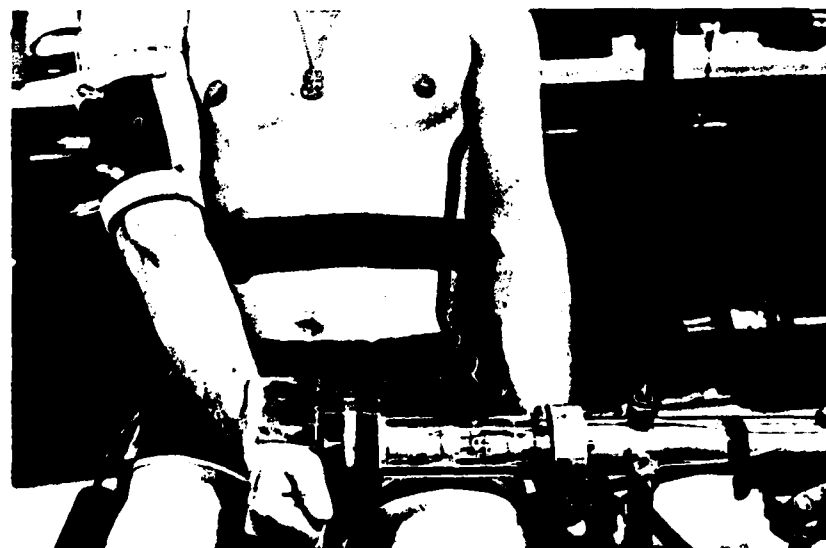


Fig. 18. Force application along the negative y direction by one of the male subjects (MS1)--D-ring force simulation.

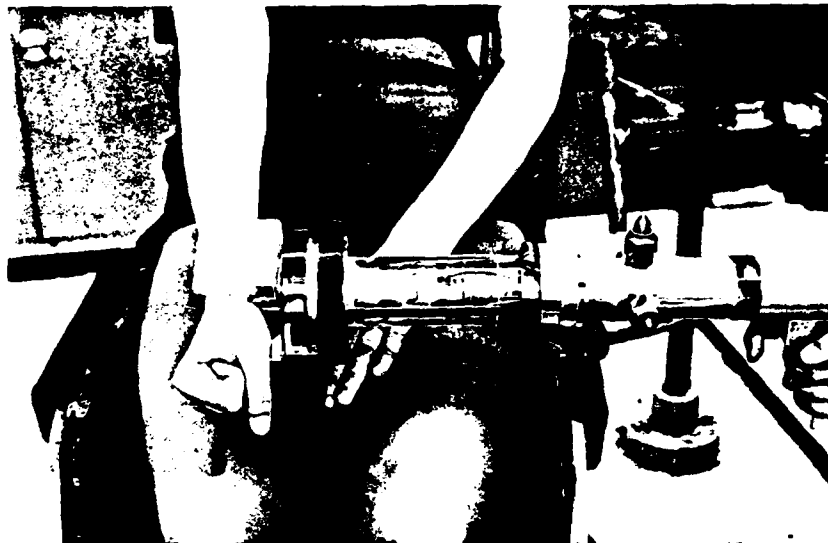


Fig. 19. Force application along the negative y direction by one of the female subjects (FS2)--D-ring force simulation.



Fig. 20. Force application on the ankle along the positive y direction by one of the male subjects (MS1).

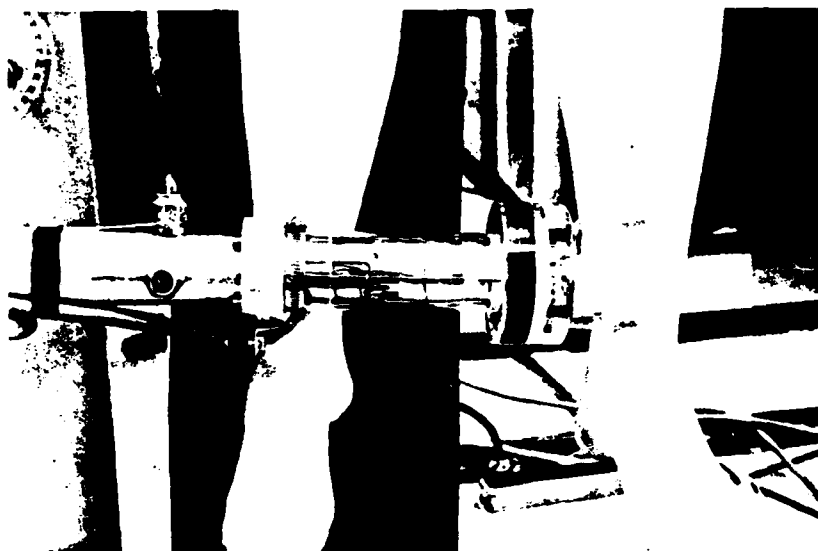


Fig. 21. Force application on the ankle along the positive y direction by one of the female subjects (FS2).



Fig. 22. Force application on the wrist by one of the male subjects (MS1) when forearm is 30° laterally rotated.

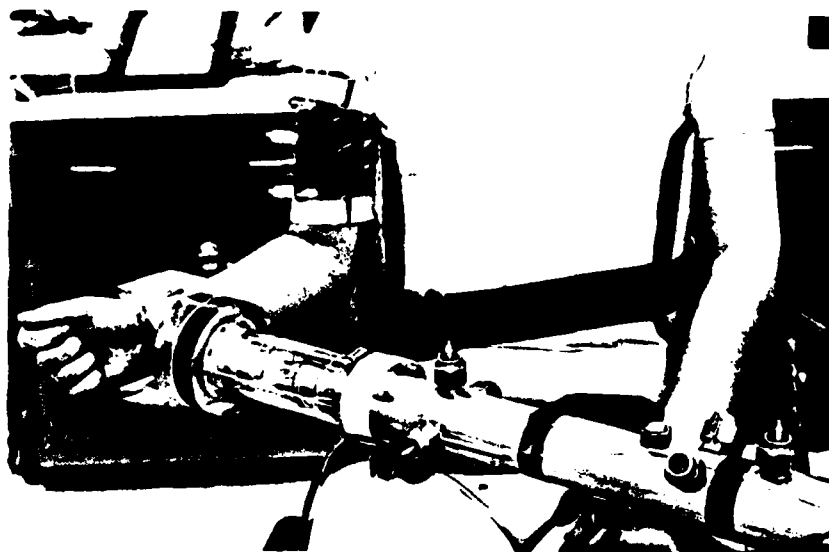


Fig. 23. Force application on the wrist by one of the female subjects (FS3) when forearm is 30° laterally rotated.

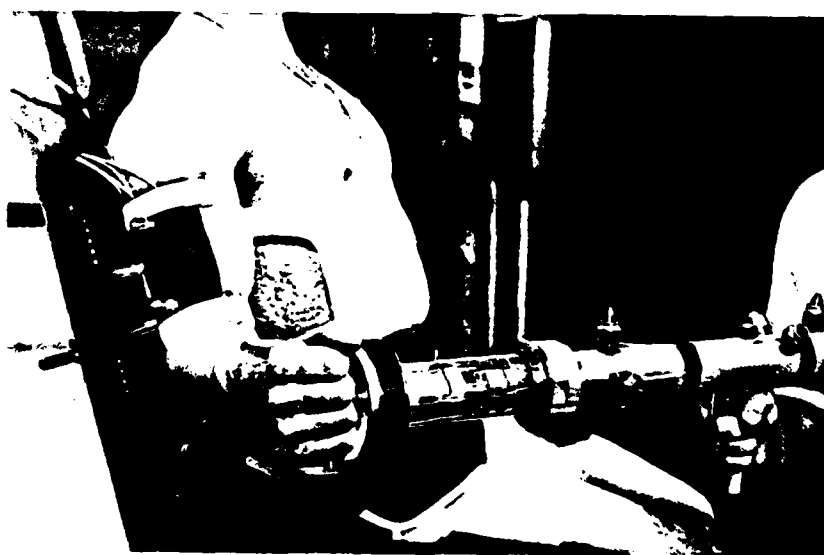


Fig. 24. Force application on the wrist by one of the male subjects (MS1) when forearm is 60° laterally rotated.



Fig. 25. Force application on the wrist by one of the female subjects (FS3) when forearm is 60° laterally rotated.



Fig. 26. Force application on the wrist by one of the male subjects (MS1) with fully extended elbow and arm orientation at $\phi = 0^\circ$ & $\theta = 30^\circ$.



Fig. 27. Force application on the elbow by one of the male subjects (MS1) with fully extended elbow and arm orientation at $\phi = 0^\circ$ & $\theta = 30^\circ$.



Fig. 28. Force application on the wrist by one of the male subjects (MS1) with fully extended elbow and arm orientation at $\phi = 0^\circ$ & $\theta = 60^\circ$.



Fig. 29. Force application on the elbow by one of the male subjects (MS1) with fully extended elbow and arm orientation at $\phi = 0^\circ$ & $\theta = 60^\circ$.



Fig. 30. Force application on the wrist by one of the male subjects (MS1) with fully extended elbow and arm orientation at $\phi = 0^\circ$ & $\theta = 120^\circ$.



Fig. 31. Force application on the elbow by one of the male subjects (MS1) with fully extended elbow and arm orientation at $\phi = 0^\circ$ & $\theta = 120^\circ$.



Fig. 32. Force application on the wrist by one of the male subjects (MS1) with fully extended elbow and arm orientation at $\phi = 30^\circ$ & $\theta = 30^\circ$.



Fig. 33. Force application on the wrist by one of the male subjects (MS1) with fully extended elbow and arm orientation at $\phi = 60^\circ$ & $\theta = 60^\circ$.

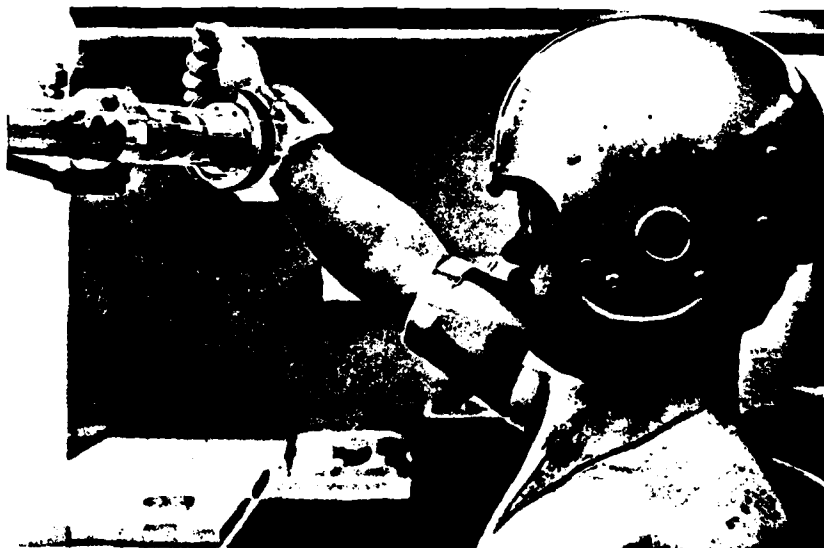


Fig. 34. Force application on the wrist by one of the male subjects (MS1) with fully extended elbow and arm orientation at $\phi = 60^\circ$ & $\theta = 120^\circ$.

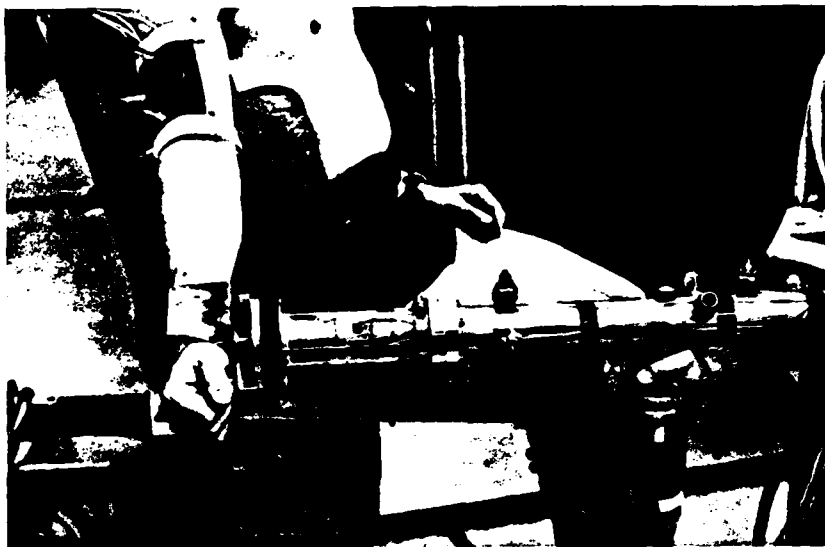


Fig. 35. Force application on the wrist by one of the male subjects (MS1) with fully extended elbow and arm orientation at $\phi = 90^\circ$ & $\theta = 30^\circ$.

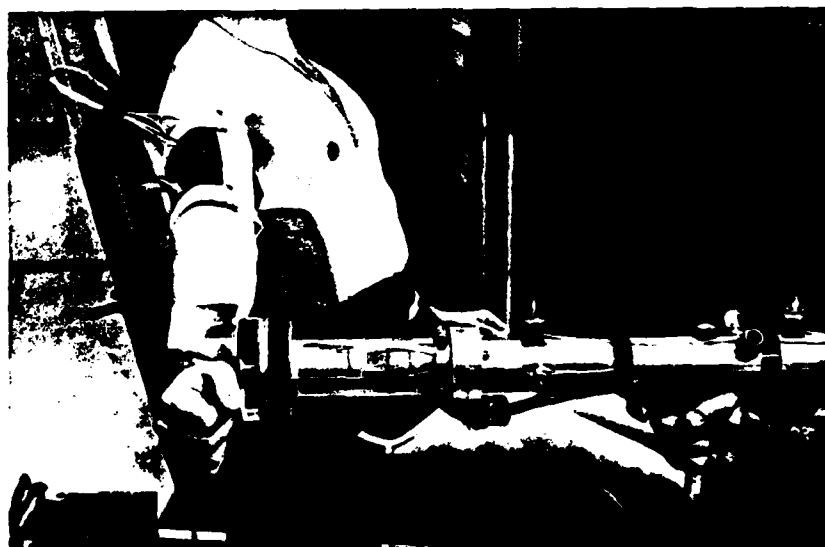


Fig. 36. Force application on the wrist by one of the male subjects (MS1) with fully extended elbow and arm orientation at $\phi = 90^\circ$ & $\theta = 60^\circ$.

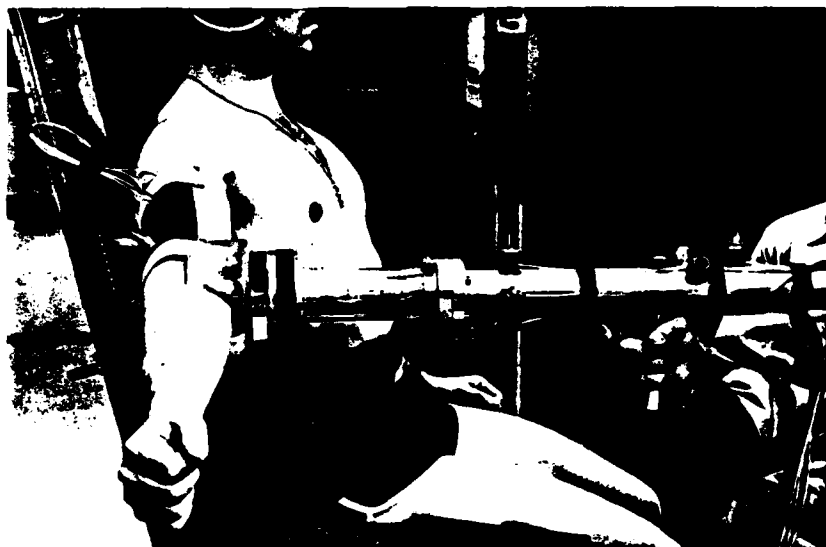


Fig. 37. Force application on the elbow by one of the male subjects (MS1) with fully extended elbow and arm orientation at $\phi = 90^\circ$ & $\theta = 60^\circ$.



Fig. 38. Force application on the wrist by one of the male subjects (MS1) with fully extended elbow and arm orientation at $\phi = 90^\circ$ & $\theta = 90^\circ$.

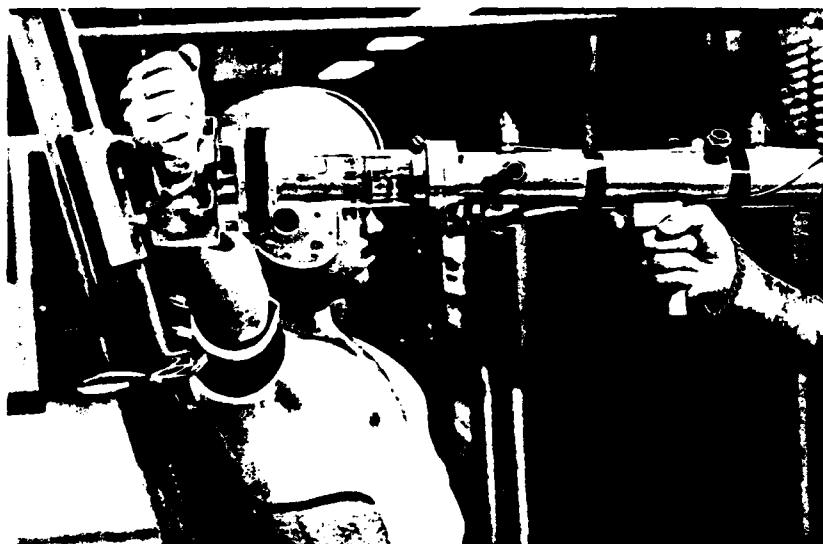


Fig. 39. Force application on the wrist by one of the male subjects (MS1) with fully extended elbow and arm at $\phi = 90^\circ$ & $\theta = 120^\circ$.

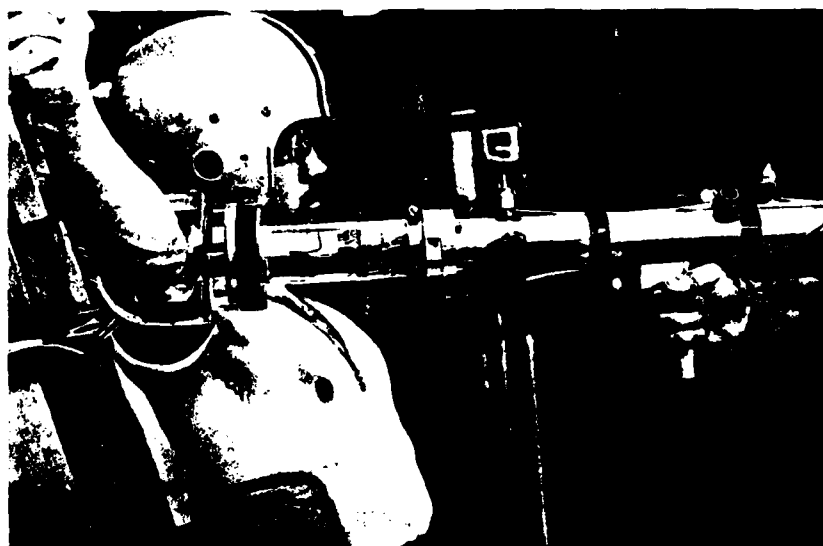


Fig. 40. Force application on the elbow by one of the male subjects (MS1) with fully extended elbow and arm at $\phi = 90^\circ$ & $\theta = 120^\circ$.



Fig. 41. Force application on the wrist by one of the female subjects (FS2) with fully extended elbow and arm orientation at $\phi = 0^\circ$ & $\theta = 30^\circ$.



Fig. 42. Force application on the elbow by one of the female subjects (FS2) with fully extended elbow and arm orientation at $\phi = 0^\circ$ & $\theta = 30^\circ$.



Fig. 43. Force application on the wrist by one of the female subjects (FS2) with fully extended elbow and arm orientation at $\phi = 0^\circ$ & $\theta = 60^\circ$.



Fig. 44. Force application on the wrist by one of the female subjects (FS2) with fully extended elbow and arm orientation at $\phi = 0^\circ$ & $\theta = 90^\circ$.

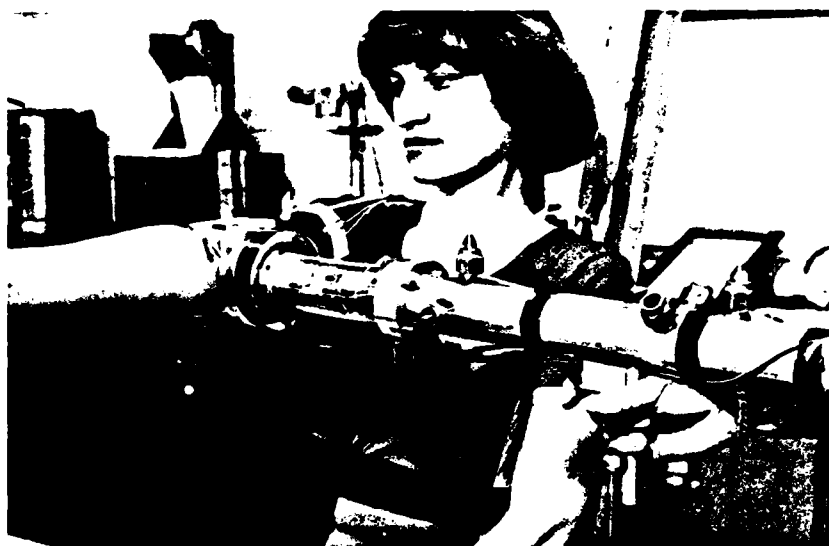


Fig. 45. Force application on the elbow by one of the female subjects (FS2) with fully extended elbow and arm orientation at $\phi = 0^\circ$ & $\theta = 90^\circ$.

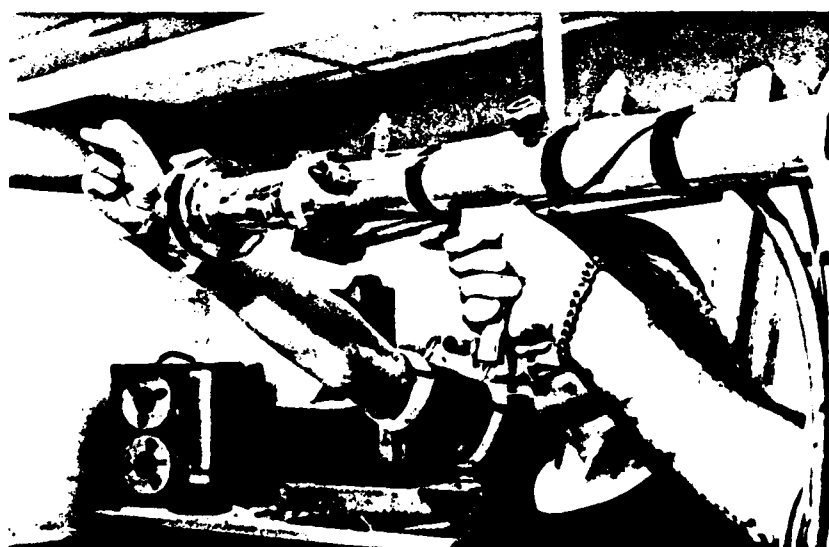


Fig. 46. Force application on the wrist by one of the female subjects (FS2) with fully extended elbow and arm orientation at $\phi = 0^\circ$ & $\theta = 120^\circ$.



Fig. 47. Force application on the wrist by one of the female subjects (FS2) with fully extended elbow and arm orientation at $\phi = 30^\circ$ & $\theta = 30^\circ$.



Fig. 48. Force application on the elbow by one of the female subjects (FS2) with fully extended elbow and arm orientation at $\phi = 30^\circ$ & $\theta = 30^\circ$.



Fig. 49. Force application on the wrist by one of the female subjects (FS2) with fully extended elbow and arm orientation at $\phi = 90^\circ$ & $\theta = 30^\circ$.

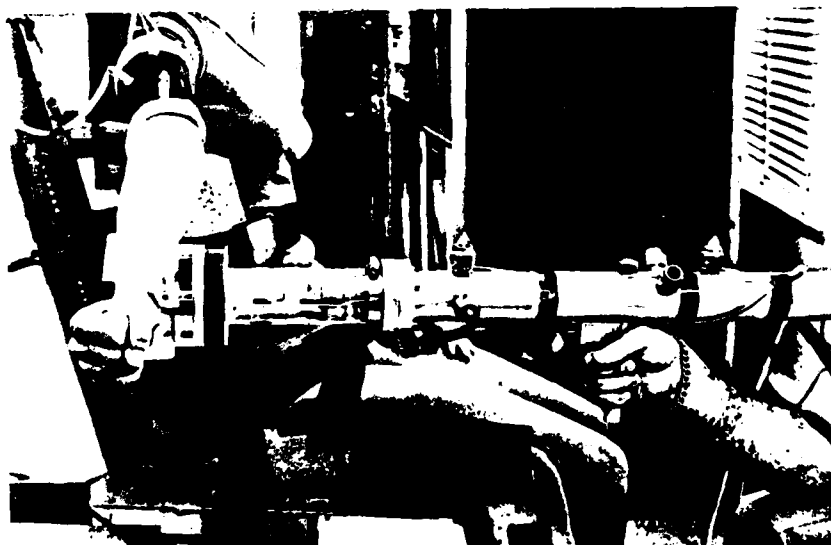


Fig. 50. Force application on the wrist by one of the female subjects (FS2) with fully extended elbow and arm orientation at $\phi = 90^\circ$ & $\theta = 60^\circ$.

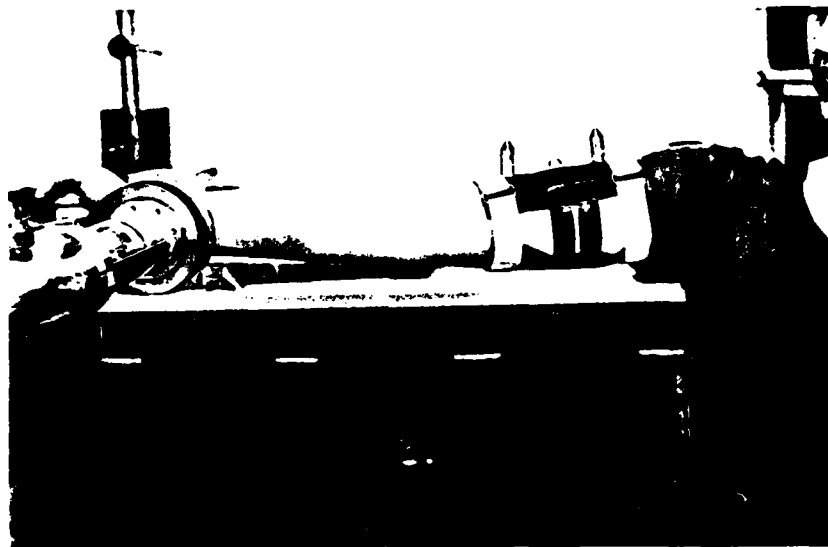


Fig. 51. Force application on the wrist by one of the female subjects (FS2) with fully extended elbow and arm orientation at $\phi = 90^\circ$ & $\theta = 90^\circ$.

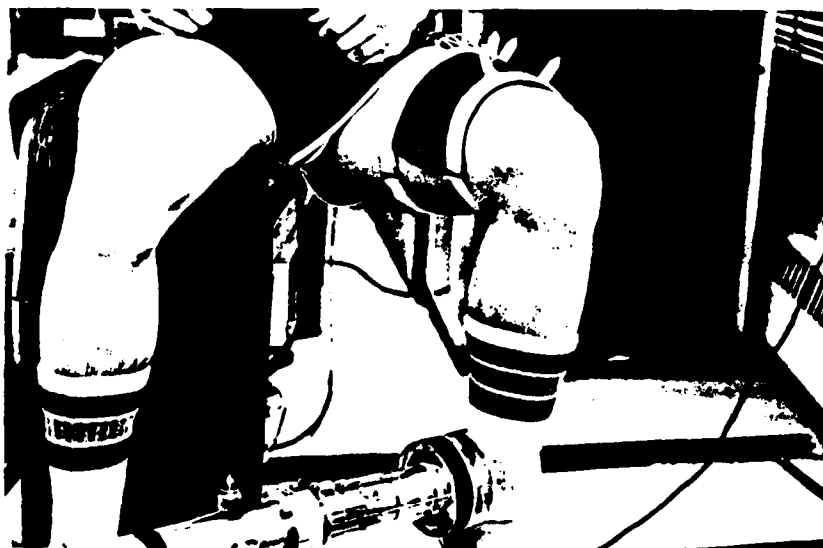


Fig. 52. Force application on the ankle by one of the male subjects (MS1) with knee at 90° flexion and upper leg is 30° abducted.

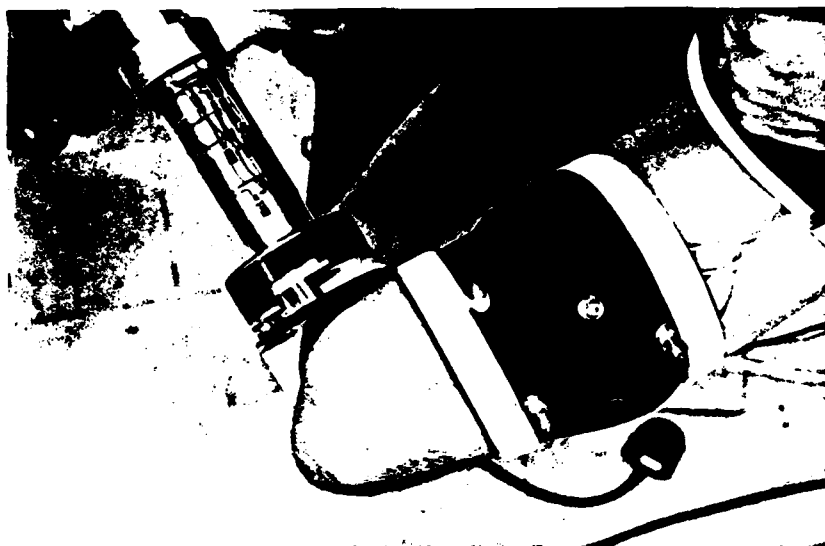


Fig. 53. Force application on the knee by one of the male subjects (MS1) with knee at 90° flexion and upper leg is 30° abducted.

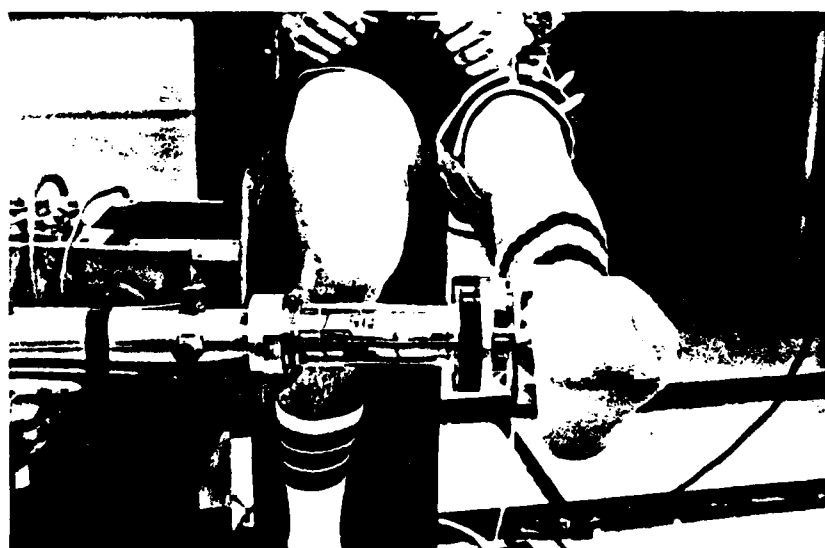


Fig. 54. Force application on the ankle by one of the male subjects (MS1) with fully extended knee and leg is along A-P direction.

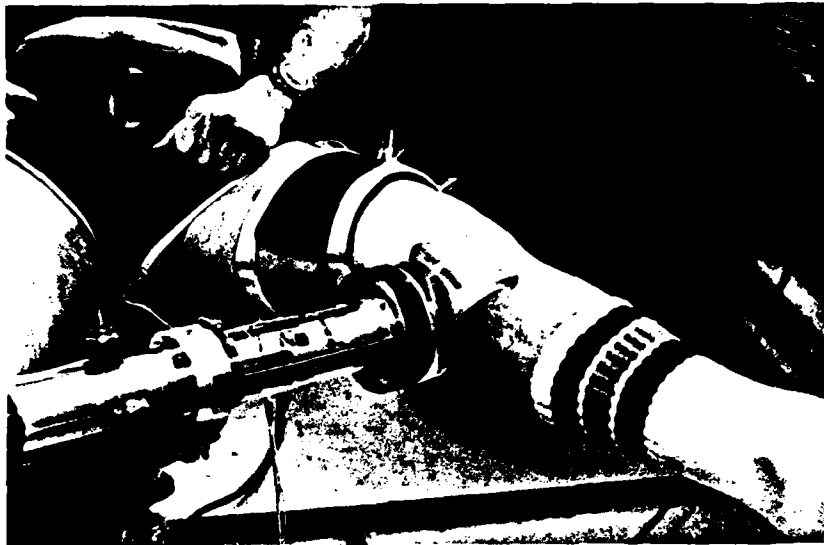


Fig. 55. Force application on the knee by one of the male subjects (MS1) with fully extended knee and leg is 30° abducted.

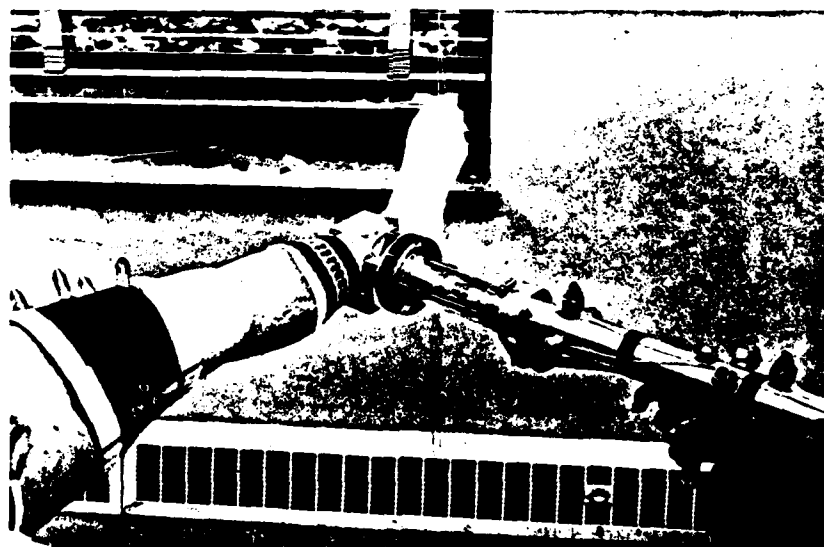


Fig. 56. Force application on the ankle by one of the male subjects (MS1) with fully extended knee and leg is 60° abducted.

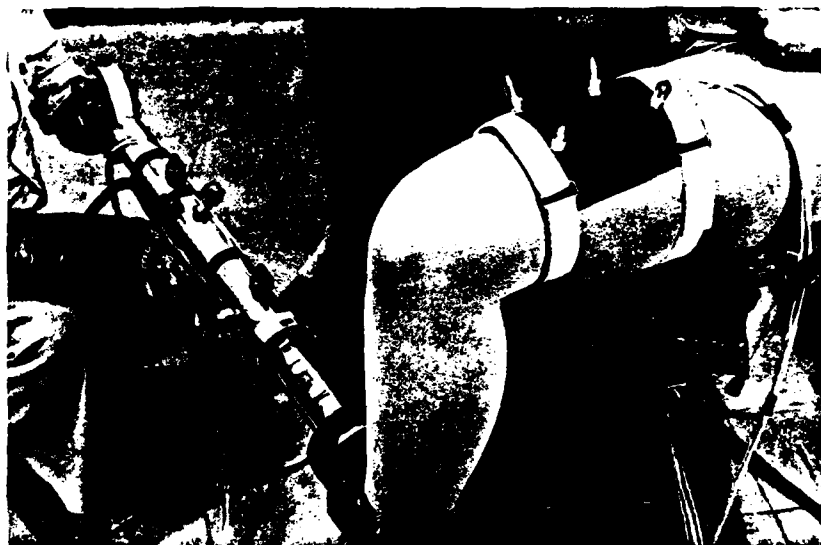


Fig. 57. Force application on the ankle by one of the female subjects (FS3) with knee at 90° flexion and upper leg is 30° abducted.

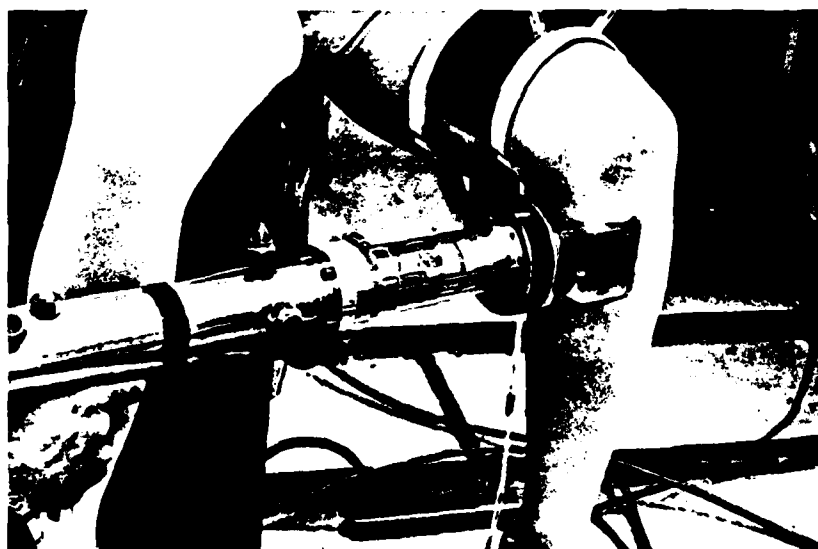


Fig. 58. Force application on the knee by one of the female subjects (FS3) with knee at 90° flexion and upper leg is 30° abducted.

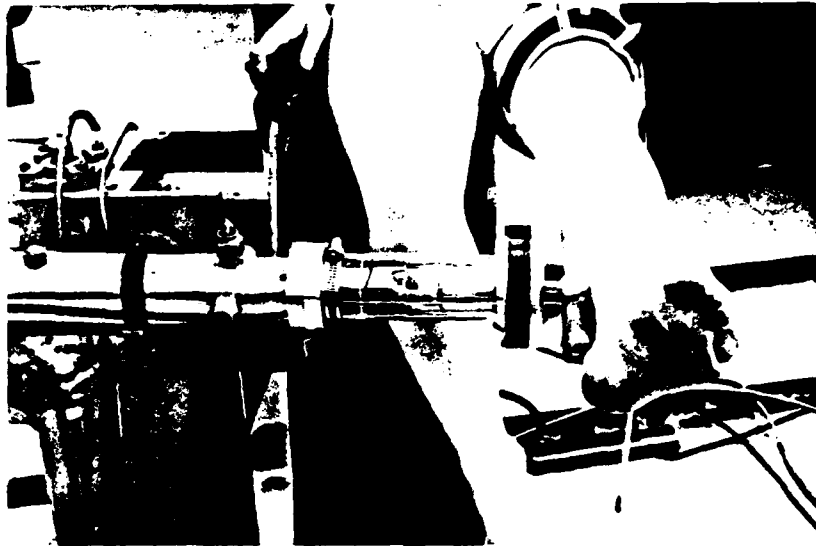


Fig. 59. Force application on the ankle by one of the female subjects (FS3) with fully extended knee and leg is along A-P direction.



Fig. 60. Force application on the knee by one of the female subjects (FS3) with fully extended knee and leg is 30° abducted.



Fig. 61 Force application on the ankle by one of the female subjects (FS3) with fully extended knee and leg is 60° abducted.

of the force applicator which was placed on the lower arm very close to the elbow joint. The same procedure was repeated for the force application on the wrist. These forces were called F_3 and F_4 for the elbow and the wrist application modes, respectively. Figures 20 & 21 show the experiment for determination of the resistance of subjects against separation of lower leg from the seated configuration.

The second set of experiments was designed to determine the active muscle resistance of subjects when their extremities were dislodged from their initial positions. If we use the spherical coordinate angles θ and ϕ to define the orientation of the upper arm or upper leg with respect to the torso we can consider various combinations of θ and ϕ in this set of experiments. Definition of θ and ϕ are given by taking the upper arm and the torso as an example in Fig. 13. Figs. 22-51 show the photographs of the second set of experiments for the upper extremities of both male and female subjects. The photographs in Figs. 52-61 contain views for the second set of experiments conducted on the lower extremities of the

subjects. In all these experiments the isometric force application the subjects was approximately three seconds and the tests were repeated twice in a test session for each subject.

ACTIVE MUSCLE FORCE AND MOMENT RESULTS FOR THE UPPER EXTREMITIES

Active muscle force and moment results for the arm and shoulder are tabulated in Tables I-XIV of Appendix D. In these tables the numerical values for the maximum magnitudes of the active muscle forces of the arms and the corresponding moments at the shoulder joints of the subjects are given for two tests. It should be emphasized that the numerical values given in these tables are the magnitudes of the force and moment vectors having all three components; although, depending upon the direction of the force application one component of the force vector predominates the other two. It should be also recognized that due to static equilibrium, the magnitude of the force vector measured by the force transducer acting on the arm also represents the magnitude of the resistive force vector in the shoulder complex.

Coordinate information obtained from the sonic emitters on the upper arm cuff was utilized to define the shoulder joint location in the following manner. The position of the cuff was first defined with respect to the bony landmarks such as the medial and lateral epicondyles of humerus; then, the long-bone axis of humerus was determined by using coordinate data of the sonic emitters. The shoulder joint point about which the moments were calculated was assumed to be at a prescribed distance on this analytically determined long-bone axis. Note that the definition of shoulder joint is somewhat arbitrary since one can choose an infinite number of points in the "shoulder complex" space.

The term "shoulder complex" refers to the combination of the shoulder joint (frequently identified as the glenohumeral joint) and the shoulder girdle which includes clavicle and scapula and their articulations. Thus, the usage of the term shoulder joint in place of the shoulder complex is somewhat misleading if one does not bear in mind the various components of the region and their articulations. The most striking feature of the

shoulder complex is the presence of four independent articulations among the bones of the shoulder complex, i.e. the clavicle, scapula, humerus, and the thorax. The sternoclavicular joint where the clavicle articulates with respect to the manubrium of sternum, and the acromioclavicular joint where the clavicle meets the acromion process of the scapula are the two articulations of the clavicle. The glenohumeral joint is the ball and socket joint where the humerus articulates with the glenoid cavity of the scapula. The fourth articulation of the shoulder complex is the scapulothoracic joint where the scapula rotates on the thorax. In the true sense, the scapulothoracic articulation is not a joint, but this definition is of some value when describing the movements of the scapula over the thorax.

Figure 62 shows a typical resistive force application by subjects as a function of time. Since the subjects were instructed not to suddenly

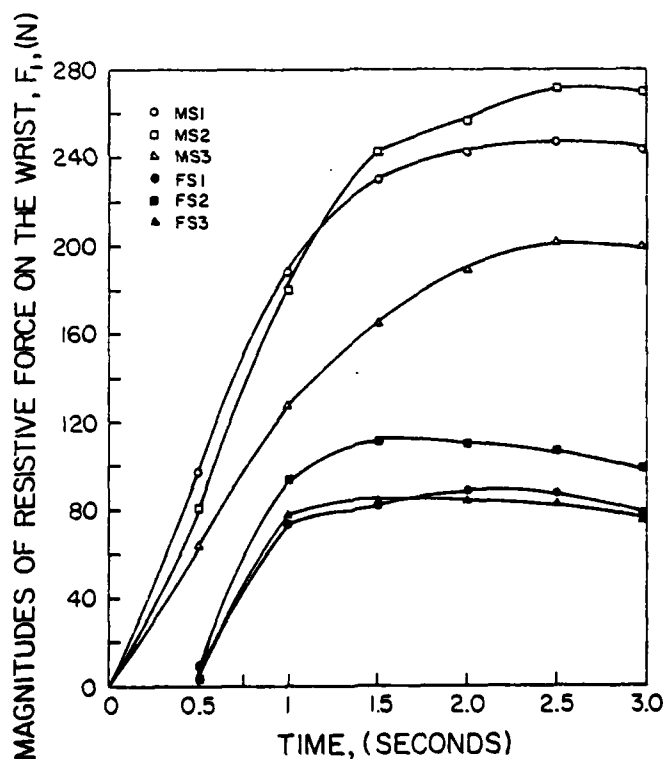


Fig. 62 Resistive muscle force vs. time curves for the force F_1 by the male (MS1, MS2, MS3) and the female (FS1, FS2, FS3) subjects.

make forceful or jerky effort during force application, the maximum values of force occurred at a later time than it was anticipated. The force values tabulated in tables are in units of newtons and they represent the maximum values of curves similar to the ones shown in Fig. 62. The contents of Tables I & II are self-explanatory. The tabulated results in Tables III & IV were obtained from the tests in which the lower arms of the subjects were dislodged from the seat armrest along the lateral direction while the upper arm orientation was kept along the torso. Fig. 63 shows results from Tables III & IV.

In the second set of experiments, in which both the lower and upper arms of the subjects were dislodged from the initial position, the results are quite extensive because of various combinations of θ and ϕ angles which define the orientation of the arm, with fully extended elbow, with respect to the torso. The θ angle refers to the angle between the z-axis of the torso and the long-bone axis of the upper arm (this angle also defines the shoulder flexion-extension in the sagittal plane). The ϕ angle refers to the angle between the projection of the long-bone axis of the upper arm on the xy-plane and the x-axis (the positive and negative values of this angle also define the shoulder abduction and adduction, respectively). The numerical results for the second set of experiments are tabulated in Tables V-XIV and associated plots are given in Figs. 64-69. In Figs. 64-69 various arm positions as a function of θ are considered in the planes of $\phi = 0^\circ$ (the sagittal plane), $\phi = 30^\circ$, $\phi = 60^\circ$, $\phi = 90^\circ$ (the frontal plane) and $\phi = 120^\circ$. In Figs. 64, 65, & 66 the angle $-\theta$ along with $\phi = 0^\circ$ defines the shoulder extension positions in the sagittal plane. Figures 64-69 can be put in three categories. In the first category, the maximum values of resistive muscle force, for the external force applications on the elbow, are plotted for various arm positions for both male and female subjects (Figs. 64 & 67). In the second category, the maximum values of resistive muscle force by the male subjects against the external force applications on the elbow and the wrist at various arm positions are plotted for various arm positions (Figs. 65, & 68). In the third category, the maximum values of resistive muscle force by the female subjects against the external force applications on

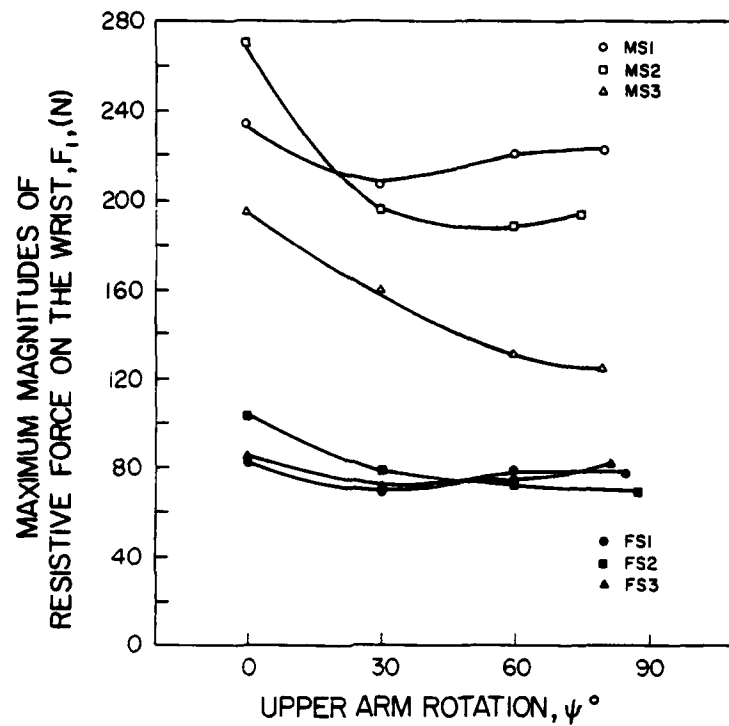


Fig. 63 Maximum values of resistive muscle force by the male (MS1, MS2, MS3) and the female (FS1, FS2, FS3) subjects at various lower arm positions while the upper arm is rotated by keeping its orientation along the torso.

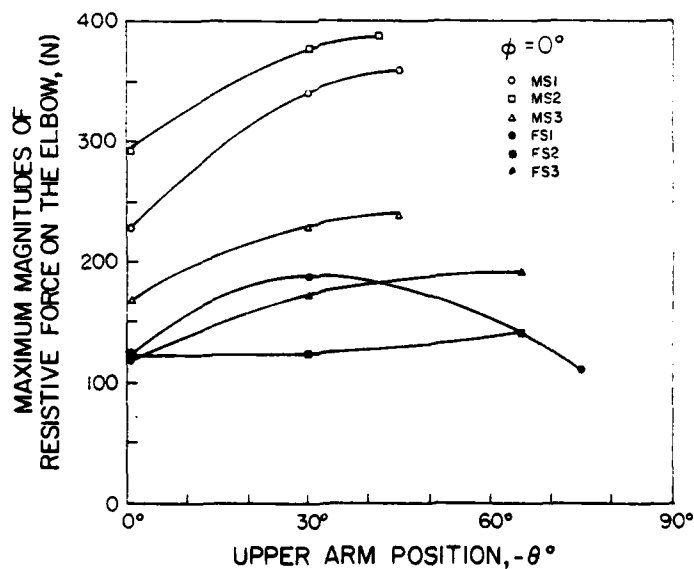


Fig. 64 Maximum values of resistive muscle force by the male (MS1, MS2, MS3) and the female (FS1, FS2, FS3) subjects at various arm positions in $\phi = 0^\circ$ plane.

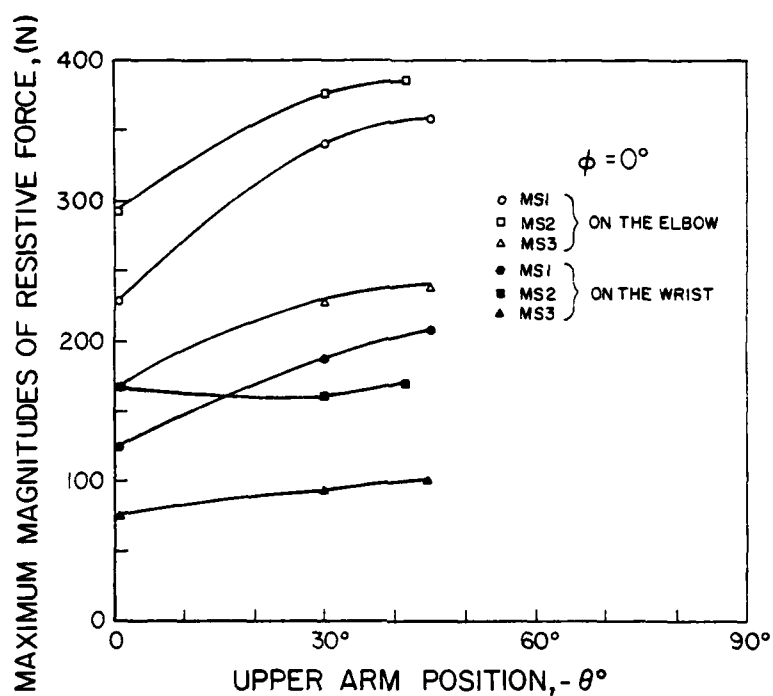


Fig. 65 Maximum values of resistive muscle force by the male subjects against the external force applications on the elbow and the wrist at various arm positions in $\phi = 0^\circ$ plane.

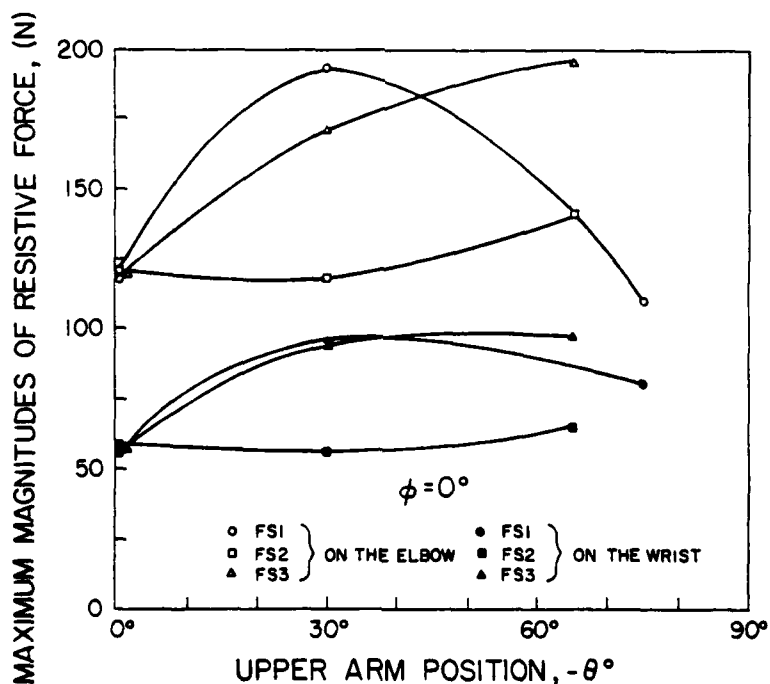


Fig. 66 Maximum values of resistive muscle force by the female subjects against the external force applications on the elbow and the wrist at various arm positions in $\phi = 0^\circ$ plane.

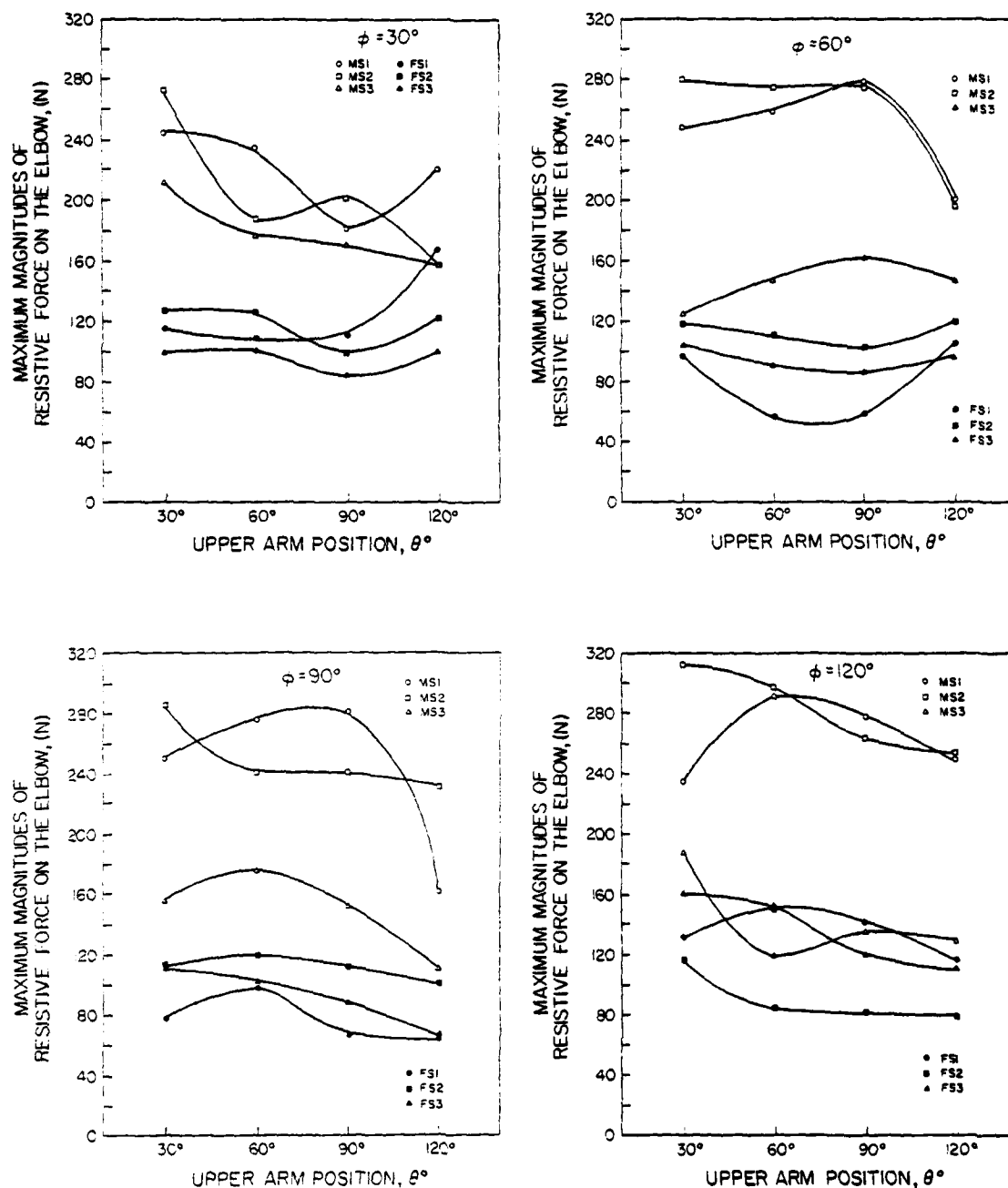


Fig. 67 Maximum values of resistive muscle force by the male (MS1, MS2, MS3) and the female (FS1, FS2, FS3) subjects against the external force applications on the elbow at various arm positions in $\phi = 30^\circ, 60^\circ, 90^\circ$, and 120° planes.

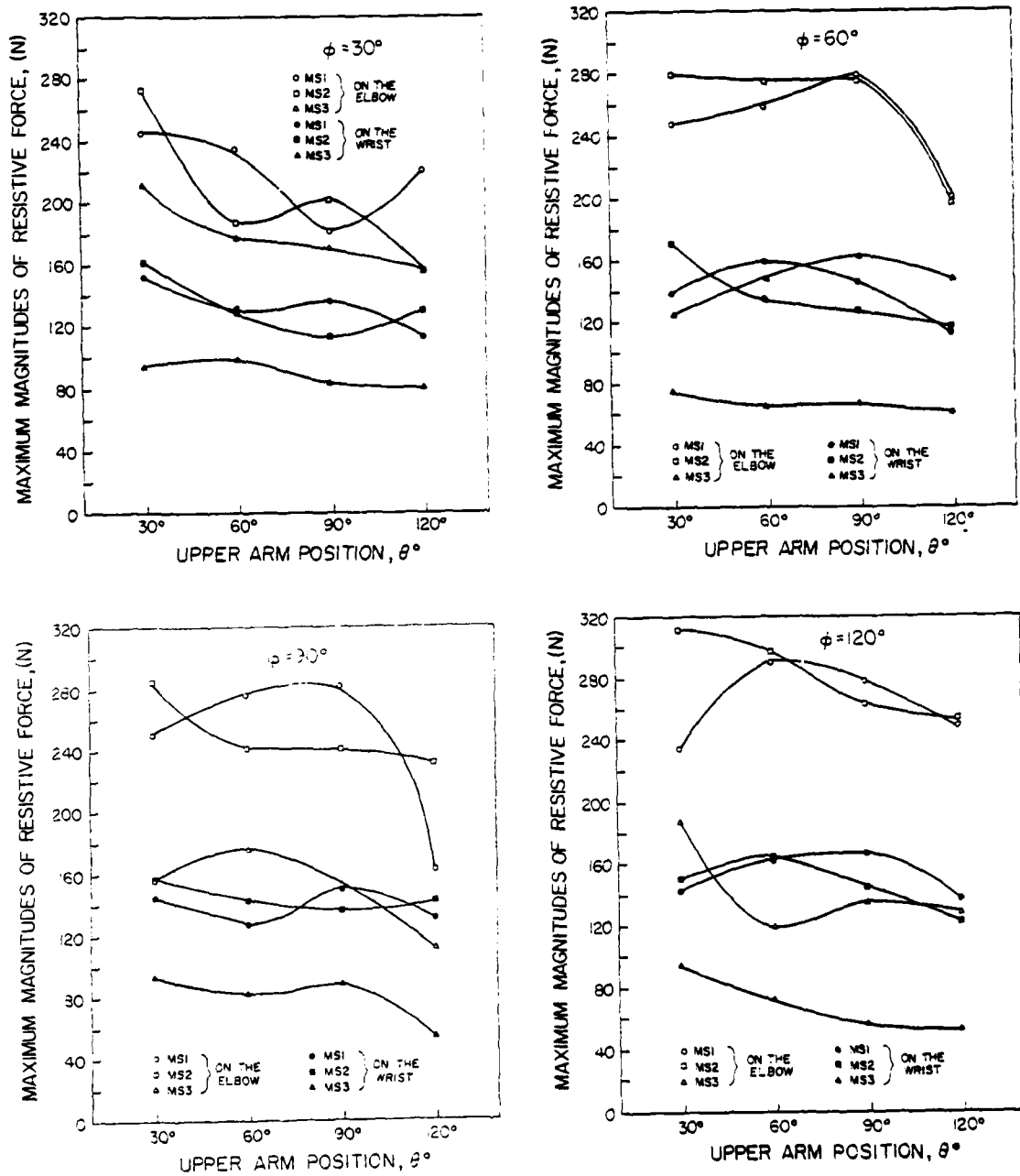


Fig. 68 Maximum values of resistive muscle force by the male subjects against the external force applications on the elbow and the wrist at various arm positions in $\phi = 30^\circ, 60^\circ, 90^\circ$, and 120° planes.

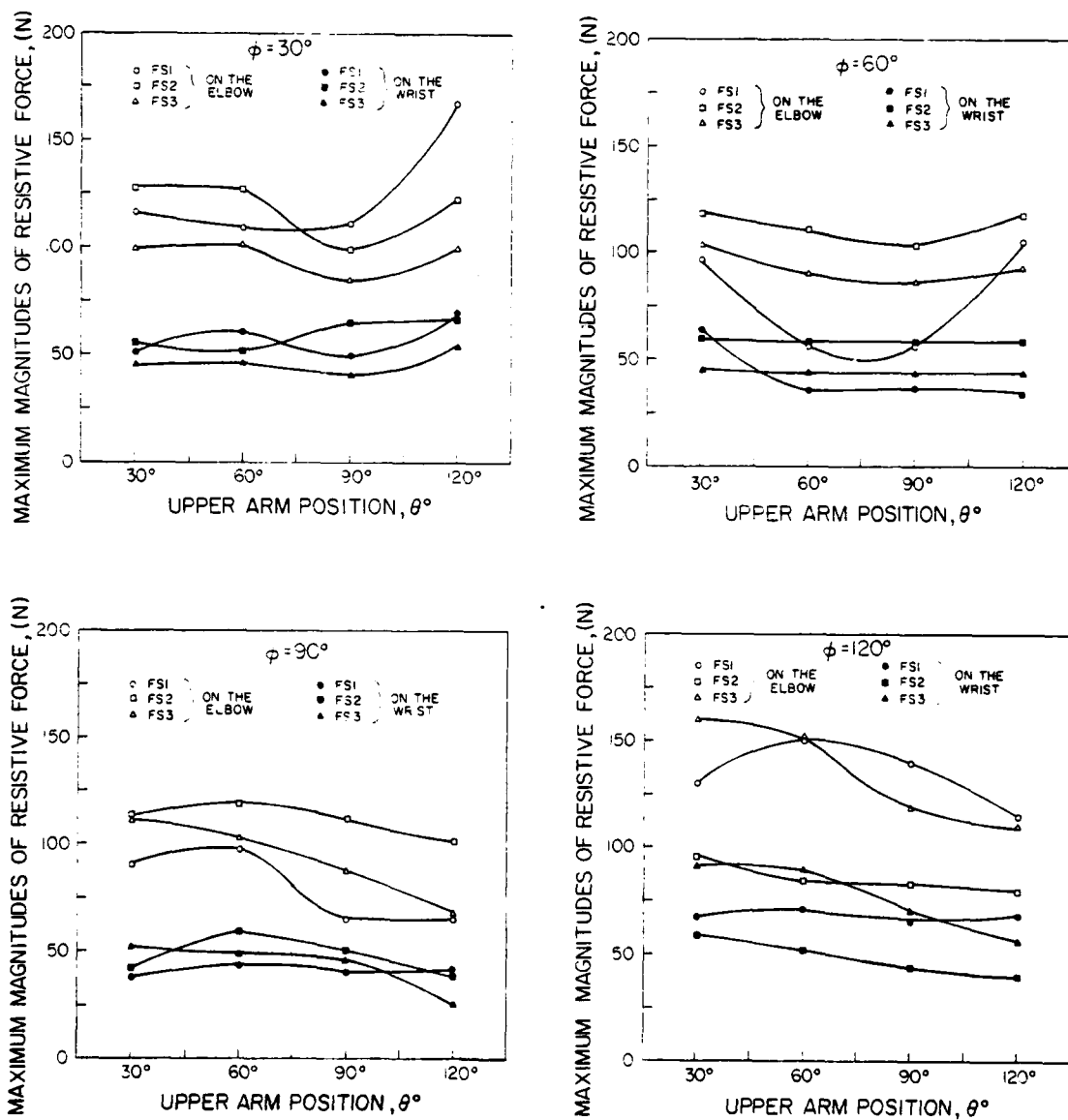


Fig. 69 Maximum values of resistive muscle force by the female subjects against the external force applications on the elbow and the wrist at various arm positions in $\phi = 30^\circ, 60^\circ, 90^\circ$, and 120° planes.

the elbow and the wrist at various arm positions are plotted (Figs. 66, & 69).

ACTIVE MUSCLE FORCE AND MOMENT RESULTS FOR THE LOWER EXTREMITIES

The maximum magnitudes of the active muscle forces of the leg and the corresponding moments at the hip joint are tabulated in Tables XV-XXVIII of Appendix E. Tests were conducted for various combinations of the spherical coordinates θ and ϕ , describing the position of the upper leg in relation to the torso with the knee flexed and the knee locked. Tests were repeated twice for each subject. The numerical values in the tables are the maximum magnitudes of the active muscle forces of the leg and the corresponding hip joint moments for the two tests. Force applications by the subjects were at the knee and just above the ankle.

The orientation of the upper leg with respect to the torso was determined in an analogous manner to the upper extremity orientation, as discussed above. The θ angle refers to the angle between the z-axis of the torso and the femoral axis ($\theta = 90^\circ$ for seated position; $\theta = 0^\circ$ for standing position). The angle ϕ measures the projection of the femoral axis on the xy plane and the x-axis.

The moments were calculated about a point in the hip which was defined similarly to the moment center of the shoulder complex. The femoral axis was determined by obtaining the coordinates of two bony landmarks of the femur: the lateral margin of the femoral condyle and the greater trochanter. Using the coordinates from the elastic cuff, an axis was defined. The moment center was assumed to be a measured distance from the elastic cuff on this axis. This gives an arbitrary point since any one of an infinite number of points could be chosen.

Figure 70 shows the resistive force applications by both male and female subjects, for the knee flexed and the knee locked configurations. On the abscissa of Fig. 70 the positions start from an initial seated position ($\theta = 90^\circ$, $\phi = 0^\circ$) and include various leg positions corresponding to dislodging the leg along the lateral direction. Maximum dislodged position is taken as the subject's indicated limit. In addition to the

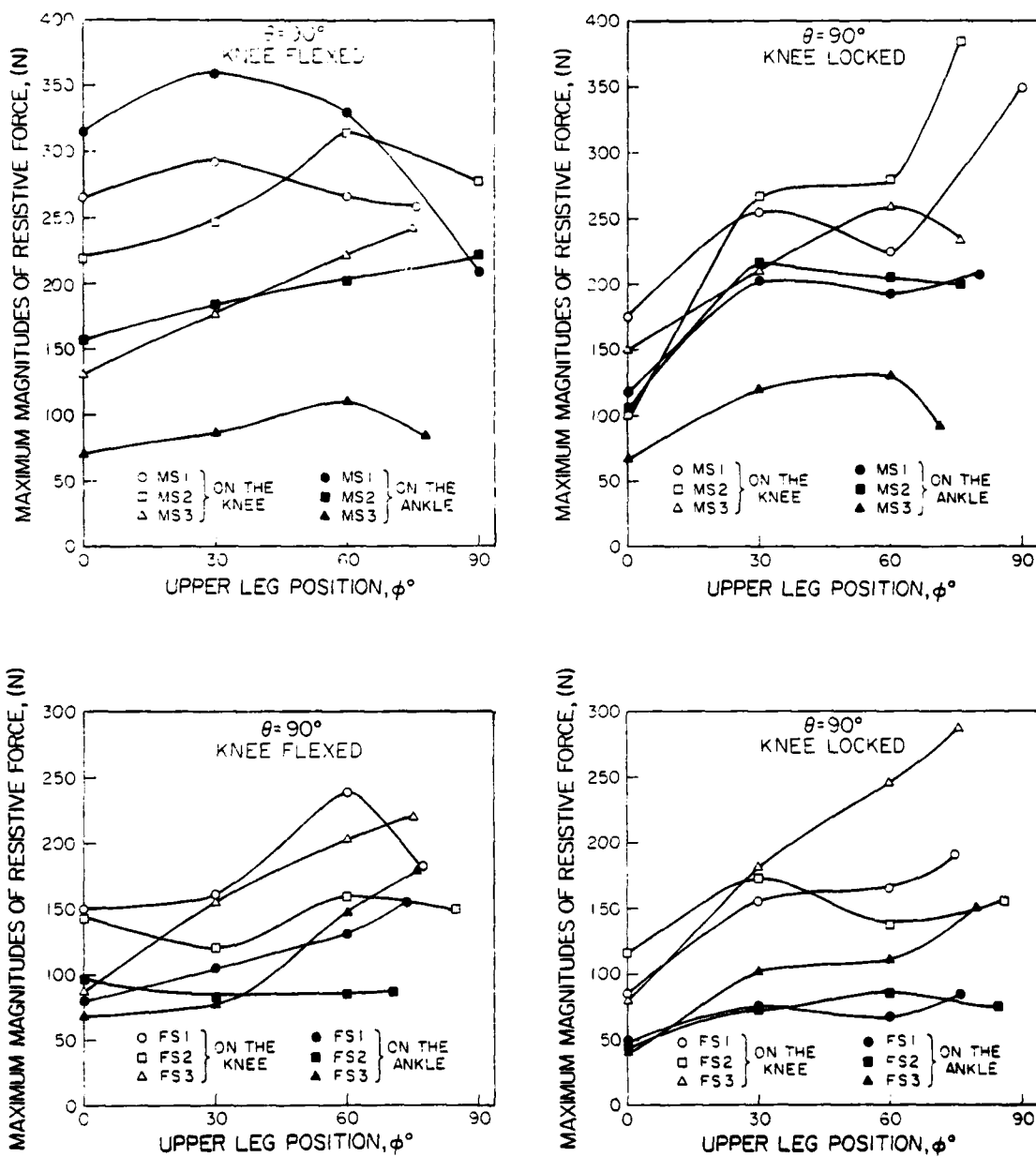


Fig. 70 Maximum values of resistive muscle force by the male (MS1, MS2, MS3) and the female (FS1, FS2, FS3) subjects for the knee flexed and the knee locked configurations for various lateral positions of the upper leg at $\theta = 90^\circ$.

seated configuration, tests were conducted for various positions of θ , with varying ϕ angles corresponding to dislodging of the leg along the lateral direction. Figures 71 and 72 show the maximum magnitudes of resistive muscle force for constant θ values of 120° and 40° respectively. Finally, Fig. 73 depicts the maximum magnitudes of resistive muscle force for two laterally dislodged positions of the leg for θ equal to zero.

RESULTS ON THE FORCED KINEMATIC MOTION OF THE SHOULDER COMPLEX

In addition to the active force/moment tests which have been discussed previously, a number of tests have been performed which involve the passive resistance of the shoulder complex to forced, drawer-type motions. In these tests the humerus is forced axially for a variety of upper arm orientations and the resistive force versus the joint center displacement is monitored. Representative results for a male subject are presented in Figs. 77-80. However, before we present the test results, we will first discuss the testing procedure.

Although the forced drawer tests are similar to the type of testing done previously, a number of changes have been made in the experimental set-up and in the data analysis and acquisition schemes. These changes were made for the following reasons:

- 1) To provide redundant data for the kinematic analysis. (More emitters are used to provide additional data in cases where certain emitters are blocked from the microphone/sensor board.)
- 2) To improve the accuracy of the data acquired.
- 3) To increase the ease of data acquisition.

An overall discussion of the experimental procedure will serve to elaborate on the effect of the hardware additions and software revisions on these tests.

As previously explained, the microphone/sensor board axis system and the fixed body axis system were always described relative to a laboratory axis system by the physical measurement of the angular orientation of the restraint chair and the microphone board with respect to the laboratory (inertial) axis system. These data were tedious to collect, cumbersome to

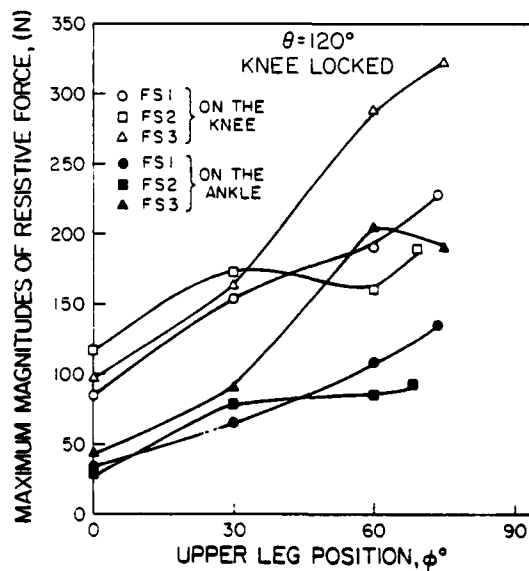
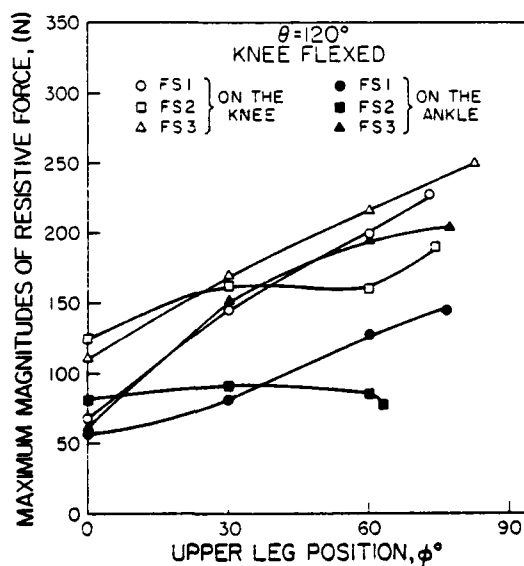
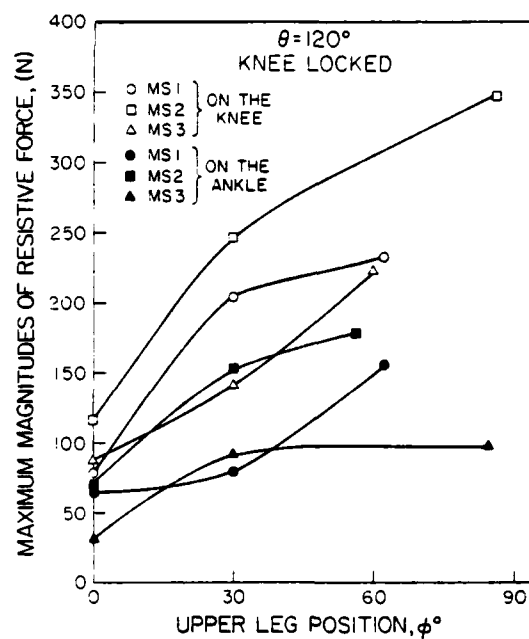
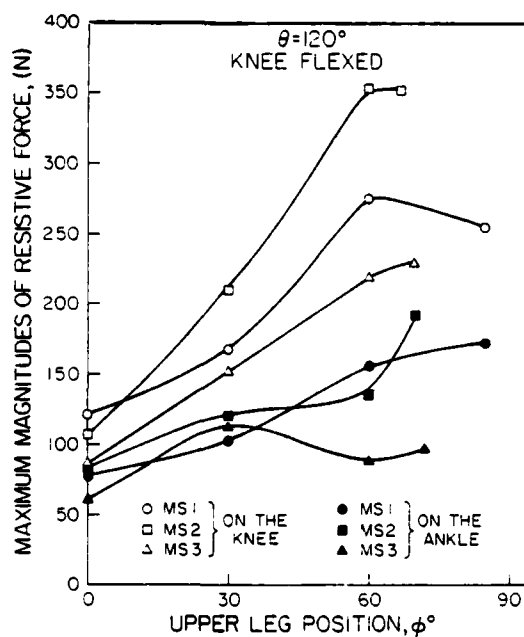


Fig. 71 Maximum values of resistive muscle force by the male (MS1, MS2, MS3) and the female (FS1, FS2, FS3) subjects for the knee flexed and the knee locked configurations for various lateral positions of the upper leg at $\theta = 120^\circ$.

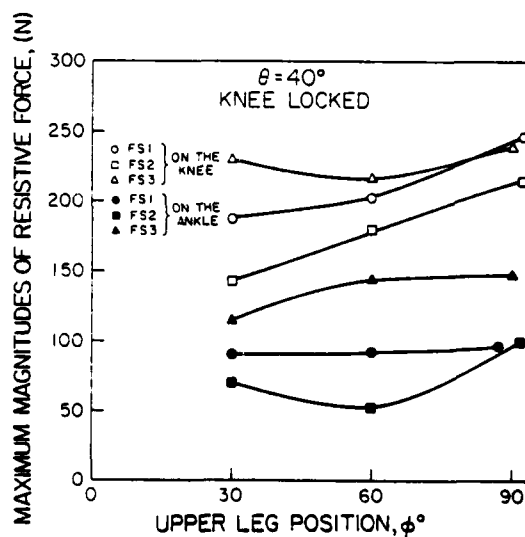
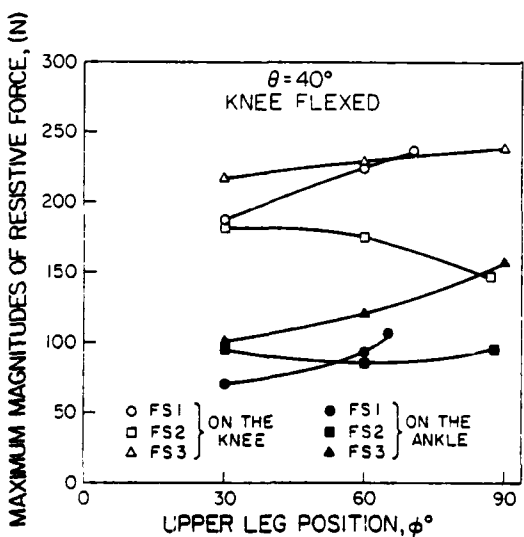
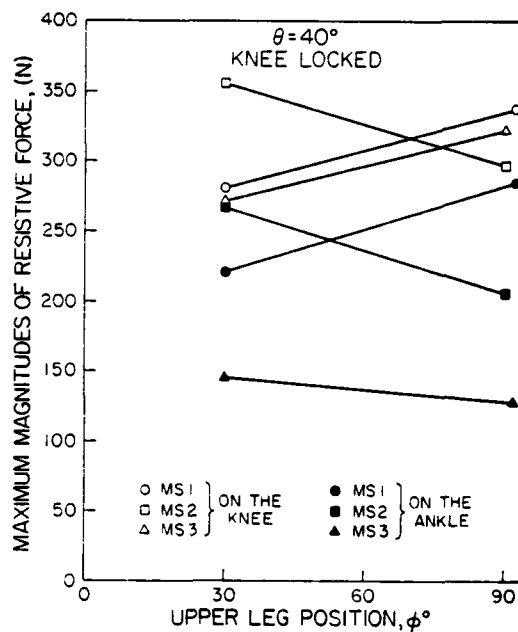
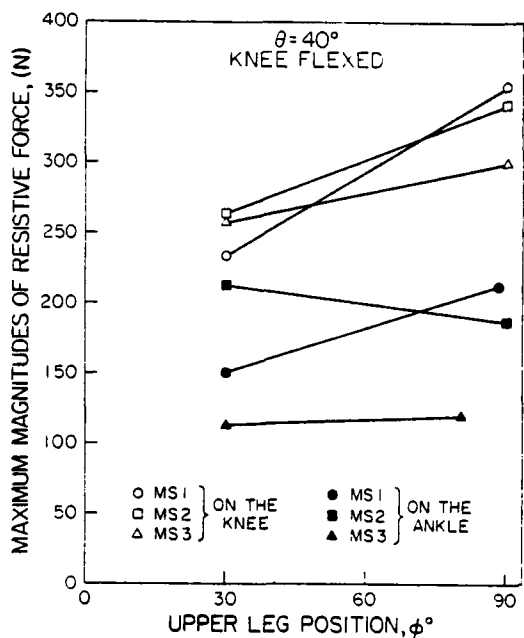


Fig. 72 Maximum values of resistive muscle force by the male (MS1, MS2, MS3) and the female (FS1, FS2, FS3) subjects for the knee flexed and the knee locked configurations for various lateral positions of the upper leg with $\theta = 40^\circ$.

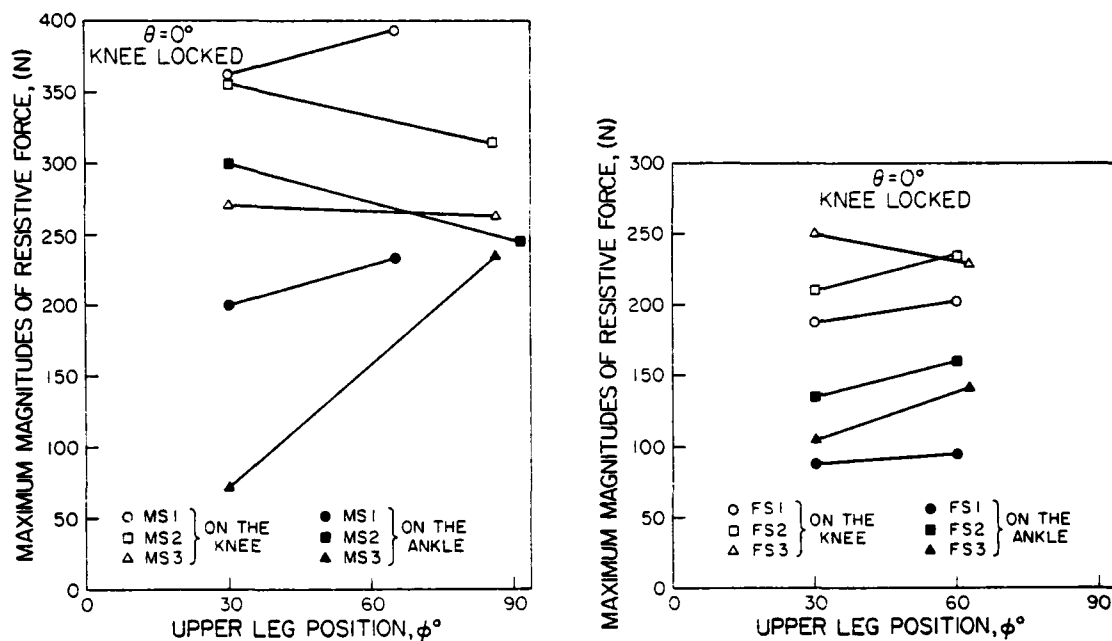


Fig. 73 Maximum values of resistive muscle force by the male (MS1, MS2, MS3) and the female (FS1, FS2, FS3) subjects for the locked knee configurations and for two lateral positions of the upper leg with $\theta = 0^\circ$.

input in the data analysis program, and subject to a degree of "judgment" by the experimenter during the actual measurement.

In order to increase both accuracy and the ease of positional data acquisition, a relative axes locator device (RALD) was developed. The RALD is shown in Fig. 74. The RALD uses four sonic emitters arranged in a prismatic fashion to describe an axis system and coordinate location in space relative to the microphone board axis system. During any test set-up, the RALD is aligned with the fixed body axis system and the sonic emitter data are used to calculate the direction cosine matrix which describes the fixed body axis system relative to the microphone board axis system. Inversely, the board axis system can always be determined with respect to the fixed body axis system from these data. Therefore, there is no need to measure any gross board or chair angular orientations. This approach is obviously easier and more flexible from a data acquisition point of view. In addition, the accuracy of the calculated data is

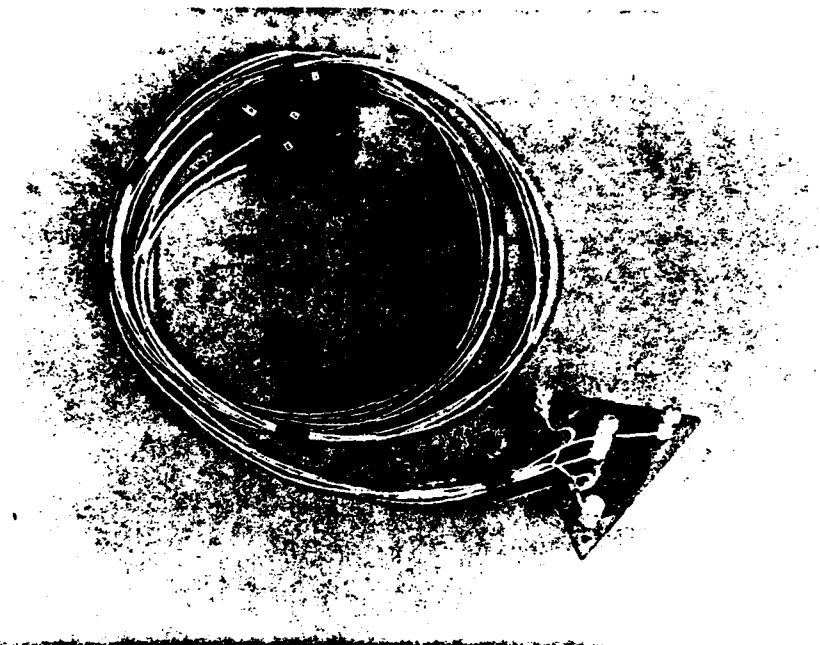


Fig. 74 Relative axes locator device (RALD).

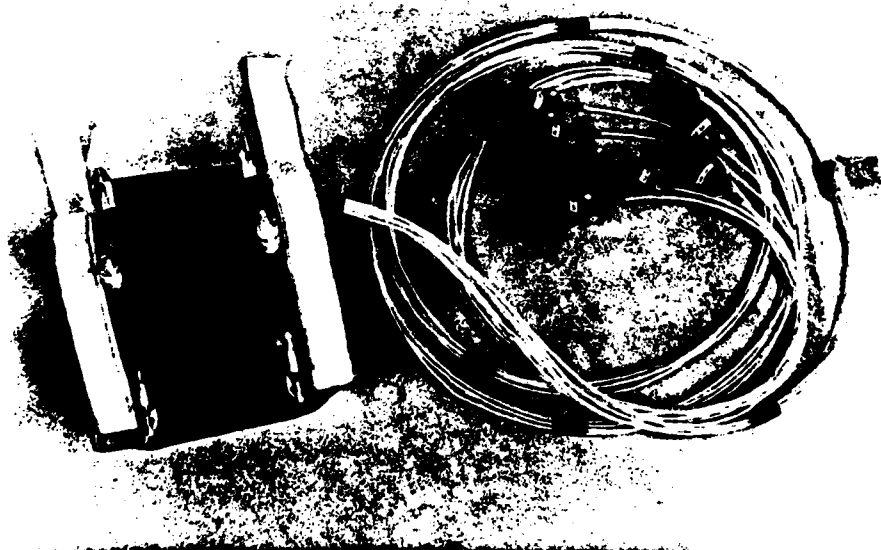


Fig. 75 Upper arm cuff fitted with six sonic emitters.

increased since multiple physical length and angle measurements are eliminated along with their more numerous transformation matrix calculations. The laboratory axis system is eliminated and the fixed body system is always established as the "inertial" axis system. Physical dimensions, which are input in the data analysis program, transfer the location of the fixed body center from the RALD origin to its actual position.

Another device which was designed to increase the data acquisition capabilities was a new arm cuff which has six emitters instead of the original four. This was made possible by the procurement of an additional digitizer multiplexor unit which expanded the previous capability to 15 emitters. The new cuff, which is shown in Fig. 75, eliminates many problematic situations in which emitters are blocked from sensors on the board due to the kinematics of the test involved. Since only three emitters are actually needed to describe the arm's location and orientation,



Fig. 76 Subject in position for superior-inferior drawer tests.

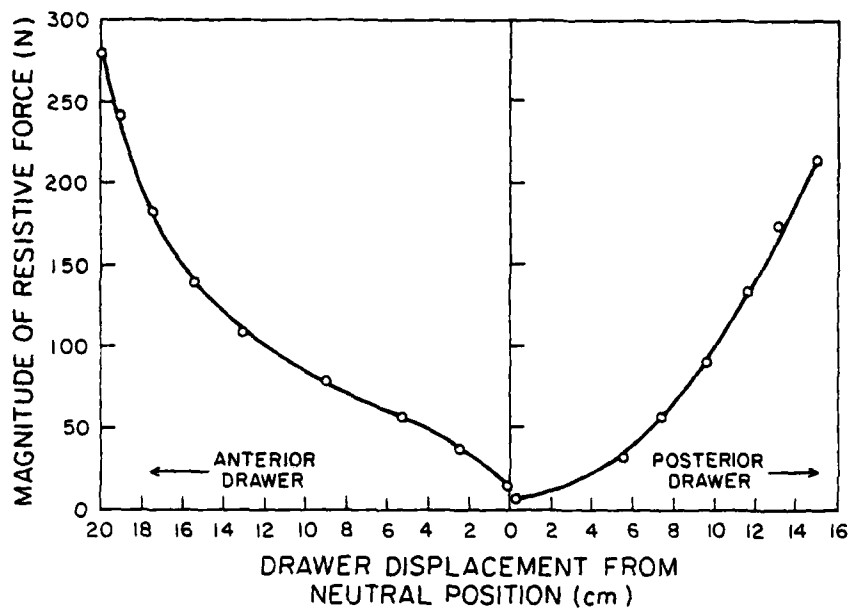


Fig. 77 Resistive force versus drawer displacement for $\theta = 90^\circ$, $\phi = 0^\circ$ upper arm orientation.

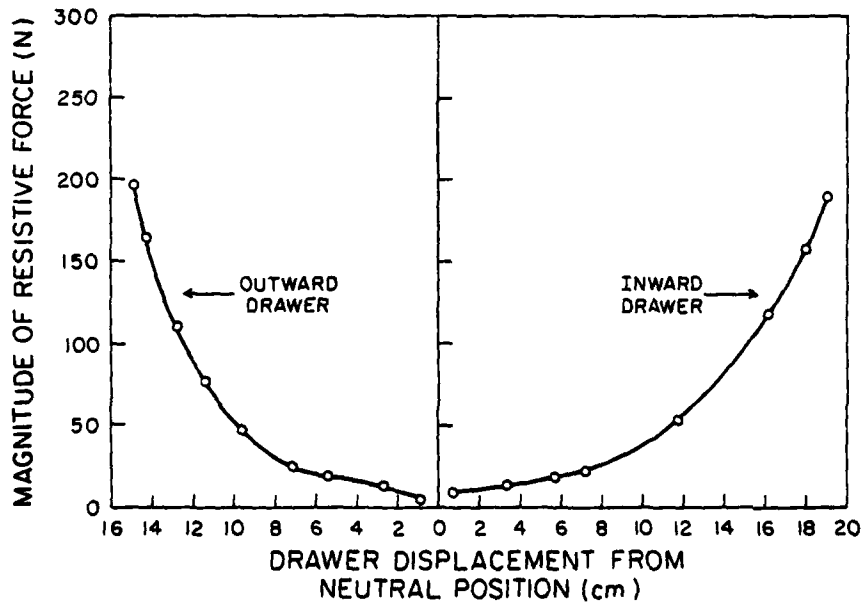
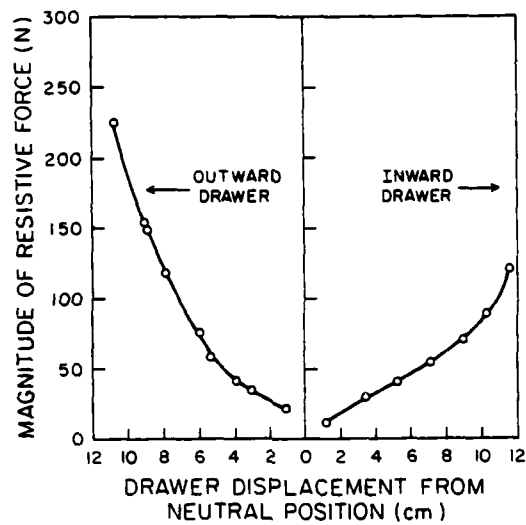
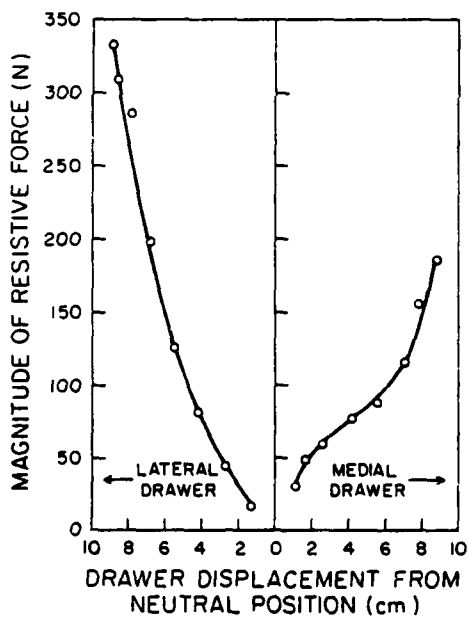


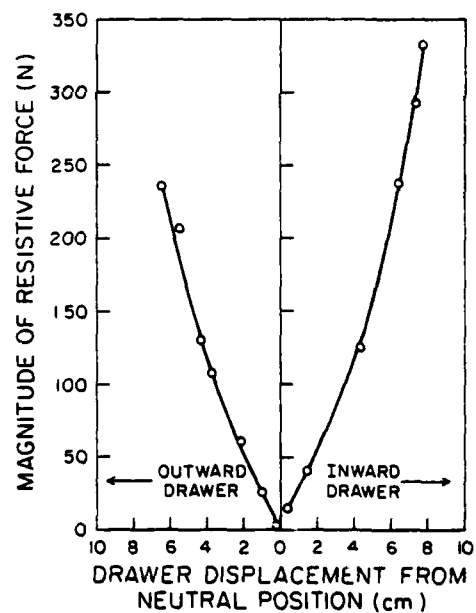
Fig. 78 Resistive force versus drawer displacement for $\theta = 90^\circ$, $\phi = 30^\circ$ upper arm orientation.



(a)



(b)



(c)

Fig. 79 Resistive force versus drawer displacement for a) $\theta = 90^\circ$, $\phi = 60^\circ$, b) $\theta = 90^\circ$, $\phi = 90^\circ$, and c) $\theta = 90^\circ$, $\phi = 115^\circ$ upper arm orientation.

three emitters can be blocked from microphone "view" without losing needed kinematic data. Of course, the appropriate computer software revisions were made to accommodate these hardware additions.

For the actual tests, the subject was secured in the chair restraint system which allows unimpeded movement of the shoulder complex. With the subject's elbow flexed to 90° , the force applicator was fixed to the arm by means of a rigid cuff extension so that the force could be applied along the humeral axis. Fig. 76 shows the subject in position for the $\theta = 0^\circ$ drawer tests. In addition, the rigid cuff placed the shoulder in a position of approximately 25° of medial rotation. This position is near the midpoint of the shoulder medial-lateral range and is a comfortable position for the subject. The test results shown in Figs. 77-79 were for drawer motions with humeral axis orientations of $\theta = 90^\circ$ and $\phi = 0^\circ, 30^\circ, 60^\circ, 90^\circ$, and 115° . Fig. 80 shows the results of a $\theta = 0^\circ$ test. For each

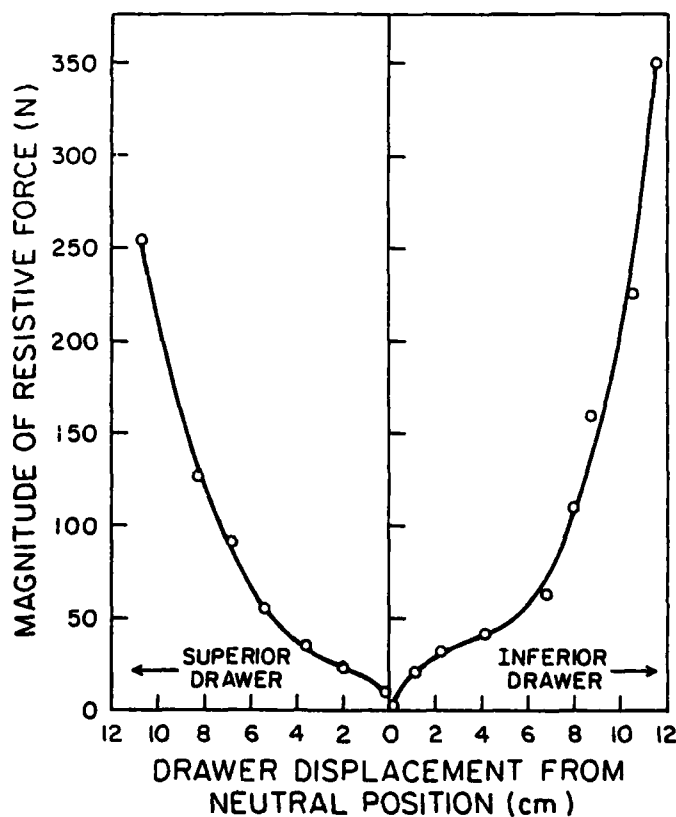


Fig. 80 Resistive force versus drawer displacement for the superior-inferior drawer ($\theta = 0^\circ$).

drawer orientation, the subject was asked to allow his shoulder complex to assume its most comfortable, "natural" position. This established the neutral position for each drawer. The test results are plots of force magnitude along the force applicator axis versus displacement of the humeral head along this same axis. In each case, the subject was instructed to avoid muscular resistance, and each test was terminated when the subject expressed discomfort. The rate of displacement for each test was maintained between 2-3 centimeters per second.

CONCLUDING REMARKS

Based on the numerical results presented in this report, several concluding remarks can be made on the active muscle force response of the upper and lower extremities of the human body to the externally applied forces:

1. On the average for the male subjects the maximum magnitudes of forces necessary to separate the lower arm, from the initial seat armrest position, along the mediolateral direction (F_1) is higher than that of inferior-superior direction (F_2); whereas, for the female subjects the results indicate F_2 is larger than F_1 . In fact, average F_1 to F_2 ratios are found to be 1.35 for males and .84 for females. In addition, the average value of the maximum magnitudes of F_1 and F_2 for male subjects are 2.58 and 1.60, respectively, times those of the female subjects.

2. For the D-ring force simulation case the average value of the maximum magnitudes of the resistive forces for the male subjects is about 2.69 times that of the female subjects. Similar male to female subject comparison gives the ratios of 2.54 and 2.64 for the forces F_3 and F_4 , respectively, of the face curtain force simulation experiment.

3. In the experiments for which the lower arm of the subject was dislodged from the seat armrest along the lateral direction while the upper arm was kept along the torso, the results for both male and female subjects show only small variations on the average value of the maximum magnitudes of force F_1 as a function of the laterally rotated lower arm position. The highest F_1 values for all subjects occur for the initial

lower arm position. The male vs. female subject comparison ratios for the F_1 forces range from 2.34 to 2.56 in this case.

4. For the shoulder extension positions in the sagittal plane, the average values of the maximum magnitudes of the resistive muscle forces, against the external force applications on the elbow, steadily increase from 229 N at $\theta = 0$ to 327 N at the maximum extension position for the male subjects. However, for the female subjects, the same resistive force starts with 120 N at $\theta = 0$ and increases to 160 N at $\theta = -30^\circ$ and decreases to 149 N at the maximum extension limit. In addition, for the same shoulder extension positions in the sagittal plane, the ratios of the average values of the maximum magnitudes of the resistive forces against the force application on the elbow to that of the wrist range from 1.89 to 2.08 for the male subjects, and 1.83 to 2.08 for the female subjects.

5. The average values of the maximum magnitudes of the resistive forces, against the external force applications on the elbow, for the dislodged positions of the arm with a fixed value of $\phi = 30^\circ$, start with 213 N at $\theta = 30^\circ$ and decrease steadily to 179 N at $\theta = 120^\circ$ for the male subjects; for the female subjects, the same quantity starts with 115 N at $\theta = 30^\circ$, exhibits a gradual decrease to 98 N at $\theta = 90^\circ$, and subsequently increase to 146 N at $\theta = 120^\circ$. The ratios of the average values of the maximum magnitudes of the resistive forces against the external force applications on the elbow to that of the wrist range from 1.58 to 1.68 for the male subjects, and 1.96 to 2.33 for the female subjects.

6. The average values of the maximum magnitudes of the resistive forces, against the external force applications on the elbow, for the dislodged positions of the arm with a fixed value of $\phi = 60^\circ$, start with 218 N at $\theta = 30^\circ$ and shows a gradual increase to 240 N at $\theta = 90^\circ$ and subsequent drop to 182 N at $\theta = 120^\circ$ for the male subjects; for the female subjects, the same quantity starts with 107 N at $\theta = 30^\circ$, decreases gradually to 82 N at $\theta = 90^\circ$ and shows an increase to 106 N at $\theta = 120^\circ$. The ratios of the average values of the maximum magnitudes of the resistive forces against the external force applications on the elbow to that of the wrist range from 1.71 to 2.12 for the male subjects, and 1.76 to 2.39 for the female subjects.

AD-A111 551

OHIO STATE UNIV RESEARCH FOUNDATION COLUMBUS
LONG BONE AND JOINT RESPONSE TO MECHANICAL LOADING. (U)
NOV 81 A E ENGIN

F/6 6/16

F49620-79-C-0110

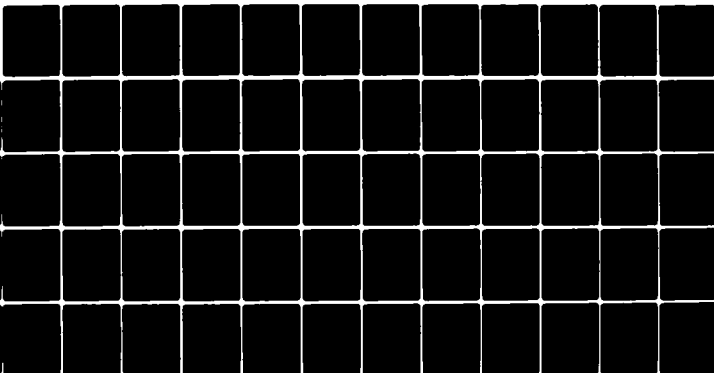
UNCLASSIFIED

AFOSR-TR-82-0013

NL

2 4 2

21 601



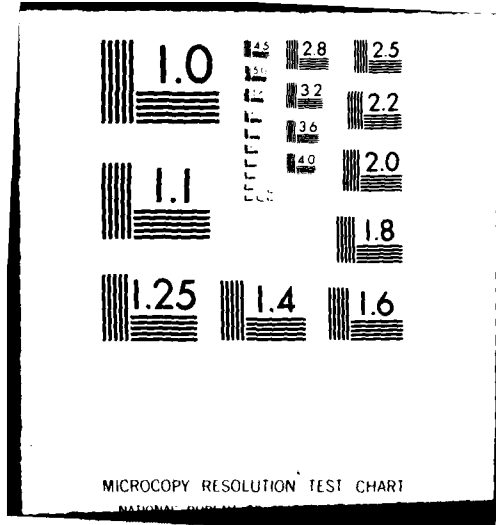
END

DATE

FILED

3-82

DTIC



7. The behavior of the average values of the maximum magnitudes of the resistive forces, against the external force applications on the elbow, for the dislodged positions of the arm with a fixed value of $\phi = 90^\circ$ (in the frontal plane) is very similar for both male and female subjects. This quantity starts with 231 N for the male subjects (101 N for the female subjects) at $\theta = 30^\circ$ and after a slight increase at $\theta = 60^\circ$, it decreases gradually to 169 N (77 N for the female subjects) at $\theta = 120^\circ$. The corresponding elbow to wrist resistive force ratios range from 1.56 to 1.98 for the male subjects, and 1.85 to 2.26 for the female subjects.

8. The behavior of the average values of the maximum magnitudes of the resistive forces, against the external force applications on the elbow, for the dislodged positions of the arm with a fixed value of $\phi = 120^\circ$ is very similar for both male and female subjects. This quantity starts with 245 N for the male subjects (129 N for the female subjects) at $\theta = 30^\circ$ and gradually decreases to 210 N (101 N for the female subjects) at $\theta = 120^\circ$. The corresponding elbow to wrist resistive force ratios range from 1.77 to 2.01 for the male subjects, and 1.77 to 1.96 for the female subjects.

9. For the initial seated position ($\theta = 90^\circ$, $\phi = 0^\circ$), the maximum magnitude of force necessary to laterally dislodge the leg is greater when the knee is flexed than when the knee is locked, greater for force applied to the knee than for force applied to the ankle, and greater for the male subjects than for the female subjects. In terms of ratios, we find that the ratio of the average values of the maximum magnitudes of the resistive forces with the knee flexed to the force with the knee locked is 1.61 for the male subjects, and 1.67 for the female subjects, when the force application is on the ankle. When the force is applied at the knee, the required force to dislodge the leg is 1.47 times the force when applied on the ankle for the male subjects, and for the female subjects, this ratio is 1.93, where, for both male and female subjects, the knee is locked. When the knee is flexed, the ratios of force on the knee to force on the ankle are 1.24 for males, and 1.55 for females.

10. The male vs. female subject comparison ratios for the initial seated position show that to dislodge the leg the male subjects require 1.51 times the force needed for the female subjects for force applied on the knee with the knee locked, and 1.98 for force application on the ankle with the knee locked position. When the knee is flexed, the male subjects' response is found to be 1.52 times the female subjects' response, for force applied at the knee, and 1.90 times the female subjects' response when the force is applied at the ankle.

11. The maximum magnitude of force required to dislodge the leg is generally greater for the knee flexed than for the knee locked. The ratios of these forces tend to decrease as the subject's limit is approached in lateral dislodgement (ϕ increasing) for any given position of θ . When the angle of dislodgement (ϕ) is held constant this force ratio for the knee flexed to the knee locked configurations tends to increase with increasing θ . Representative ratios are cited here for $\theta = 120^\circ$ with force application on the knee, and dislodgement (ϕ) going from 0° to the subject's limit. For the male subjects the range is 1.11 to 1.03; for the female subjects, the range is 1.02 to 0.90. For the case of a constant ϕ with force application on the ankle and θ going from 0° to 120° , we see a range of 0.75 to 1.37, for the male subjects, and a range of 1.22 to 1.45 for the female subjects.

12. An interesting observation can also be made by examining the ratios of the required dislodging force applied to the knee and the required dislodging force applied to the ankle. For the male subjects, this ratio tends to increase as the leg is dislodged (ϕ increasing) for all values of θ with either the knee locked or flexed positions. This range, for example, is from 1.40 to 1.85, for $\theta = 120^\circ$, and ϕ going from 0° to the subject's lateral limit, with the knee flexed positions. On the other hand, for the female subjects, this ratio decreases for the same position sequences. For example, with $\theta = 120^\circ$, and ϕ going from 0° to the subject's limit, the range decreases from 2.72 to 1.77, for the knee locked case.

Following concluding remarks are appropriate for the results of the forced kinematic motion (drawer tests) of the shoulder complex. These

preliminary tests provided quantitative data on the variability of the "stiffness" of the shoulder complex dependent upon the upper arm orientation. The shoulder complex appears least stiff for the $\theta = 90^\circ$, $\phi = 30^\circ$ drawer for the tests which were performed. This is very close to the midpoint of possible ϕ angle orientations with $\theta = 90^\circ$. In addition, as we increase or decrease the ϕ orientation from $\phi = 30^\circ$ the stiffness for a given displacement increases. A number of the curves exhibit a rapid increase in resistance initially followed by a region of less rapid increase. It is believed that this phenomenon is an artifact of the testing procedure. It is possibly due to a reflex resistance caused by the activation of stretch receptors in the muscles of the shoulder complex.

The results presented in this report were obtained from three male and three female subjects who are young, healthy and with no special training to increase muscular strength. It is reasonable to expect that the values of the resistive muscle forces and their corresponding moments at the joints depend not only on sex and anthropometry of the subjects as shown in this research but also on age, physical fitness, and, particularly, degree of training for muscular strength. We can also point out that, although there are both intra- and inter-subject variations for the maximum values of the active muscle force and moment data for the extremities, there are some trends one can establish for the behavior of their magnitudes.

It is expected that incorporation of the active muscle force and moment data into the multi-segmented mathematical models of the human body should improve the long-time response capabilities of these models so that they can simulate more realistically the biodynamic events which take place prior to flail injuries. Improvement in mathematical models with incorporation of the active muscle force and moment data results from the notion that calculated deceleration profiles of the limbs with respect to the torso when the body is ejected into the windblast will be substantially different than those calculated from a model including only the passive resistive force and moments in major articulating joints. Recognizing that dislocations of the major articulating joints along with associated soft and hard tissue injuries are closely related to the

magnitude of the deceleration forces, one can see the importance of incorporating active muscle force and moment data into the multi-segmented mathematical models of the human body.


```

100  FORMAT(' ', 'INPUT HAS ONLY ONE NON-ZERO READING.  MAXIMA =
      $MINIMA, STANDARD DEVIATION = 0.0  .')
      STOP
      END

```

```

C
C .....
C
C      SUBROUTINE TALLY
C
C      PURPOSE
C          CALCULATE TOTAL, MEAN, STANDARD DEVIATION, MINIMUM, MAXIMUM
C          FOR EACH VARIABLE IN A SET (OR A SUBSET) OF OBSERVATIONS
C
C      USAGE
C          CALL TALLY(A,S,TOTAL,AVER,SD,VMIN,VMAX,NO,NV,IER)
C
C      DESCRIPTION OF PARAMETERS
C          A      - OBSERVATION MATRIX, NO BY NV
C          S      - INPUT VECTOR INDICATING SUBSET OF A. ONLY THOSE
C                  OBSERVATIONS WITH A NON-ZERO S(J) ARE CONSIDERED.
C                  VECTOR LENGTH IS NO.
C          TOTAL  - OUTPUT VECTOR OF TOTALS OF EACH VARIABLE. VECTOR
C                  LENGTH IS NV.
C          AVER   - OUTPUT VECTOR OF AVERAGES OF EACH VARIABLE. VECTOR
C                  LENGTH IS NV.
C          SD     - OUTPUT VECTOR OF STANDARD DEVIATIONS OF EACH
C                  VARIABLE. VECTOR LENGTH IS NV.
C          VMIN   - OUTPUT VECTOR OF MINIMA OF EACH VARIABLE. VECTOR
C                  LENGTH IS NV.
C          VMAX   - OUTPUT VECTOR OF MAXIMA OF EACH VARIABLE. VECTOR
C                  LENGTH IS NV.
C          NO     - NUMBER OF OBSERVATIONS
C          NV     - NUMBER OF VARIABLES FOR EACH OBSERVATION
C          IER    - ZERO, IF NO ERROR.
C                  - 1, IF S IS NULL. VMIN=1.E37, VMAX=-1.E37., SD=AVER=0
C                  - 2, IF S HAS ONLY ONE NON-ZERO ELEMENT. VMIN=VMAX.
C                  SD=0.0
C
C      REMARKS
C          NONE
C
C      SUBROUTINES AND FUNCTION SUBPROGRAMS REQUIRED
C          NONE
C
C      METHOD
C          ALL OBSERVATIONS CORRESPONDING TO A NON-ZERO ELEMENT IN S

```

```

C      VECTOR ARE ANALYZED FOR EACH VARIABLE IN MATRIX A.
C      TOTALS ARE ACCUMULATED AND MINIMUM AND MAXIMUM VALUES ARE
C      FOUND. FOLLOWING THIS, MEANS AND STANDARD DEVIATIONS ARE
C      CALCULATED. THE DIVISOR FOR STANDARD DEVIATION IS ONE LESS
C      THAN THE NUMBER OF OBSERVATIONS USED.
C      .....
C
C      SUBROUTINE TALLY(A,S,TOTAL,AVER,SD,VMIN,VMAX,NO,NV,IER)
C      DIMENSION A(1),S(1),TOTAL(1),AVER(1),SD(1),VMIN(1),VMAX(1)
C
C      CLEAR OUTPUT VECTORS AND INITIALIZE VMIN,VMAX
C
C      IER=0
C      DO 1 K=1,NV
C      TOTAL(K)=0.0
C      AVER(K)=0.0
C      SD(K)=0.0
C      VMIN(K)=1.0E37
C      1 VMAX(K)=-1.0E37
C
C      TEST SUBSET VECTOR
C
C      SCNT=0.0
C      DO 7 J=1,NO
C      IJ=J-NO
C      IF(S(J)) 2,7,2
C      2 SCNT=SCNT+1.0
C
C      CALCULATE TOTAL, MINIMA, MAXIMA
C
C      DO 6 I=1,NV
C      IJ=IJ+NO
C      X=A(IJ)
C      TOTAL(I)=TOTAL(I)+X
C      IF(X-VMIN(I)) 3,4,4
C      3 VMIN(I)=X
C      4 IF(X-VMAX(I)) 6,6,5
C      5 VMAX(I)=X
C      6 SD(I)=SD(I)+X*X
C      7 CONTINUE
C
C      CALCULATE MEANS AND STANDARD DEVIATIONS
C
C      IF (SCNT)8,8,9
C      8 IER=1
C      GO TO 15
C      9 DO 10 I=1,NV
C      10 AVER(I)=TOTAL(I)/SCNT
C      IF (SCNT-1.0) 13,11,13

```

```

11 IER=2
   DO 12 I=1,NV
12 SD(I)=0.0
   GO TO 15
13 DO 14 I=1,NV
14 SD(I)=SQRT(ABS((SD(I)-TOTAL(I)*TOTAL(I)/SCNT)/(SCNT-1.0)))
15 RETURN
   END

```

.ENABL LC

#Enable LOWER CASE

; OSUATD

; The function of this routine is to control a DATA TRANSLATION
 ; A-to-D. This routine is callable from FORTRAN. This routine
 ; operates in a 'SINGLE SHOT' MODE only. In addition, this routine
 ; operates in a programmed request mode (no interrupt).

; FORTRAN CALL:

; CALL OSUATD(ICHAN,IGAIN,IDATA,ISTAT)

; where

; ICHAN - Is an INTEGER*2 variable specifying the CHANNEL
 ; to read. Must be .GE. 0 .AND. .LE. 127.

; IGAIN - Is an INTEGER*2 variable specifying the GAIN to
 ; to use.

; if = 0 means gain of 1
 ; if = 1 means gain of 2
 ; if = 2 means gain of 4
 ; if = 3 means gain of 8.

; IDATA - Is an INTEGER*2 variable for the DATA read

; ISTAT - Is an INTEGER*2 variable for a STATUS word.
 ; (see OUTPUTS & NOTES for meanings)

; INPUTS:

; R5 Points to a PARAMETER LIST

```

;
;          DISPLACEMENT   FUNCTION
;          IN LIST
;          -----
;          0               Number of parameters
;          2               Address of CHANNEL
;          4               Address of GAIN
;          6               Address of DATA
;          8               Address of STAT
;
;
; OUTPUTS:
;
;      If ISTAT = 1 then CONVERSION was successful & DATA contains the value
;
;      If ISTAT = -1 then CONVERSION was not successful
;
;
; NOTES:
;
;      Four arguments MUST be specified!! If not, control will return
;      immediately & no operation will be performed.
;

```

```

.PSECT OSUATD,RW,I,GBL,REL,CON

```

```

ADCSR   =      170000           ;Define the A-to-D CSR
ADBUF   =      ADCSR+2         ;Define the A-to-D Buffer
DACSR   =      ADCSR+16        ;Define the D/A CSR
DAXBUF  =      ADCSR+20        ;Define D/A X-data register
DAYBUF  =      ADCSR+22        ;Define D/A Y-data register
DMACSR  =      ADCSR+32        ;Define DMA CSR
DMAWCR  =      ADCSR+34        ;Define DMA word count register
DMAADR  =      ADCSR+36        ;Define the DMA current address register

```

```

OSUATD::                                ;Entry point

```

```

MOV     #ADCSR,R3                   ;Point R0 to A to D CSR
MOV     R5,R4                       ;Point R4 to the PARM list

```

	MOV	(R4)+,R0	;Move the ARG COUNT into R0
	TSTB	R0	;Is the number of ARGs > 0?
	BMI	RTN	;NO, Br.
	CMPB	R0,#4.	;Is the number of ARGs = 4.?
	BNE	RTN	;NO, Br. (Unable to service)
	MOV	@(R4)+,R1	;Move the CHANNEL NUMBER into R1
	CMP	R1,#177	;Is the CHANNEL NUMBER .LE. Max
	BHI	140\$;NO, Br. (Bad Channel)
	SWAB	R1	;Position the CHANNEL NUMBER in the high byte
	MOV	@(R4)+,R2	;Set R4 = IGAIN
	CMP	R2,#3	;Is the IGAIN .LE. 3?
	BLOS	160\$;YES, Br. (Good gain supplied)
140\$:	MOV	#-1,R0	;Set ISTAT to return = -1
	BR	RTNSTA	;Br. to RETURN with status
160\$:	ASL	R2	;Position the IGAIN bits
	ASL	R2	; ...
	BIS	R2,R1	;Construct the BIT MASK in R1
	MOV	R1,@R3	;Set the CSR for the convert
	INC	@R3	;Start the conversion
200\$:	TSTB	@R3	;Is the conversion DONE?
	BPL	200\$;NO, Br. (Loop to recheck)
	MOV	ADBUF-ADCSR(R3),@(R4)+	;Move the converted value to the IDATA slot
	MOV	#1,R0	;Set R0 = 1 to imply success
RTNSTA:	MOV	R0,@B.(R5)	;Set the ISTAT
RTN:	RTS	PC	;Return to the CALLER
	.END		;That's all folks

```

;      INDIRECT COMMAND FILE <TRNCAL>
;
;      PROMPTS FOR NAME OR TYPE OF CALIBRATION TEST
;
;      PROMPTS FOR AMOUNT OF APPLIED LOAD
;
;
;
;      INSTALLS AND RUNS <CHNCAL> WHENEVER
;      A CARRIAGE RETURN IS ENTERED AFTER THE
;      AMOUNT OF APPLIED LOAD.
;
;      STOP BY TYPING CTRL Z
;
;
;
;
TIM
.ENABLE SUBSTITUTION
.ASKS XXXXXX WHAT IS THIS TEST (AXIAL,MOMENT,ETC.)?
TIM
.NEW: .ASKS XXXXXX WHAT IS THE AMOUNT OF APPLIED LOAD?
TIM
RUN CHNCAL
TIM
.GOTO NEW
/
>

```

APPENDIX B

DATA ACQUISITION PROGRAM

```

PROGRAM BIGQIO
DIMENSION BIGBUF(224,40),TEMP(28),OUTPUT(34)
LOGICAL*1 BIGBUF,TRANS(224)
LOGICAL*1 RECDAT(224,2)
LOGICAL*1 FNAME(13)
DIMENSION IPARAM(6,2),IOSB(2,2),ATDOUT(6)
DIMENSION IPARM(6),IOSTOP(2)
DIMENSION SUM(6,2),ATDDAT(6,40)
INTEGER COLUMN,TEST(1),CUT,CHECK
DATA TEST/-1/CHECK/0/COLUMN/1/KOUNT/0/CUT/0/
DATA IORAL/'1010/IREC/1/
DATA MODE/1/LMODE/2/

C
C   CREATE & OPEN OUTPUT FILE
C
WRITE(5,5)
READ(5,10) (FNAME(I),I=1,13)
WRITE(5,15)
READ (5,20) NREC
MREC=NREC*2
CALL ASSIGN (1,FNAME,13)
DEFINE FILE 1 (MREC,68,U,IREC)

C
C   GET THE BUFFER ADDRESSES
C
CALL GETADR(IPARAM(1,1),RECDAT(1,1))
CALL GETADR(IPARAM(1,2),RECDAT(1,2))
IPARAM(2,1)=224
IPARAM(2,2)=224
CALL GETADR(IPARM(1),TEST(1))
IPARM(2)=1

C
C   QUEUE THE FIRST I/O
C
CALL QIO(IORAL,4,10,10,IOSB(1,1),IPARAM(1,1))
DO 25 I=1,150
DO 25 J=32,37
      K=J-31
      CALL OSUATD(J,0,IDATA,ISTAT)
      DATA=IDATA*0.00030571578
      SUM(K,1)=SUM(K,1)+DATA
25  CONTINUE
C

```

```

C      INITIALIZE THE NUMBER OF RECORDS TRANSFERRED
C
100    NMODE=MODE
      MODE=LMODE
      LMODE=NMODE

C
C      WAIT FOR THE BUFFER TO FILL
C
      CALL WAITFR(10)
      CALL QIO(IORAL,4,10,10,IOSB(1,MODE),IPARAM(1,MODE))
1      DO 90 I=1,224
          BIGBUF(I,COLUMN)=RECDAT(I,LMODE)
90     CONTINUE
      DO 30 I=1,150
      DO 30 J=32,37
          K=J-31
          CALL OSUATD(J,0,IDATA,ISTAT)
          DATA=IDATA*0.00030571578
          SUM(K,MODE)=SUM(K,MODE)+DATA
30     CONTINUE
2      DO 35 I=1,6
          ATDDAT(I,COLUMN)=SUM(I,LMODE)
          SUM(I,LMODE)=0.0
35     CONTINUE
      IF(CHECK .EQ. NREC)GOTO 1200
C
C      INCREMENT THE NUMBER OF RECORDS
C
      COLUMN=COLUMN+1
      CHECK=COLUMN-1
      GOTO 100
1200   WRITE(5,45)CHECK
      DO 999 K=1,CHECK
          DO 998 I=1,224
              TRANS(I)=BIGBUF(I,K)
998     CONTINUE
          DECODE (224,530,TRANS) (OUTPUT(J),J=1,28)
          DO 997 I=1,6
              ATDOUT(I)=ATDDAT(I,K)
              OUTPUT(28+I)=ATDOUT(I)*0.006666667
997     CONTINUE
          DO 996 I=1,25,4
              IND=IFIX(OUTPUT(I))
              INDEX=IND+(IND-1)*3
              TEMP(INDEX)=OUTPUT(I)
              IF(TEMP(INDEX) .EQ. 0.0)GOTO 992
              TEMP(INDEX+1)=OUTPUT(I+1)
              IF(TEMP(INDEX+1) .EQ. 0.0) GOTO 992
              TEMP(INDEX+2)=OUTPUT(I+2)
              IF(TEMP(INDEX+2) .EQ. 0.0) GOTO 992

```

```

TEMP(INDEX+3)=OUTPUT(I+3)
IF(TEMP(INDEX+3) .EQ. 0.0) GOTO 992
996      CONTINUE
        DO 995 I=1,28
          OUTPUT(I)=TEMP(I)
995      CONTINUE
        IF(KOUNT .GT. 0) GOTO 993
994      WRITE(5,535) (FNAME(I),I=1,13)
        WRITE(5,540) (OUTPUT(I),I=1,16)
        WRITE(5,545) (OUTPUT(I),I=17,28)
        WRITE(5,550) (OUTPUT(I),I=29,34)
993      WRITE(1'IREC) (OUTPUT(I),I=1,34)
        GOTO 991
992      WRITE(5,560) KOUNT
        CUT=CUT+1
991      DO 899 I=1,34
          OUTPUT(I)=0.0
899      CONTINUE
        DO 888 I=1,6
          ATDOUT(I)=0.0
888      CONTINUE
        DO 887 I=1,224
          TRANS(I)= ' '
887      CONTINUE
        DO 886 I=1,28
          TEMP(I)=0.0
886      CONTINUE
        KOUNT=KOUNT+1
999      CONTINUE
1500     CLOSE (UNIT=1)
        WRITE(5,555) (FNAME(I),I=1,13),KOUNT-CUT
        CALL CLREF(10)
5        FORMAT('$','Enter the name to be given to the data file [S-13]: ')
10       FORMAT(13A1)
15       FORMAT('$','Enter the number of records (disitizer sweeps) to b
    $e allocated to the data file [N-5]: ')
20       FORMAT(I5)
45       FORMAT('0','SUCCESS.','I6,' SWEEPS RECORDED.')
530      FORMAT(7(1X,F4.0,3F8.2,3X))
535      FORMAT('0','PROCESSED DATA FOR FILE: ',13A1)
540      FORMAT('0',4(F4.0,3F8.2))
545      FORMAT('0',3(F4.0,3F8.2))
550      FORMAT('0',6F17.9)
555      FORMAT('0','DATA WRITTEN TO DISK. ',13A1,'CONTAINS',I5,' RECORD
    $S. ')
560      FORMAT('0','RECORD NUMBER: ',I5,' CONTAINED ZERO VALUES AND
    $ HAS BEEN DELETED.')
2000     STOP
        END

```

```

      .ENABL  LC                      ;Enable LOWER CASE
;
; OSUATD
;
; The function of this routine is to control a DATA TRANSLATION
; A-to-D. This routine is callable from FORTRAN. This routine
; operates in a 'SINGLE SHOT' MODE only. In addition, this routine
; operates in a programmed request mode (no interrupt).
;
;
; FORTRAN CALL:
;
;      CALL OSUATD(ICHAN,IGAIN,IDATA,ISTAT)
;
;      where
;
;          ICHAN - Is an INTEGER*2 variable specifying the CHANNEL
;                  to read. Must be .GE. 0 .AND. .LE. 127.
;
;          IGAIN - Is an INTEGER*2 variable specifying the GAIN to
;                  to use.
;
;                  if = 0 means gain of 1
;                  if = 1 means gain of 2
;                  if = 2 means gain of 4
;                  if = 3 means gain of 8.
;
;          IDATA - Is an INTEGER*2 variable for the DATA read
;
;          ISTAT - Is an INTEGER*2 variable for a STATUS word.
;                  (see OUTPUTS & NOTES for meanings)
;
; INPUTS:
;
;      R5 Points to a PARAMETER LIST
;
;          DISPLACEMENT    FUNCTION
;          IN LIST
;          -----
;          0                Number of parameters
;          2                Address of CHANNEL
;          4                Address of GAIN
;          6                Address of DATA
;          8                Address of STAT

```

```

;
; OUTPUTS:
;
; If ISTAT = 1 then CONVERSION was successful & DATA contains the value
;
; If ISTAT = -1 then CONVERSION was not successful
;

```

; NOTES:

```

; Four arguments MUST be specified!! If not, control will return
; immediately & no operation will be performed.
;

```

.PSECT OSUATD,RW,I,GBL,REL,CON

```

ADCSR = 170000 ;Define the A-to-D CSR
ADBUF = ADCSR+2 ;Define the A-to-D Buffer
DACSR = ADCSR+16 ;Define the D/A CSR
DAXBUF = ADCSR+20 ;Define D/A X-data register
DAYBUF = ADCSR+22 ;Define D/A Y-data register
DMACSR = ADCSR+32 ;Define DMA CSR
DMAWCR = ADCSR+34 ;Define DMA word count register
DMAADR = ADCSR+36 ;Define the DMA current address register

```

OSUATD:: ;Entry point

```

MOV #ADCSR,R3 ;Point R0 to A to D CSR
MOV R5,R4 ;Point R4 to the PARM list

MOV (R4)+,R0 ;Move the ARG COUNT into R0
TSTB R0 ;Is the number of ARGs > 0?
BMI RTN ;NO, Br.

CMPB R0,#4. ;Is the number of ARGs = 4.?
BNE RTN ;NO, Br. (Unable to service)

MOV @R4+,R1 ;Move the CHANNEL NUMBER into R1
CMP R1,#177 ;Is the CHANNEL NUMBER .LE. Max
BHI 140$ ;NO, Br. (Bad Channel)

```

```

SWAB    R1                                ;Position the CHANNEL NUMBER in the high byte

MOV     @R4)+,R2                          ;Set R4 = IGAIN
CMP     R2,#3                             ;Is the IGAIN .LE. 3?
BLOS    160$                              ;YES, Br. (Good gain supplied)

140$:   MOV     #-1,R0                     ;Set ISTAT to return = -1
BR      RTNSTA                            ;Br. to RETURN with status

160$:   ASL     R2                          ;Position the IGAIN bits
ASL     R2                                ;
BIS     R2,R1                             ;Construct the BIT MASK in R1

MOV     R1,@R3                            ;Set the CSR for the convert

INC     @R3                               ;Start the conversion

200$:   TSTB    @R3                        ;Is the conversion DONE?
BPL     200$                              ;NO, Br. (Loop to recheck)

MOV     ADBUF-ADCSR(R3),@R4)+             ;Move the converted value to the IDATA slot

MOV     #1,R0                             ;Set R0 = 1 to imply success

RTNSTA: MOV     R0,@8.(R5)                 ;Set the ISTAT

RTN:    RTS     PC                         ;Return to the CALLER

.END                                         ;That's all folks

```

>

APPENDIX C
DATA PROCESSING PROGRAM

```

C
PROGRAM TABLE
C
C DECLARE & TYPE VARIABLES; DIMENSION ARRAYS; INITIALIZE CONSTANTS
C
    DIMENSION POSIT1(3),RECDAT(34),CAL(6,6)
    DIMENSION STORE(40,10)
    DIMENSION X(6),OUTPUT(3),F1(6),G1(6)
    DIMENSION PTAXIS(3,3)
    DIMENSION PT1PT2(3),PT2PT3(3),PT1PT3(3),PT5PT7(3)
    DIMENSION PT4PT7(3),PT6PT7(3)
    LOGICAL*1 FNAME(13),JTNAME(9),SNAME(25),MESS(80)
    LOGICAL*1 DAY(9),HOUR(8)
    REAL NORMAL,LENG1
    REAL MOMNTX,MOMNTY,MOMNTZ
    INTEGER ANS,Y,N,BODYSD
    DATA Y/'Y'/N/'N'/
    COMMON /AC/ PT4PT5(3)
    COMMON /BC/ POINT1(3),POINT2(3),POINT3(3)
    COMMON /DC/ POINT4(3),POINTS(3),POINT6(3),POINT7(3)
    COMMON /EC/ PTAPP(3),FIXCNT(3),FORCE(6)
    COMMON /FC/ SONICX,SONICY,SONICZ,TILT,BDROTO,CHTILT,CHROTO,
    $ BODYSD,XSUB,TRNS(3,3)
    DATA IREC/1/BODYSD/1/FORCE/6*0.0/
    DATA KOUNT/1/

C
C PROMPT FOR DATA AND OUTPUT INFORMATION
C
    WRITE(5,1)
    505 WRITE(5,5)
    READ(5,10,ERR=505) (JTNAME(I),I=1,9)
    510 WRITE(5,15)
    READ(5,20,ERR=510) (SNAME(I),I=1,25)
    515 WRITE(5,25)
    READ (5,30,ERR=515) (MESS(I),I=1,80)
    520 WRITE(5,35)
    READ (5,40,ERR=520) (FNAME(I),I=1,13)
    525 WRITE(5,45)
    READ (5,50,ERR=525) NREC

C
C LOCATE THE ORIGIN OF THE 3-D BOARD WITH RESPECT TO THE

```

```

C      FIXED BODY SEGMENT
C
530    WRITE(5,55)
535    WRITE(5,60)
      READ(5,65,ERR=535) SONICX
540    WRITE(5,70)
      READ(5,65,ERR=540) SONICY
545    WRITE(5,75)
      READ(5,65,ERR=545) SONICZ
      WRITE(5,3)
550    WRITE(5,4)
      READ(5,65,ERR=550) XSUB
555    WRITE(5,80)
      READ(5,65,ERR=555) TILT
560    WRITE(5,85)
      READ(5,65,ERR=560) BDROTO
565    WRITE(5,87)
      READ(5,65,ERR=565) LENG1
570    WRITE(5,275)
      READ(5,65,ERR=570) CHTILT
575    WRITE(5,280)
      READ(5,65,ERR=575) CHROTO
C
C      CONVERT THE INPUT ANGLES TO RADIANs
C
      OUTROT=CHROTO
      OUTTIL=CHTILT
      TILT = TILT*0.0174532925
      BDROTO = BDROTO*0.0174532925
      CHTILT = CHTILT*0.0174532925
      CHROTO = CHROTO*0.0174532925
C
C      CHECK WHICH SIDE OF THE BODY IS BEING TESTED
C
      IF(SONICX .GE. 0.0) BODYSD=-1
C
C      LOCATE, IDENTIFY AND ACCESS THE DATA FILE
C
2000   CONTINUE
      CALL ASSIGN (1,FNAME,13)
      DEFINE FILE 1 (NREC,68,U,IREF)
C
C      READ ONE RECORD
C
500    READ (1,IREF,ERR=4000) (RECDAT(I),I=1,34)
C
C      ASSIGN DATA TO VARIABLES
C
      DO 499 I=1,3
          POINT1(I)=RECDAT(I+1)

```

```

POINT2(I)=RECDAT(I+5)
POINT3(I)=RECDAT(I+9)
POINT4(I)=RECDAT(I+13)
POINT5(I)=RECDAT(I+17)
POINT6(I)=RECDAT(I+21)
POINT7(I)=RECDAT(I+25)
499  CONTINUE
501  FORCE(1)=RECDAT(33)
      FORCE(2)=RECDAT(34)
      FORCE(3)=RECDAT(29)
      FORCE(4)=RECDAT(31)
      FORCE(5)=RECDAT(32)
      FORCE(6)=RECDAT(30)

C
C  AFTER INITIAL RECORD, GO ON; OTHERWISE
C
      IF(IREC .GE. 3)GOTO 605

C
C  FILL THE CALIBRATION MATRIX
C

      CAL(1,1)=-0.10616
      CAL(1,2)=0.00164
      CAL(1,3)=0.00047
      CAL(1,4)=0.00094
      CAL(1,5)=-0.00030
      CAL(1,6)=-0.00011
      CAL(2,1)=-0.00106
      CAL(2,2)=0.10876
      CAL(2,3)=-0.00001
      CAL(2,4)=-0.00021
      CAL(2,5)=-0.00149
      CAL(2,6)=0.00008
      CAL(3,1)=0.00090
      CAL(3,2)=0.00108
      CAL(3,3)=0.01532
      CAL(3,4)=0.0
      CAL(3,5)=-0.00016
      CAL(3,6)=0.00023
      CAL(4,1)=0.00229
      CAL(4,2)=0.00028
      CAL(4,3)=0.00037
      CAL(4,4)=0.02987
      CAL(4,5)=-0.00009
      CAL(4,6)=0.00012
      CAL(5,1)=0.00033
      CAL(5,2)=0.00707
      CAL(5,3)=0.00045
      CAL(5,4)=-0.00028
      CAL(5,5)=0.02924
      CAL(5,6)=0.00003

```

```

CAL(6,1)=-0.00020
CAL(6,2)=-0.00390
CAL(6,3)=-0.00090
CAL(6,4)=0.0
CAL(6,5)=0.00097
CAL(6,6)=0.03986

C
C   INVERT THE CALIBRATION MATRIX
C
C   CALL MINV(CAL,6,D,F1,G1)
C
C   OUTPUT HEADER INFORMATION
C
CALL DATE(DAY)
CALL TIME(HOUR)
WRITE (5,200)
WRITE(5,100) (JTNAME(I),I=1,9)
WRITE(5,205)
WRITE(5,105) DAY,HOUR,OUTROT,(SNAME(I),I=1,25),OUTTIL
WRITE(5,110) (FNAME(I),I=1,13),NREC-1,(MESS(I),I=1,80)
WRITE(5,205)
WRITE(5,320)
WRITE(5,325)
605  CONTINUE
600  CALL FORPT(PTAPP,PTAXIS,BODYSD)
C
C   MULTIPLY THE TRANSDUCER VALUES BY THE CALIBRATION MATRIX
C   TO GET THE FORCES
C
CALL GMPRD(CAL,FORCE,X,6,6,1)
DO 492 I=1,6
    FORCE(I)=X(I)
492  CONTINUE
C
C   CALCULATE THE POSITION OF THE MOVING BODY SEGMENT
C
CALL POSITN(POSIT1,PT4PT5)
C
C   CALCULATE THETA AND PHI FOR THIS POSITION
C
CALL SPHERE(THETA,PHI)
RECDAT(1)=THETA
RECDAT(2)=PHI
C
C   CALCULATE THE JOINT CENTER AND PRINT RESULTS
C
CALL FJTCNT(POSIT1,LENG1,FXCNT)
CALL MATRIX(FIXCNT,OUTPUT)
RECDAT(16)=OUTPUT(1)
RECDAT(17)=OUTPUT(2)

```

```

RECDAT(18)=OUTPUT(3)
701 CALL RESULT(PTAXIS,TOTFOX,TOTFOY,TOTFOZ,TOTMOX,
TOTMOY,TOTMOZ,2,RECDAT)
RECDAT(3)=TOTFOX*-4.44898
RECDAT(4)=TOTFOY*-4.44898
RECDAT(5)=TOTFOZ*-4.44898
RECDAT(6)=SQRT(RECDAT(3)**2+RECDAT(4)**2+RECDAT(5)**2)
RECDAT(13)=SQRT(RECDAT(7)**2+RECDAT(9)**2+RECDAT(11)**2)
RECDAT(14)=SQRT(RECDAT(8)**2+RECDAT(10)**2+RECDAT(12)**2)
RECDAT(15)=SQRT((RECDAT(7)+RECDAT(8))**2+(RECDAT(9)+RECDAT(10))
**2+(RECDAT(11)+RECDAT(12))**2)
DO 705 I=1,3
PT1PT2(I)=POINT1(I)-POINT2(I)
PT2PT3(I)=POINT2(I)-POINT3(I)
PT1PT3(I)=POINT1(I)-POINT3(I)
PT4PT5(I)=POINT4(I)-POINT5(I)
PT5PT7(I)=POINT5(I)-POINT7(I)
PT4PT7(I)=POINT4(I)-POINT7(I)
PT6PT7(I)=POINT6(I)-POINT7(I)
705 CONTINUE
STORE(KOUNT,4)=SQRT(PT1PT2(1)**2+PT1PT2(2)**2+PT1PT2(3)**2)
STORE(KOUNT,5)=SQRT(PT2PT3(1)**2+PT2PT3(2)**2+PT2PT3(3)**2)
STORE(KOUNT,6)=SQRT(PT1PT3(1)**2+PT1PT3(2)**2+PT1PT3(3)**2)
STORE(KOUNT,7)=SQRT(PT4PT5(1)**2+PT4PT5(2)**2+PT4PT5(3)**2)
STORE(KOUNT,8)=SQRT(PT5PT7(1)**2+PT5PT7(2)**2+PT5PT7(3)**2)
STORE(KOUNT,9)=SQRT(PT4PT7(1)**2+PT4PT7(2)**2+PT4PT7(3)**2)
STORE(KOUNT,10)=SQRT(PT6PT7(1)**2+PT6PT7(2)**2+PT6PT7(3)**2)
C
C WRITE THE OUTPUT IN COMPACT FORM
C
DO 702 I=1,3
STORE(KOUNT,I)=RECDAT(I+15)
702 CONTINUE
WRITE(5,330) (RECDAT(I),I=1,15)
C
C IF THERE ARE ANY MORE RECORDS, GO GET THEM!
C
KOUNT=KOUNT+1
IF(IREC.NE.NREC)GOTO 500
WRITE(5,335)
DO 703 I=1,KOUNT-1
WRITE(5,350) (STORE(I,J),J=1,10)
703 CONTINUE
C
C FORMAT STATEMENTS FOR PROMPTS AND RESULTS
C
1 FORMAT('1','Enter requested LENGTHS in CENTIMETRES and requeste
$d ANGLES in DEGREES: '/')
5 FORMAT('$','Enter name of Joint tested [S-9]: ')
10 FORMAT(9A1)

```

```

15     FORMAT('$','Enter subject name or number [S-25]: ')
20     FORMAT(25A1)
25     FORMAT('0','Enter a description of the test [S-80]: ')
30     FORMAT(80A1)
35     FORMAT('$','Enter data file name [S-13]: ')
40     FORMAT(13A1)
45     FORMAT('$','Enter number of records to be read [N-5]: ')
50     FORMAT(I5)
55     FORMAT('0','Enter the coordinates of the fixed body segment ori
    $sin, with respect to the 3-D board origin:')
60     FORMAT('$',T15,'Enter the X-COORDINATE [N-8]: ')
65     FORMAT(F8.2)
70     FORMAT('$',T15,'Enter the Y-COORDINATE [N-8]: ')
75     FORMAT('$',T15,'Enter the Z-COORDINATE [N-8]: ')
3     FORMAT('0','Enter distance from FIXED BODY ORIGIN to SONIC POI
    $NT COORDINATE in CENTIMETRES: ')
4     FORMAT('$',T15,'Enter the X-DISTANCE with respect to the
    $ fixed body coordinate system [N-8]: ')
80     FORMAT('$','Enter, in degrees, the rotation of the 3-D board fr
    $om the vertical [N-8]: ')
85     FORMAT('$','Enter, in degrees, the rotation of the 3-D board fr
    $om the X-Z plane [N-8]: ')
87     FORMAT('$','Enter the length to the fixed Joint center [N-8]:
    $')
100    FORMAT('0',T78,9A1,'JOINT')
105    FORMAT('0',T5,'DATE: ',9A1,T138,'CHAIR POSITION:',/,T5,'TIME: '
    $,8A1,T143,'ROTATION:',F8.2,' degrees',/,T5,'SUBJECT NAME AND NUMB
    $ER: ',25A1,T143,'TILT: ',F8.2,' degrees')
110    FORMAT(' ',T5,'DATA FILE NAME: ',13A1,/,T5,'NUMBER OF RECORDS:
    $',I5,/,T5,'DESCRIPTION: ',80A1)
200    FORMAT('1',170('-',/))
205    FORMAT('0',170('-',/))
206    FORMAT(' ',170('-',/))
207    FORMAT('0',170('.',/))
275    FORMAT('$','Enter the tilt of the chair, in degrees, from the v
    $ertical [N-8]: ')
280    FORMAT('$','Enter the rotation of the chair, in degrees [N-8]:
    $ ')
300    FORMAT('0',T30,'ERROR ON ATTEMPT TO READ NEXT RECORD')
320    FORMAT('0',T3,'THETA',T15,'PHI',T44,'FORCES (newtons)',T88,
    $'MOMENTS (newton metres)')
325    FORMAT(' ',T7,'(degrees)',T26,'FX',T37,'FY',T48,'FZ',T55,
    $'MAGNITUDE',T69,'X:rxF',T79,'X:pure',T91,'Y:rxF',T102,
    $'Y:pure',T114,'Z:rxF',T124,'Z:pure',T134,'MAG:rxF',
    $T144,'MAG:pure',T158,'TOTAL')
330    FORMAT('0',15(F7.2,4X))
335    FORMAT('0','FIXED JOINT CENTERS:',T88,'SPARK GAP DISTANCES:',
    $/T47,'1 to 2',8X,'2 to 3',8X,'1 to 3',8X,'4 to 5',8X,'5 to 7',8X,
    $'4 to 7',8X,'6 to 7')
340    FORMAT('0',/'$','Are there other files to be processed?

```

```

      $[Y/N]: ')
345   FORMAT(A4)
350   FORMAT(' ',10(F9.2,5X))
C
C     CLOSE UP DATA FILE & THAT'S ALL FOLKS!
C
      WRITE(5,207)
2001  WRITE(5,340)
      READ(5,345)ANS
      IF(ANS .EQ. 'N')GOTO 5000
      CLOSE(UNIT=1)
      WRITE(5,35)
      READ(5,40) (FNAME(I),I=1,13)
      WRITE(5,45)
      READ(5,50) NREC
      NREC=NREC+1
      WRITE(5,25)
      READ(5,30) (MESS(I),I=1,80)
      IREC=1
      KOUNT=1
      DO 2222 I=1,34
          RECDAT(I)=0.0
2222  CONTINUE
      GOTO 2000
4000  WRITE(5,205)
      WRITE(5,300)
      GOTO 2001
5000  WRITE(5,205)
      CLOSE(UNIT=1)
      STOP
      END

```

```

      SUBROUTINE FORPT(PTAPP,PTAXIS,BODYSD)
C
C     SUBROUTINE TO CALCULATE THE POINT OF FORCE APPLICATION
C     AND THE AXIS SYSTEM OF THE FORCE APPLICATOR
C
      COMMON /BC/ POINT1(3),POINT2(3),POINT3(3)
      DIMENSION PTAPP(3),NORMAL(3),PT1PT2(3),PT2PT3(3)
      DIMENSION PTAXIS(3,3),X(3),Y(3)
      REAL NORMAL,NORLEN
      INTEGER BODYSD
      DO 10 I=1,3
          PT1PT2(I)=POINT2(I)-POINT1(I)
          PT2PT3(I)=POINT3(I)-POINT2(I)
10    CONTINUE

```

```

CALL CRSRD(P1PT2,PT2PT3,NORMAL)
IF(BODYSO .GT. 0)GOTO 15
NORMAL(1)=-1.0*NORMAL(1)
NORMAL(2)=-1.0*NORMAL(2)
NORMAL(3)=-1.0*NORMAL(3)
15 NORLEN=SQRT(PT2PT3(1)**2+PT2PT3(2)**2+PT2PT3(3)**2)*0.5
CALL UNITVR(NORMAL)
DO 20 I=1,3
    NORMAL(I)=NORMAL(I)*NORLEN
    PT2PT3(I)=PT2PT3(I)*0.5+POINT2(I)
    PTAPP(I)=NORMAL(I)+PT2PT3(I)
    X(I)=POINT3(I)-PTAPP(I)
    Y(I)=POINT2(I)-PTAPP(I)
20 CONTINUE
CALL UNITVR(P1PT2)
CALL UNITVR(X)
CALL UNITVR(Y)
DO 30 I=1,3
    PTAPP(I)=PTAPP(I)+P1PT2(I)*28.1305
    PTAXIS(1,I)=X(I)
    PTAXIS(2,I)=Y(I)
    PTAXIS(3,I)=P1PT2(I)
30 CONTINUE
RETURN
END

```

```

SUBROUTINE FJTCNT(POSIT1,LENG1,FXCNT)
C
C CALCULATES A FIXED JOINT CENTER
C
COMMON /AC/ PT4PT5(3)
DIMENSION POSIT1(3),FXCNT(3)
REAL LENG1
DO 5 I=1,3
    FXCNT(I)=-1.0*PT4PT5(I)
5 CONTINUE
CALL UNITVR(FXCNT)
DO 10 I=1,3
    FXCNT(I)=FXCNT(I)*LENG1+POSIT1(I)
10 CONTINUE
RETURN
END

```

```

SUBROUTINE POSITN(POSIT1,PT4PT5)

```

```

C      SUBROUTINE TO CALCULATE THE POSITION OF THE MOVING BODY SEGMENT
C

```

```

COMMON /DC/ POINT4(3),POINT5(3),POINT6(3),POINT7(3)
DIMENSION PT4PT5(3),PT5PT7(3),POSIT1(3),NORMAL(3)
REAL NORMAL
DO 10 I=1,3
    PT4PT5(I)=POINT5(I)-POINT4(I)
    PT5PT7(I)=POINT7(I)-POINT5(I)
10  CONTINUE
CALL CRSPRD(PT4PT5,PT5PT7,NORMAL)
15  CALL UNITVR(NORMAL)
DIST=SQRT(PT5PT7(1)**2+PT5PT7(2)**2+PT5PT7(3)**2)*0.5
DO 25 I=1,3
    NORMAL(I)=NORMAL(I)*DIST
    PT5PT7(I)=POINT5(I)+PT5PT7(I)*0.5
    POSIT1(I)=NORMAL(I)+PT5PT7(I)
25  CONTINUE
RETURN
END

```

```

SUBROUTINE SPHERE(THETA,PHI)

```

```

C
C      SUBROUTINE TO CALCULATE THE SPHERICAL COORDINATES OF THE
C      MOVING BODY SEGMENT
C

```

```

DIMENSION A(3),B(3)
COMMON /AC/ PT4PT5(3)
DATA PI/3.141592654/
A(1)=PT4PT5(1)
A(2)=PT4PT5(2)
A(3)=PT4PT5(3)
CALL UNITVR(A)
CALL MATRIX(A,B)
THETA=SQRT(B(1)**2+B(2)**2)/B(3)
THETA=ATAN(THETA)
IF(B(3)) 5,10,15
5   THETA=PI+THETA
    GOTO 15
10  THETA=PI*0.5
15  PHI=ATAN2(B(2),B(1))
    IF(B(1) .NE. 0.0)GOTO 20
    IF(B(2) .GT. 0.0)PHI=PI*0.5
    GOTO 1000
    IF(B(2) .LT. 0.0)PHI=PI*-0.5
    GOTO 1000

```

```

20     IF(PHI) 25,30,35
25     IF(B(2) .GE. 0.0) PHI=PI+PHI
      GOTO 1000
30     PHI=0.0
      IF(B(1) .LT. 0.0) PHI=PI
      GOTO 1000
35     IF(B(2) .LT. 0.0) PHI=-1.0*PI+PHI
1000    PHI=PHI*180.0/PI
      THETA=THETA*180.0/PI
      RETURN
      END

```

SUBROUTINE MATRIX(X,OUTPUT)

```

C
C     SUBROUTINE TO DETERMINE THE ROTATION AND
C     TRANSLATION OF THE 3-D BOARD TO THE FIXED BODY SEGMENT
C     COORDINATE SYSTEM
C
      COMMON /FC/ SONICX,SONICY,SONICZ,TILT,BDROTO,CHTILT,CHROTO,
$     BODYSD,XSUB,TRNS(3,3)
      DIMENSION THAT(6,3),T1(3,3),T2(3,3),T3(3,3),T32(3,3)
      DIMENSION X(3),OUTPUT(3),F5(3),G5(3),XX(3)
      INTEGER BODYSD
      DATA KOUNT/1/T1/9*0.0/
      IFLAG=0
      XX(1)=X(1)
      XX(2)=X(2)
      XX(3)=X(3)
      ARGV=X(1)**2+X(2)**2+X(3)**2
      IF(ARGV .LE. 1.2) GOTO 5
      IFLAG=1
      XX(1)=X(1)-SONICX
      XX(2)=X(2)-SONICY
      XX(3)=X(3)-SONICZ
5     IF(KOUNT .GT. 1) GOTO 15
      T1(1,1)=.9702957
      T1(1,3)=.2419219
      T1(2,2)=1.0
      T1(3,1)=-.2419219
      T1(3,3)=.9702957
      DO 10 I=1,4,3
          IF(I.EQ.1) PHI=CHROTO+1.570798
          IF(I.EQ.1) THETA=CHTILT
          IF(I.EQ.4) PHI=BDROTO
          IF(I.EQ.4) THETA=TILT
          THAT(I,1)=COS(PHI)

```

```

      TMAT(I,2)=SIN(PHI)
      TMAT(I,3)=0.0
      TMAT(I+1,1)=-SIN(PHI)*COS(THETA)
      TMAT(I+1,2)=COS(PHI)*COS(THETA)
      TMAT(I+1,3)=SIN(THETA)
      TMAT(I+2,1)=SIN(PHI)*SIN(THETA)
      TMAT(I+2,2)=-COS(PHI)*SIN(THETA)
      TMAT(I+2,3)=COS(THETA)
10  CONTINUE
      CALL RCUT(TMAT,4,T2,T3,6,3,0)
      CALL GMPRD(T3,T2,T32,3,3,3)
      CALL GMPRD(T32,T1,TRNS,3,3,3)
      KOUNT=KOUNT+1
15  DO 20 I=1,3
      OUTPUT(I)=XX(1)*TRNS(1,I)+XX(2)*TRNS(2,I)+XX(3)*TRNS(3,I)
20  CONTINUE
      IF(IFLAG .EQ. 0) GOTO 25
      OUTPUT(1)=OUTPUT(1)+XSUB
25  RETURN
      END

```

```

      SUBROUTINE RESULT(PTAXIS,TOTFOX,TOTFOY,TOTFOZ,TOTMOX,
$TOTMOY,TOTMOZ,I,RECDAT)
C
C      ASSOCIATES FORCE & MOMENT MAGNITUDES WITH THE POINT OF
C      FORCE APPLICATION VECTOR, CALCULATES THE MOMENTS (r x F),
C      PREPARES THE TOTALS FOR OUTPUT
C
      COMMON /EC/ PTAPP(3),FIXCNT(3),FORCE(6)
      COMMON /FC/ SONICX,SONICY,SONICZ,TILT,BDROTO,CHTILT,CHROTO,
$      BODYSD,XSUB,TRNS(3,3)
      DIMENSION Y(3),PTAXIS(3,3),XMO(3),YMO(3),ZMO(3),WORK(6,3)
      DIMENSION WORKX(3),WORKY(3),WORKZ(3)
      DIMENSION RECDAT(34),CPTAPP(3),X(3),Z(3)
      INTEGER BODYSD
      CPTAPP(1)=PTAPP(1)
      CPTAPP(2)=PTAPP(2)
      CPTAPP(3)=PTAPP(3)
      CALL MATRIX(CPTAPP,Y)
      DO 10 J=1,3
          CPTAPP(J)=Y(J)
10  CONTINUE
      CALL MATRIX(FIXCNT,Y)
      DO 15 J=1,3
          CPTAPP(J)=CPTAPP(J)-Y(J)
15  CONTINUE

```

```

1      DO 7 J=1,3
          X(J)=FORCE(1)*PTAXIS(1,J)
          Y(J)=FORCE(2)*PTAXIS(2,J)
          Z(J)=FORCE(3)*PTAXIS(3,J)
          WORKX(J)=FORCE(4)*PTAXIS(1,J)
          WORKY(J)=FORCE(5)*PTAXIS(2,J)
          WORKZ(J)=FORCE(6)*PTAXIS(3,J)
7      CONTINUE
      FRCXB=X(1)+Y(1)+Z(1)
      FRCYB=X(2)+Y(2)+Z(2)
      FRCZB=X(3)+Y(3)+Z(3)
      WRKXB=WORKX(1)+WORKY(1)+WORKZ(1)
      WRKYB=WORKX(2)+WORKY(2)+WORKZ(2)
      WRKZB=WORKX(3)+WORKY(3)+WORKZ(3)
      DO 8 J=1,3
          WORK(1,J)=FRCXB*TRNS(1,J)
          WORK(2,J)=FRCYB*TRNS(2,J)
          WORK(3,J)=FRCZB*TRNS(3,J)
          WORK(4,J)=WRKXB*TRNS(1,J)
          WORK(5,J)=WRKYB*TRNS(2,J)
          WORK(6,J)=WRKZB*TRNS(3,J)
8      CONTINUE
      RECDAT(8)=(WORK(4,1)+WORK(5,1)+WORK(6,1))*-0.11298
      RECDAT(10)=(WORK(4,2)+WORK(5,2)+WORK(6,2))*-0.11298
      RECDAT(12)=(WORK(4,3)+WORK(5,3)+WORK(6,3))*-0.11298
      DO 20 J=1,3
          X(J)=WORK(1,J)
          Y(J)=WORK(2,J)
          Z(J)=WORK(3,J)
20     CONTINUE
      CALL CRSPRD(CPTAPP,X,XMO)
      CALL CRSPRD(CPTAPP,Y,YMO)
      CALL CRSPRD(CPTAPP,Z,ZMO)
      DO 30 J=1,3
          WORK(4,J)=WORK(4,J)+XMO(J)
          WORK(5,J)=WORK(5,J)+YMO(J)
          WORK(6,J)=WORK(6,J)+ZMO(J)
30     CONTINUE
      TOTFOX=WORK(1,1)+WORK(2,1)+WORK(3,1)
      TOTFOY=WORK(1,2)+WORK(2,2)+WORK(3,2)
      TOTFOZ=WORK(1,3)+WORK(2,3)+WORK(3,3)
      TOTMOX=WORK(4,1)+WORK(5,1)+WORK(6,1)
      TOTMOY=WORK(4,2)+WORK(5,2)+WORK(6,2)
      TOTMOZ=WORK(4,3)+WORK(5,3)+WORK(6,3)
      RECDAT(7)=(XMO(1)+YMO(1)+ZMO(1))*-0.0444898
      RECDAT(9)=(XMO(2)+YMO(2)+ZMO(2))*-0.0444898
      RECDAT(11)=(XMO(3)+YMO(3)+ZMO(3))*-0.0444898
      RETURN
      END

```

```

C
C .....
C
C SUBROUTINE GMPRD
C
C PURPOSE
C   MULTIPLY TWO GENERAL MATRICES TO FORM A RESULTANT GENERAL
C   MATRIX
C
C USAGE
C   CALL GMPRD(A,B,R,N,M,L)
C
C DESCRIPTION OF PARAMETERS
C   A - NAME OF FIRST INPUT MATRIX
C   B - NAME OF SECOND INPUT MATRIX
C   R - NAME OF OUTPUT MATRIX
C   N - NUMBER OF ROWS IN A
C   M - NUMBER OF COLUMNS IN A AND ROWS IN B
C   L - NUMBER OF COLUMNS IN B
C
C REMARKS
C   ALL MATRICES MUST BE STORED AS GENERAL MATRICES
C   MATRIX R CANNOT BE IN THE SAME LOCATION AS MATRIX A
C   MATRIX R CANNOT BE IN THE SAME LOCATION AS MATRIX B
C   NUMBER OF COLUMNS OF MATRIX A MUST BE EQUAL TO NUMBER OF ROW
C   OF MATRIX B
C
C SUBROUTINES AND FUNCTION SUBPROGRAMS REQUIRED
C   NONE
C
C METHOD
C   THE M BY L MATRIX B IS PREMULTIPLIED BY THE N BY M MATRIX A
C   AND THE RESULT IS STORED IN THE N BY L MATRIX R.
C .....
C
C SUBROUTINE GMPRD(A,B,R,N,M,L)
C   DIMENSION A(1),B(1),R(1)
C
C   IR=0
C   IK=-M
C   DO 10 K=1,L
C     IK=IK+M
C     DO 10 J=1,N
C       IR=IR+1
C       JI=J-M

```

```

      IB=IK
      R(IR)=0
      DO 10 I=1,M
      JI=JI+N
      IB=IB+1
10  R(IR)=R(IR)+A(JI)*B(IB)
      RETURN
      END

```

```

C
C .....
C
C      SUBROUTINE MINV
C
C      PURPOSE
C          INVERT A MATRIX
C
C      USAGE
C          CALL MINV(A,N,D,L,M)
C
C      DESCRIPTION OF PARAMETERS
C          A - INPUT MATRIX, DESTROYED IN COMPUTATION AND REPLACED BY
C              RESULTANT INVERSE.
C          N - ORDER OF MATRIX A
C          D - RESULTANT DETERMINANT
C          L - WORK VECTOR OF LENGTH N
C          M - WORK VECTOR OF LENGTH N
C
C      REMARKS
C          MATRIX A MUST BE A GENERAL MATRIX
C
C      SUBROUTINES AND FUNCTION SUBPROGRAMS REQUIRED
C          NONE
C
C      METHOD
C          THE STANDARD GAUSS-JORDAN METHOD IS USED. THE DETERMINANT
C          IS ALSO CALCULATED. A DETERMINANT OF ZERO INDICATES THAT
C          THE MATRIX IS SINGULAR.
C
C .....
C
C      SUBROUTINE MINV(A,N,D,L,M)
C      DIMENSION A(1),L(1),M(1)
C
C .....
C
C      IF A DOUBLE PRECISION VERSION OF THIS ROUTINE IS DESIRED, THE

```

```

C      C IN COLUMN 1 SHOULD BE REMOVED FROM THE DOUBLE PRECISION
C      STATEMENT WHICH FOLLOWS.
C
C      DOUBLE PRECISION A,D,BIGA,HOLD,DABS
C
C      THE C MUST ALSO BE REMOVED FROM DOUBLE PRECISION STATEMENTS
C      APPEARING IN OTHER ROUTINES USED IN CONJUNCTION WITH THIS
C      ROUTINE.
C
C      THE DOUBLE PRECISION VERSION OF THIS SUBROUTINE MUST ALSO
C      CONTAIN DOUBLE PRECISION FORTRAN FUNCTIONS. ABS IN STATEMENT
C      10 MUST BE CHANGED TO DABS.
C
C      .....
C
C      SEARCH FOR LARGEST ELEMENT
C
      D=1.0
      NK=-N
      DO 80 K=1,N
      NK=NK+N
      L(K)=K
      M(K)=K
      KK=NK+K
      BIGA=A(KK)
      DO 20 J=K,N
      IZ=N*(J-1)
      DO 20 I=K,N
      IJ=IZ+I
10      IF( ABS(BIGA)- ABS(A(IJ))) 15,20,20
15      BIGA=A(IJ)
      L(K)=I
      M(K)=J
20      CONTINUE
C
C      INTERCHANGE ROWS
C
      J=L(K)
      IF(J-K) 35,35,25
25      KI=K-N
      DO 30 I=1,N
      KI=KI+N
      HOLD=-A(KI)
      JI=KI-K+J
      A(KI)=A(JI)
30      A(JI) =HOLD
C
C      INTERCHANGE COLUMNS
C
35      I=M(K)

```

```

      IF(I-K) 45,45,38
38 JP=N*(I-1)
   DO 40 J=1,N
      JK=NK+J
      JI=JP+J
      HOLD=-A(JK)
      A(JK)=A(JI)
40 A(JI) =HOLD

C
C      DIVIDE COLUMN BY MINUS PIVOT (VALUE OF PIVOT ELEMENT IS
C      CONTAINED IN BIGA)
C
45 IF(BIGA) 48,46,48
46 D=0.0
   RETURN
48 DO 55 I=1,N
      IF(I-K) 50,55,50
50 IK=NK+I
      A(IK)=A(IK)/(-BIGA)
55 CONTINUE

C
C      REDUCE MATRIX
C
   DO 65 I=1,N
      IK=NK+I
      HOLD=A(IK)
      IJ=I-N
      DO 65 J=1,N
         IJ=IJ+N
         IF(I-K) 60,65,60
60 IF(J-K) 62,65,62
62 KJ=IJ-I+K
      A(IJ)=HOLD*A(KJ)+A(IJ)
65 CONTINUE

C
C      DIVIDE ROW BY PIVOT
C
      KJ=K-N
      DO 75 J=1,N
         KJ=KJ+N
         IF(J-K) 70,75,70
70 A(KJ)=A(KJ)/BIGA
75 CONTINUE

C
C      PRODUCT OF PIVOTS
C
      D=D*BIGA

C
C      REPLACE PIVOT BY RECIPROCAL
C

```

```

      A(KK)=1.0/BIGA
80  CONTINUE
C
C      FINAL ROW AND COLUMN INTERCHANGE
C
      K=N
100 K=(K-1)
      IF(K) 150,150,105
105 I=L(K)
      IF(I-K) 120,120,108
108 JQ=N*(K-1)
      JR=N*(I-1)
      DO 110 J=1,N
      JK=JQ+J
      HOLD=A(JK)
      JI=JR+J
      A(JK)=-A(JI)
110 A(JI) =HOLD
120 J=M(K)
      IF(J-K) 100,100,125
125 KI=K-N
      DO 130 I=1,N
      KI=KI+I
      HOLD=A(KI)
      JI=KI-K+J
      A(KI)=-A(JI)
130 A(JI) =HOLD
      GO TO 100
150 RETURN
      END

C
C .....
C
C      SUBROUTINE RCUT
C
C      PURPOSE
C      PARTITION A MATRIX BETWEEN SPECIFIED ROWS TO FORM TWO
C      RESULTANT MATRICES
C
C      USAGE
C      CALL RCUT (A,L,R,S,N,M,MS)
C
C      DESCRIPTION OF PARAMETERS
C      A - NAME OF INPUT MATRIX
C      L - ROW OF A ABOVE WHICH PARTITIONING TAKES PLACE

```

```

C      R - NAME OF MATRIX TO BE FORMED FROM UPPER PORTION OF A
C      S - NAME OF MATRIX TO BE FORMED FROM LOWER PORTION OF A
C      N - NUMBER OF ROWS IN A
C      M - NUMBER OF COLUMNS IN A
C      MS - ONE DIGIT NUMBER FOR STORAGE MODE OF MATRIX A
C           0 - GENERAL
C           1 - SYMMETRIC
C           2 - DIAGONAL
C
C      REMARKS
C      MATRIX R CANNOT BE IN SAME LOCATION AS MATRIX A
C      MATRIX S CANNOT BE IN SAME LOCATION AS MATRIX A
C      MATRIX R CANNOT BE IN SAME LOCATION AS MATRIX S
C      MATRIX R AND MATRIX S ARE ALWAYS GENERAL MATRICES
C
C      SUBROUTINES AND FUNCTION SUBPROGRAMS REQUIRED
C      LOC
C
C      METHOD
C      ELEMENTS OF MATRIX A ABOVE ROW L ARE MOVED TO FORM MATRIX R
C      OF L-1 ROWS AND M COLUMNS. ELEMENTS OF MATRIX A IN ROW L
C      AND BELOW ARE MOVED TO FORM MATRIX S OF N-L+1 ROWS AND M
C      COLUMNS
C
C      .....
C
C      SUBROUTINE RCUT(A,L,R,S,N,M,MS)
C      DIMENSION A(1),R(1),S(1)
C
C      IR=0
C      IS=0
C      DO 70 J=1,M
C      DO 70 I=1,N
C
C      FIND LOCATION IN OUTPUT MATRIX AND SET TO ZERO
C
C      IF(I-L) 20,10,10
C 10 IS=IS+1
C      S(IS)=0.0
C      GO TO 30
C 20 IR=IR+1
C      R(IR)=0.0
C
C      LOCATE ELEMENT FOR ANY MATRIX STORAGE MODE
C
C 30 CALL LOC(I,J,IJ,N,M,MS)
C
C      TEST FOR ZERO ELEMENT IN DIAGONAL MATRIX
C
C      IF(IJ) 40,70,40

```

```
C
C      DETERMINE WHETHER ABOVE OR BELOW L
C
40 IF(I-L) 60,50,50
50 S(IS)=A(IJ)
   GO TO 70
60 R(IR)=A(IJ)
70 CONTINUE
   RETURN
   END
>
```

TABLE I
MAXIMUM MAGNITUDES OF THE ACTIVE MUSCLE FORCE & MOMENT VECTORS
AT THE SHOULDER JOINTS OF THREE MALE SUBJECTS
DURING DISLODGING OF THE ARM FROM THE INDICATED POSITIONS

ARM POSITION	MAGNITUDE	SUBJECT MS 1	SUBJECT MS 2	SUBJECT MS 3
POSITION #1 SEAT ARMREST INITIATION FORCE F_1	FORCE (N)	225.33	270.60	189.11
		243.62	271.90	201.03
	MOMENT (N-m)	105.18	108.00	99.88
		107.56	109.70	105.88
POSITION #1 SEAT ARMREST INITIATION FORCE F_2	FORCE (N)	174.92	217.95	111.81
		181.18	235.39	113.62
	MOMENT (N-m)	58.08	54.79	37.54
		73.19	65.78	38.68
POSITION #2 D-RING FORCE SIMULATION	FORCE (N)	144.12	147.04	122.71
		174.33	153.83	155.23
	MOMENT (N-m)	69.96	70.79	69.98
		81.33	75.45	87.46
POSITION #3 FACE CURTAIN FORCE SIMULATION F_3	FORCE (N)	216.91	225.98	189.63
		269.93	244.42	206.04
	MOMENT (N-m)	65.81	55.08	83.55
		85.06	58.41	89.95
POSITION #3 FACE CURTAIN FORCE SIMULATION F_4	FORCE (N)	232.41	225.42	195.55
		277.27	250.85	210.67
	MOMENT (N-m)	86.99	68.70	83.21
		89.51	78.64	89.72

TABLE II
MAXIMUM MAGNITUDES OF THE ACTIVE MUSCLE FORCE & MOMENT VECTORS AT THE
SHOULDER JOINTS OF THREE FEMALE SUBJECTS DURING DISLODGING OF
THE ARM FROM THE INDICATED POSITIONS

ARM POSITION	MAGNITUDE	SUBJECT FS 1	SUBJECT FS 2	SUBJECT FS 3
POSITION #1 SEAT ARMREST INITIATION FORCE F ₁	FORCE (N)	79.54	95.05	83.47
		88.31	111.62	84.80
	MOMENT (N-m)	36.12	38.14	35.36
		37.00	46.25	38.06
POSITION #1 SEAT ARMREST INITIATION FORCE F ₂	FORCE (N)	86.03	95.74	139.88
		88.27	98.81	140.05
	MOMENT (N-m)	21.58	30.07	51.12
		22.35	31.52	63.81
POSITION #2 D-RING FORCE SIMULATION	FORCE (N)	56.56	57.19	45.54
		63.56	59.18	51.27
	MOMENT (N-m)	25.89	28.76	22.00
		28.82	29.14	24.57
POSITION #3 FACE CURTAIN FORCE SIMULATION F ₃	FORCE (N)	86.86	96.52	67.10
		92.99	120.79	68.88
	MOMENT (N-m)	30.78	30.42	22.24
		34.95	33.35	23.62
POSITION # 3 FACE CURTAIN FORCE SIMULATION F ₄	FORCE (N)	68.52	92.95	87.01
		73.43	100.71	103.87
	MOMENT (N-m)	30.74	32.60	30.74
		31.25	35.22	37.45

TABLE III
MAXIMUM MAGNITUDES OF THE ACTIVE MUSCLE FORCE & MOMENT VECTORS
AT THE SHOULDER JOINTS OF THREE MALE SUBJECTS AT THE
DISLODGED POSITIONS OF THE LOWER ARM FROM THE SEAT ARMREST

LOWER ARM POSITION	MAGNITUDE	SUBJECT MS 1	SUBJECT MS 2	SUBJECT MS 3
30° Laterally Rotated F_1	FORCE (N)	190.08	186.70	150.63
		223.62	205.05	170.97
	MOMENT (N-m)	81.06	70.25	74.57
		89.61	75.36	84.05
60° Laterally Rotated F_1	FORCE (N)	216.58	182.32	126.24
		224.26	195.10	130.89
	MOMENT (N-m)	81.10	65.45	62.66
		83.33	69.20	62.95
Rotated to the Lateral Limit F_1	FORCE (N)	201.02	184.65	120.30
		244.17	207.39	124.43
	MOMENT (N-m)	79.27	64.45	55.40
		97.62	72.95	58.68

TABLE IV
MAXIMUM MAGNITUDES OF THE ACTIVE MUSCLE FORCE & MOMENT VECTORS
AT THE SHOULDER JOINTS OF THREE FEMALE SUBJECTS AT THE
DISLODGED POSITIONS OF THE LOWER ARM FROM THE SEAT ARMREST

LOWER ARM POSITION	MAGNITUDE	SUBJECT FS 1	SUBJECT FS 2	SUBJECT FS 3
30° Laterally Rotated F_1	FORCE (N)	68.06 70.83	77.18 80.63	68.14 74.57
	MOMENT (N-m)	27.47 29.12	30.72 33.88	25.57 31.06
60° Laterally Rotated F_1	FORCE (N)	77.61 80.17	72.34 75.20	69.20 85.87
	MOMENT (N-m)	30.56 32.98	28.26 29.30	29.06 31.58
Rotated to the Lateral Limit F_1	FORCE (N)	74.61 77.89	63.34 69.37	79.15 85.15
	MOMENT (N-m)	26.96 27.29	23.29 26.95	33.04 39.40

TABLE V
MAXIMUM MAGNITUDES OF THE ACTIVE MUSCLE FORCE & MOMENT VECTORS
AT THE SHOULDER JOINTS OF THREE MALE SUBJECTS
FOR THE INDICATED POSITIONS OF THE ARM WITH $\phi = 0^\circ$

ARM POSITION	MAGNITUDE	SUBJECT MS 1	SUBJECT MS 2	SUBJECT MS 3
FORCE APPLICATION ON THE ELBOW $\theta = 0^\circ$	FORCE (N)	195.43	278.34	165.49
		257.96	304.91	169.84
	MOMENT (N-m)	55.74	77.34	59.80
		74.80	89.41	60.87
FORCE APPLICATION ON THE WRIST $\theta = 0^\circ$	FORCE (N)	113.93	163.43	70.81
		131.51	170.81	74.76
	MOMENT (N-m)	59.20	76.15	38.18
		65.49	81.71	38.99
FORCE APPLICATION ON THE ELBOW $\theta = -30^\circ$	FORCE (N)	336.28	349.22	220.20
		348.20	358.60	228.40
	MOMENT (N-m)	109.09	100.82	77.38
		112.64	103.64	82.46
FORCE APPLICATION ON THE WRIST $\theta = -30^\circ$	FORCE (N)	187.47	158.38	92.30
		192.11	162.46	94.25
	MOMENT (N-m)	86.84	77.80	49.50
		89.12	79.78	51.71
FORCE APPLICATION ON THE ELBOW $\theta = -\text{LIMIT}$	FORCE (N)	343.56	368.62	234.70
		369.63	403.54	240.85
	MOMENT (N-m)	113.54	105.08	81.49
		117.80	117.95	82.10
FORCE APPLICATION ON THE WRIST $\theta = -\text{LIMIT}$	FORCE (N)	175.52	167.15	97.32
		227.63	174.98	102.26
	MOMENT (N-m)	78.85	80.69	50.75
		103.15	87.54	52.86

TABLE VI
MAXIMUM MAGNITUDES OF THE ACTIVE MUSCLE FORCE & MOMENT VECTORS
AT THE SHOULDER JOINTS OF THREE FEMALE SUBJECTS
FOR THE INDICATED POSITIONS OF THE ARM WITH $\phi = 0^\circ$

ARM POSITION	MAGNITUDE	SUBJECT FS 1	SUBJECT FS 2	SUBJECT FS 3
FORCE APPLICATION ON THE ELBOW $\theta = 0^\circ$	FORCE (N)	110.41	111.21	117.04
		127.22	131.74	119.67
	MOMENT (N-m)	32.82	36.84	30.59
		34.07	43.54	33.87
FORCE APPLICATION ON THE WRIST $\theta = 0^\circ$	FORCE (N)	59.51	58.47	57.35
		54.22	58.95	60.04
	MOMENT (N-m)	30.65	31.11	28.64
		28.50	31.46	31.28
FORCE APPLICATION ON THE ELBOW $\theta = -30^\circ$	FORCE (N)	183.55	112.05	171.31
		193.77	123.24	175.78
	MOMENT (N-m)	55.32	35.91	50.44
		56.63	38.26	50.96
FORCE APPLICATION ON THE WRIST $\theta = -30^\circ$	FORCE (N)	90.12	53.50	90.17
		97.93	57.25	94.04
	MOMENT (N-m)	40.39	27.30	41.66
		45.56	28.58	42.15
FORCE APPLICATION ON THE ELBOW $\theta = -\text{LIMIT}$	FORCE (N)	106.57	141.38	194.15
		111.54	142.33	197.63
	MOMENT (N-m)	34.09	41.49	57.72
		34.75	43.72	59.42
FORCE APPLICATION ON THE WRIST $\theta = -\text{LIMIT}$	FORCE (N)	75.40	64.17	90.99
		87.19	66.94	103.36
	MOMENT (N-m)	35.02	31.96	44.22
		42.43	32.30	54.76

TABLE VII
MAXIMUM MAGNITUDES OF THE ACTIVE MUSCLE FORCE & MOMENT VECTORS
AT THE SHOULDER JOINTS OF THREE MALE SUBJECTS
FOR THE DISLODGED POSITIONS OF THE ARM WITH $\phi = 30^\circ$

ARM POSITION	MAGNITUDE	SUBJECT MS 1	SUBJECT MS 2	SUBJECT MS 3
FORCE APPLICATION ON THE ELBOW $\theta = 30^\circ$	FORCE	239.41	262.51	110.97
	(N)	249.87	284.39	128.48
	MOMENT	75.62	59.03	42.89
	(N-m)	81.66	61.76	49.41
FORCE APPLICATION ON THE WRIST $\theta = 30^\circ$	FORCE	142.44	155.99	88.05
	(N)	166.42	163.92	92.52
	MOMENT	69.91	73.59	53.26
	(N-m)	76.09	80.01	56.95
FORCE APPLICATION ON THE ELBOW $\theta = 60^\circ$	FORCE	211.71	183.68	144.58
	(N)	261.64	189.12	210.57
	MOMENT	71.94	51.93	56.38
	(N-m)	86.92	61.35	80.81
FORCE APPLICATION ON THE WRIST $\theta = 60^\circ$	FORCE	130.69	123.70	96.44
	(N)	132.63	132.28	101.70
	MOMENT	65.85	52.56	61.05
	(N-m)	67.27	54.52	63.55
FORCE APPLICATION ON THE ELBOW $\theta = 90^\circ$	FORCE	175.82	199.97	156.30
	(N)	186.68	208.88	183.83
	MOMENT	60.30	53.20	56.34
	(N-m)	62.51	56.44	67.10
FORCE APPLICATION ON THE WRIST $\theta = 90^\circ$	FORCE	117.19	104.66	79.50
	(N)	155.61	120.30	85.31
	MOMENT	59.31	48.47	44.99
	(N-m)	69.14	56.75	47.91
FORCE APPLICATION ON THE ELBOW $\theta = 120^\circ$	FORCE	209.91	156.46	153.83
	(N)	233.27	159.02	161.54
	MOMENT	63.20	46.82	60.77
	(N-m)	70.80	46.88	63.14
FORCE APPLICATION ON THE WRIST $\theta = 120^\circ$	FORCE	95.74	125.07	81.19
	(N)	127.94	134.72	82.21
	MOMENT	57.02	62.68	54.98
	(N-m)	66.70	64.66	56.21

TABLE VIII

MAXIMUM MAGNITUDES OF THE ACTIVE MUSCLE FORCE & MOMENT VECTORS
AT THE SHOULDER JOINTS OF THREE FEMALE SUBJECTS
FOR THE DISLODGED POSITIONS OF THE ARM WITH $\phi = 30^\circ$

ARM POSITION	MAGNITUDE	SUBJECT FS 1	SUBJECT FS 2	SUBJECT FS 3
FORCE APPLICATION ON THE ELBOW $\theta = 30^\circ$	FORCE (N)	111.90	126.84	92.03
		121.68	128.23	107.61
	MOMENT (N-m)	35.90	41.55	25.99
		39.59	43.16	31.59
FORCE APPLICATION ON THE WRIST $\theta = 30^\circ$	FORCE (N)	44.83	53.40	40.65
		57.75	56.89	51.59
	MOMENT (N-m)	22.12	28.92	21.41
		27.48	30.92	26.82
FORCE APPLICATION ON THE ELBOW $\theta = 60^\circ$	FORCE (N)	107.70	124.52	97.55
		110.93	130.20	105.38
	MOMENT (N-m)	35.08	37.75	30.17
		35.45	42.19	32.89
FORCE APPLICATION ON THE WRIST $\theta = 60^\circ$	FORCE (N)	61.40	48.58	45.36
		62.09	53.23	48.47
	MOMENT (N-m)	29.11	24.79	22.33
		31.52	26.86	25.13
FORCE APPLICATION ON THE ELBOW $\theta = 90^\circ$	FORCE (N)	109.36	83.32	83.65
		113.13	110.23	84.73
	MOMENT (N-m)	39.09	22.26	23.40
		40.81	38.31	24.15
FORCE APPLICATION ON THE WRIST $\theta = 90^\circ$	FORCE (N)	37.74	58.95	41.07
		48.51	71.67	42.49
	MOMENT (N-m)	20.92	27.84	20.21
		22.54	34.94	21.07
FORCE APPLICATION ON THE ELBOW $\theta = 120^\circ$	FORCE (N)	160.39	109.67	97.65
		173.74	134.43	99.79
	MOMENT (N-m)	50.73	31.07	29.80
		53.14	35.57	30.98
FORCE APPLICATION ON THE WRIST $\theta = 120^\circ$	FORCE (N)	65.96	60.57	53.09
		73.15	69.78	54.58
	MOMENT (N-m)	36.87	29.00	27.75
		41.51	35.30	27.97

TABLE IX
MAXIMUM MAGNITUDES OF THE ACTIVE MUSCLE FORCE & MOMENT VECTORS
AT THE SHOULDER JOINTS OF THREE MALE SUBJECTS
FOR THE DISLODGED POSITIONS OF THE ARM WITH $\phi = 60^\circ$

ARM POSITION	MAGNITUDE	SUBJECT MS 1	SUBJECT MS 2	SUBJECT MS 3
FORCE APPLICATION ON THE ELBOW $\theta = 30^\circ$	FORCE	231.59	273.04	122.72
	(N)	265.38	288.02	128.31
	MOMENT	71.94	72.03	46.68
	(N-m)	86.33	75.89	47.69
FORCE APPLICATION ON THE WRIST $\theta = 30^\circ$	FORCE	135.39	166.15	70.74
	(N)	142.05	175.66	76.16
	MOMENT	67.88	82.25	43.22
	(N-m)	68.20	83.40	45.11
FORCE APPLICATION ON THE ELBOW $\theta = 60^\circ$	FORCE	221.19	255.48	128.97
	(N)	297.04	294.77	162.52
	MOMENT	94.27	58.04	50.44
	(N-m)	97.53	61.36	63.22
FORCE APPLICATION ON THE WRIST $\theta = 60^\circ$	FORCE	153.05	132.97	61.22
	(N)	162.77	134.47	69.89
	MOMENT	79.13	58.35	38.46
	(N-m)	82.29	61.35	42.74
FORCE APPLICATION ON THE ELBOW $\theta = 90^\circ$	FORCE	279.48	266.66	154.85
	(N)	281.73	289.51	165.20
	MOMENT	82.88	57.42	52.06
	(N-m)	84.16	62.15	54.70
FORCE APPLICATION ON THE WRIST $\theta = 90^\circ$	FORCE	135.38	115.52	68.37
	(N)	154.43	135.58	69.18
	MOMENT	65.30	53.44	42.75
	(N-m)	75.98	60.25	43.69
FORCE APPLICATION ON THE ELBOW $\theta = 120^\circ$	FORCE	191.87	189.28	144.49
	(N)	209.96	204.40	148.61
	MOMENT	55.41	53.12	49.67
	(N-m)	63.19	56.10	57.76
FORCE APPLICATION ON THE WRIST $\theta = 120^\circ$	FORCE	106.95	113.14	59.89
	(N)	114.70	117.04	63.32
		56.12	55.86	40.36
	(N-m)	57.21	56.63	42.55

TABLE X
MAXIMUM MAGNITUDES OF THE ACTIVE MUSCLE FORCE & MOMENT VECTORS
AT THE SHOULDER JOINTS OF THREE FEMALE SUBJECTS
FOR THE DISLODGED POSITIONS OF THE ARM WITH $\phi = 60^\circ$

ARM POSITION	MAGNITUDE	SUBJECT FS 1	SUBJECT FS 2	SUBJECT FS 3
FORCE APPLICATION ON THE ELBOW $\theta = 30^\circ$	FORCE (N)	87.00	110.12	99.11
		107.62	128.26	110.32
	MOMENT (N-m)	25.60	34.29	27.67
		31.20	40.10	32.26
FORCE APPLICATION ON THE WRIST $\theta = 30^\circ$	FORCE (N)	60.43	53.69	44.48
		66.36	64.96	46.39
	MOMENT (N-m)	29.03	26.49	20.76
		31.36	32.64	22.41
FORCE APPLICATION ON THE ELBOW $\theta = 60^\circ$	FORCE (N)	50.67	106.58	89.47
		62.50	115.55	93.84
	MOMENT (N-m)	17.20	30.76	24.52
		20.25	33.65	26.18
FORCE APPLICATION ON THE WRIST $\theta = 60^\circ$	FORCE (N)	33.01	56.45	43.46
		39.81	58.22	46.08
	MOMENT (N-m)	16.63	28.75	23.88
		19.56	30.79	25.26
FORCE APPLICATION ON THE ELBOW $\theta = 90^\circ$	FORCE (N)	52.51	95.78	85.49
		60.87	110.53	87.08
	MOMENT (N-m)	13.46	22.29	21.49
		18.46	23.41	22.88
FORCE APPLICATION ON THE WRIST $\theta = 90^\circ$	FORCE (N)	35.38	56.41	44.70
		38.09	59.69	45.27
	MOMENT (N-m)	16.70	25.02	20.66
		19.80	26.52	21.70
FORCE APPLICATION ON THE ELBOW $\theta = 120^\circ$	FORCE (N)	85.92	116.93	91.87
		126.16	120.65	97.20
	MOMENT (N-m)	27.66	28.85	23.09
		38.02	30.01	24.43
FORCE APPLICATION ON THE WRIST $\theta = 120^\circ$	FORCE (N)	32.22	55.02	38.90
		34.90	57.79	48.45
	MOMENT (N-m)	18.07	27.41	21.77
		19.18	28.60	26.49

TABLE XI
 MAXIMUM MAGNITUDES OF THE ACTIVE MUSCLE FORCE & MOMENT VECTORS
 AT THE SHOULDER JOINTS OF THREE MALE SUBJECTS
 FOR THE DISLODGED POSITIONS OF THE ARM WITH $\phi = 90^\circ$

ARM POSITION	MAGNITUDE	SUBJECT MS 1	SUBJECT MS 2	SUBJECT MS 3
FORCE APPLICATION ON THE ELBOW $\theta = 30^\circ$	FORCE (N)	242.17 258.91	271.56 298.58	150.16 162.89
	MOMENT (N-m)	82.09 86.48	77.14 81.24	56.40 58.53
FORCE APPLICATION ON THE WRIST $\theta = 30^\circ$	FORCE (N)	128.28 159.72	154.37 159.21	79.44 107.75
	MOMENT (N-m)	65.18 84.07	71.70 76.98	43.34 58.24
FORCE APPLICATION ON THE ELBOW $\theta = 60^\circ$	FORCE (N)	272.55 282.05	241.18 242.61	162.34 189.96
	MOMENT (N-m)	88.52 91.36	65.35 66.48	56.71 70.75
FORCE APPLICATION ON THE WRIST $\theta = 60^\circ$	FORCE (N)	115.30 138.25	139.65 145.75	76.88 86.38
	MOMENT (N-m)	54.39 65.97	65.10 67.60	44.46 46.05
FORCE APPLICATION ON THE ELBOW $\theta = 90^\circ$	FORCE (N)	274.79 288.15	239.06 244.58	145.39 156.17
	MOMENT (N-m)	77.34 81.76	64.72 66.24	53.02 57.30
FORCE APPLICATION ON THE WRIST $\theta = 90^\circ$	FORCE (N)	171.14 178.44	134.31 138.19	81.39 91.84
	MOMENT (N-m)	77.34 86.27	61.70 66.70	47.96 54.50
FORCE APPLICATION ON THE ELBOW $\theta = 120^\circ$	FORCE (N)	153.98 168.87	226.00 238.61	109.79 113.48
	MOMENT (N-m)	47.93 62.96	49.83 57.34	37.48 43.00
FORCE APPLICATION ON THE WRIST $\theta = 120^\circ$	FORCE (N)	127.83 132.02	134.38 145.78	52.80 54.11
	MOMENT (N-m)	64.29 65.25	63.12 71.79	31.18 32.31

TABLE XII
MAXIMUM MAGNITUDES OF THE ACTIVE MUSCLE FORCE & MOMENT VECTORS
AT THE SHOULDER JOINTS OF THREE FEMALE SUBJECTS
FOR THE DISLODGED POSITIONS OF THE ARM WITH $\phi = 90^\circ$

ARM POSITION	MAGNITUDE	SUBJECT FS 1	SUBJECT FS 2	SUBJECT FS 3
FORCE APPLICATION ON THE ELBOW $\theta = 30^\circ$	FORCE	74.77	110.96	108.56
	(N)	81.77	114.49	115.19
	MOMENT	20.47	34.08	30.39
	(N-m)	24.59	36.15	32.38
FORCE APPLICATION ON THE WRIST $\theta = 30^\circ$	FORCE	37.54	41.82	50.59
	(N)	38.80	45.62	53.53
	MOMENT	20.98	17.38	24.86
	(N-m)	21.74	19.53	26.48
FORCE APPLICATION ON THE ELBOW $\theta = 60^\circ$	FORCE	82.00	105.37	93.52
	(N)	113.11	134.07	111.81
	MOMENT	21.44	31.32	28.31
	(N-m)	30.53	36.17	33.00
FORCE APPLICATION ON THE WRIST $\theta = 60^\circ$	FORCE	39.97	57.53	47.47
	(N)	47.76	61.99	52.28
	MOMENT	20.02	30.81	24.25
	(N-m)	22.97	32.90	26.53
FORCE APPLICATION ON THE ELBOW $\theta = 90^\circ$	FORCE	59.69	105.33	82.48
	(N)	70.72	118.81	93.33
	MOMENT	14.88	30.12	24.59
	(N-m)	17.94	32.07	27.68
FORCE APPLICATION ON THE WRIST $\theta = 90^\circ$	FORCE	38.48	49.64	48.48
	(N)	42.89	51.27	56.44
	MOMENT	18.58	25.37	23.59
	(N-m)	19.41	26.17	27.08
FORCE APPLICATION ON THE ELBOW $\theta = 120^\circ$	FORCE	61.91	96.00	62.37
	(N)	68.25	105.48	70.15
	MOMENT	30.90	45.99	19.81
	(N-m)	33.89	51.18	21.36
FORCE APPLICATION ON THE WRIST $\theta = 120^\circ$	FORCE	36.28	38.44	23.74
	(N)	46.82	39.30	26.49
	MOMENT	17.45	23.33	13.65
	(N-m)	20.53	24.24	15.01

TABLE XIII
MAXIMUM MAGNITUDES OF THE ACTIVE MUSCLE FORCE & MOMENT VECTORS
AT THE SHOULDER JOINTS OF THREE MALE SUBJECTS
FOR THE DISLODGED POSITIONS OF THE ARM WITH $\phi = 120^\circ$

ARM POSITION	MAGNITUDE	SUBJECT MS 1	SUBJECT MS 2	SUBJECT MS 3
FORCE APPLICATION ON THE ELBOW $\theta = 30^\circ$	FORCE (N)	232.37	311.03	187.99
		237.60	313.11	189.25
	MOMENT (N-m)	74.79	92.98	68.50
		79.90	93.13	68.73
FORCE APPLICATION ON THE WRIST $\theta = 30^\circ$	FORCE (N)	136.84	138.64	89.37
		149.78	163.92	102.06
	MOMENT (N-m)	65.56	67.48	48.52
		72.25	77.29	55.96
FORCE APPLICATION ON THE ELBOW $\theta = 60^\circ$	FORCE (N)	288.36	289.94	105.18
		293.48	305.39	129.64
	MOMENT (N-m)	94.11	80.83	36.33
		95.55	87.81	43.55
FORCE APPLICATION ON THE WRIST $\theta = 60^\circ$	FORCE (N)	176.40	154.86	68.49
		181.44	171.18	76.49
	MOMENT (N-m)	84.98	77.47	38.80
		87.58	81.65	43.29
FORCE APPLICATION ON THE ELBOW $\theta = 90^\circ$	FORCE (N)	282.09	237.45	130.68
		293.72	288.61	138.09
	MOMENT (N-m)	92.61	68.43	50.85
		95.88	81.46	52.07
FORCE APPLICATION ON THE WRIST $\theta = 90^\circ$	FORCE (N)	157.57	135.00	57.08
		172.01	155.79	56.33
	MOMENT (N-m)	75.89	63.14	32.07
		82.02	71.28	31.82
FORCE APPLICATION ON THE ELBOW $\theta = 120^\circ$	FORCE (N)	242.36	248.94	127.24
		255.76	258.96	130.89
	MOMENT (N-m)	70.87	65.25	49.42
		84.12	68.23	50.58
FORCE APPLICATION ON THE WRIST $\theta = 120^\circ$	FORCE (N)	131.63	121.65	51.67
		143.31	123.97	54.42
	MOMENT (N-m)	66.34	53.29	29.18
		68.84	54.88	30.58

TABLE XIV
MAXIMUM MAGNITUDES OF THE ACTIVE MUSCLE FORCE & MOMENT VECTORS
AT THE SHOULDER JOINTS OF THREE FEMALE SUBJECTS
FOR THE DISLODGED POSITIONS OF THE ARM WITH $\phi = 120^\circ$

ARM POSITION	MAGNITUDE	SUBJECT FS 1	SUBJECT FS 2	SUBJECT FS 3
FORCE APPLICATION ON THE ELBOW $\theta = 30^\circ$	FORCE (N)	123.64 137.82	96.08 96.34	159.53 161.00
	MOMENT (N-m)	38.07 42.29	31.20 31.22	49.07 49.85
FORCE APPLICATION ON THE WRIST $\theta = 30^\circ$	FORCE (N)	65.77 68.25	56.79 59.33	88.96 90.48
	MOMENT (N-m)	31.15 33.89	29.73 31.10	45.04 46.93
FORCE APPLICATION ON THE ELBOW $\theta = 60^\circ$	FORCE (N)	137.73 163.10	80.46 87.29	141.90 160.51
	MOMENT (N-m)	42.51 49.77	25.47 26.66	39.06 44.16
FORCE APPLICATION ON THE WRIST $\theta = 60^\circ$	FORCE (N)	70.91 71.63	51.93 52.81	87.19 88.96
	MOMENT (N-m)	35.61 36.37	26.91 27.87	43.07 43.47
FORCE APPLICATION ON THE ELBOW $\theta = 90^\circ$	FORCE (N)	141.04 142.08	77.37 89.85	113.56 124.98
	MOMENT (N-m)	42.58 43.02	23.28 29.42	31.23 35.45
FORCE APPLICATION ON THE WRIST $\theta = 90^\circ$	FORCE (N)	63.86 67.13	40.11 46.64	58.16 76.43
	MOMENT (N-m)	31.53 33.31	20.62 22.50	29.05 34.39
FORCE APPLICATION ON THE ELBOW $\theta = 120^\circ$	FORCE (N)	110.62 119.85	76.51 80.79	107.82 112.13
	MOMENT (N-m)	34.42 37.13	29.04 33.68	28.87 29.81
FORCE APPLICATION ON THE WRIST $\theta = 120^\circ$	FORCE (N)	70.67 77.66	37.76 44.07	54.33 58.01
	MOMENT (N-m)	32.81 34.73	18.30 21.32	25.01 27.25

APPENDIX E

TABULATED NUMERICAL RESULTS (TABLES XV-XXVIII)
FOR THE LOWER EXTREMITIES

TABLE XV
MAXIMUM MAGNITUDES OF THE ACTIVE MUSCLE FORCE AND MOMENT VECTORS
AT THE HIP JOINTS OF THREE MALE SUBJECTS FOR THE INDICATED
POSITIONS OF THE LEG WITH $\theta = 0$, KNEE LOCKED.

LEG POSITION	MAGNITUDE	SUBJECT MS 1	SUBJECT MS 2	SUBJECT MS 3
FORCE APPLIED ON THE KNEE $\phi = 30^\circ$	FORCE	363.60	355.90	269.78
	(N)	360.47	326.85	251.76
	MOMENT	171.31	185.96	134.68
	(N-m)	171.94	174.60	125.10
FORCE APPLIED ON THE ANKLE $\phi = 30^\circ$	FORCE	200.20	299.60	72.15
	(N)	182.44	274.15	71.90
	MOMENT	157.24	225.64	36.19
	(N-m)	137.62	208.13	28.31
FORCE APPLIED ON THE KNEE $\phi = \text{LIMIT}$	FORCE	395.50	315.84	263.29
	(N)	392.38	305.42	228.96
	MOMENT	188.34	158.56	101.65
	(N-m)	189.84	153.90	84.40
FORCE APPLIED ON THE ANKLE $\phi = \text{LIMIT}$	FORCE	233.98	248.35	236.88
	(N)	231.03	225.70	224.02
	MOMENT	183.13	183.39	142.20
	(N-m)	181.84	164.16	128.11

TABLE XVI
MAXIMUM MAGNITUDES OF THE ACTIVE MUSCLE FORCE AND MOMENT VECTORS
AT THE HIP JOINTS OF THREE FEMALE SUBJECTS FOR THE INDICATED
POSITIONS OF THE LEG WITH $\theta = 0$, KNEE LOCKED.

LEG POSITION	MAGNITUDE	SUBJECT FS 1	SUBJECT FS 2	SUBJECT FS 3
FORCE APPLIED ON THE KNEE $\phi = 30^\circ$	FORCE	187.70	210.83	250.16
	(N)	179.53	180.61	244.26
	MOMENT	84.04	76.28	120.61
	(N-m)	81.44	64.78	117.65
FORCE APPLIED ON THE ANKLE $\phi = 30^\circ$	FORCE	87.77	135.85	102.29
	(N)	66.52	131.49	101.66
	MOMENT	68.22	44.87	71.85
	(N-m)	53.18	39.73	66.19
FORCE APPLIED ON THE KNEE $\phi = 60^\circ$	FORCE	202.43	235.41	229.59
	(N)	171.53	219.00	227.35
	MOMENT	92.92	79.32	112.51
	(N-m)	76.92	75.77	110.22
FORCE APPLIED ON THE ANKLE $\phi = 60^\circ$	FORCE	92.83	159.06	139.46
	(N)	82.05	152.79	133.20
	MOMENT	69.58	38.13	111.08
	(N-m)	62.51	30.38	105.28

TABLE XVII

MAXIMUM MAGNITUDES OF THE ACTIVE MUSCLE FORCE AND MOMENT VECTORS
AT THE HIP JOINTS OF THREE MALE SUBJECTS FOR THE INDICATED
POSITIONS OF THE LEG WITH $\theta = 40^\circ$, KNEE LOCKED.

LEG POSITION	MAGNITUDE	SUBJECT MS 1	SUBJECT MS 2	SUBJECT MS 3
FORCE APPLIED ON THE KNEE $\phi = 30^\circ$	FORCE (N)	280.75	354.66	273.60
		279.54	290.08	259.66
	MOMENT (N-m)	126.14	184.87	169.88
		112.62	155.78	166.26
FORCE APPLIED ON THE ANKLE $\phi = 30^\circ$	FORCE (N)	221.50	271.14	146.71
		218.16	258.20	137.21
	MOMENT (N-m)	162.71	204.23	124.76
		157.10	196.21	92.74
FORCE APPLIED ON THE KNEE $\phi = \text{LIMIT}$	FORCE (N)	328.91	297.32	322.74
		344.12	283.29	314.97
	MOMENT (N-m)	162.98	147.71	159.79
		164.58	141.79	157.63
FORCE APPLIED ON THE ANKLE $\phi = \text{LIMIT}$	FORCE (N)	282.86	204.69	126.13
		281.36	179.79	122.85
	MOMENT (N-m)	221.30	151.02	85.70
		221.20	126.05	83.42

TABLE XVIII
MAXIMUM MAGNITUDES OF THE ACTIVE MUSCLE FORCE AND MOMENT VECTORS
AT THE HIP JOINTS OF THREE MALE SUBJECTS FOR THE INDICATED
POSITIONS OF THE LEG WITH $\theta = 40^\circ$, KNEE FLEXED.

LEG POSITION	MAGNITUDE	SUBJECT MS 1	SUBJECT MS 2	SUBJECT MS 3
FORCE APPLIED ON THE KNEE $\phi = 30^\circ$	FORCE	235.97	261.16	261.98
	(N)	233.59	252.96	249.76
	MOMENT	115.01	126.40	137.74
	(N-m)	113.38	123.86	130.77
FORCE APPLIED ON THE ANKLE $\phi = 30^\circ$	FORCE	150.60	212.05	113.12
	(N)	150.19	211.80	106.22
	MOMENT	93.73	158.23	32.88
	(N-m)	93.14	196.02	31.09
FORCE APPLIED ON THE KNEE $\phi = \text{LIMIT}$	FORCE	352.08	344.08	301.40
	(N)	349.02	309.57	287.37
	MOMENT	169.38	165.56	148.51
	(N-m)	168.57	149.20	143.03
FORCE APPLIED ON THE ANKLE $\phi = \text{LIMIT}$	FORCE	212.26	188.14	119.06
	(N)	196.85	186.31	117.53
	MOMENT	117.41	142.24	79.46
	(N-m)	104.79	146.95	76.34

TABLE XIX
MAXIMUM MAGNITUDES OF THE ACTIVE MUSCLE FORCE AND MOMENT VECTORS
AT THE HIP JOINTS OF THREE FEMALE SUBJECTS FOR THE INDICATED
POSITIONS OF THE LEG WITH $\theta = 40^\circ$, KNEE LOCKED.

LEG POSITION	MAGNITUDE	SUBJECT FS 1	SUBJECT FS 2	SUBJECT FS 3
FORCE APPLIED ON THE KNEE $\phi = 30^\circ$	FORCE	187.70	142.93	230.44
	(N)	182.98	138.58	217.97
	MOMENT	84.04	69.34	118.87
	(N-m)	82.67	67.21	113.14
FORCE APPLIED ON THE ANKLE $\phi = 30^\circ$	FORCE	90.84	72.98	114.32
	(N)	87.77	63.82	107.73
	MOMENT	70.69	55.46	73.25
	(N-m)	68.22	50.28	60.54
FORCE APPLIED ON THE KNEE $\phi = 60^\circ$	FORCE	202.43	178.80	215.65
	(N)	200.16	173.00	211.64
	MOMENT	92.92	87.92	102.08
	(N-m)	91.02	78.67	100.42
FORCE APPLIED ON THE ANKLE $\phi = 60^\circ$	FORCE	92.83	54.67	147.56
	(N)	92.20	54.35	135.67
	MOMENT	69.58	42.60	90.81
	(N-m)	68.88	42.38	85.58
FORCE APPLIED ON THE KNEE $\phi = \text{LIMIT}$	FORCE	248.66	214.24	240.61
	(N)	237.98	203.18	233.66
	MOMENT	111.52	104.75	114.86
	(N-m)	106.46	97.92	105.56
FORCE APPLIED ON THE ANKLE $\phi = \text{LIMIT}$	FORCE	133.51	107.64	147.95
	(N)	121.57	83.15	143.17
	MOMENT	97.69	85.58	87.78
	(N-m)	91.37	70.68	81.78

TABLE XX
MAXIMUM MAGNITUDES OF THE ACTIVE MUSCLE FORCE AND MOMENT VECTORS
AT THE HIP JOINTS OF THREE FEMALE SUBJECTS FOR THE INDICATED
POSITIONS OF THE LEG WITH $\theta = 40^\circ$, KNEE FLEXED.

LEG POSITION	MAGNITUDE	SUBJECT FS 1	SUBJECT FS 2	SUBJECT FS 3
FORCE APPLIED ON THE KNEE $\phi = 30^\circ$	FORCE	187.86	186.09	216.10
	(N)	168.84	185.33	213.08
	MOMENT	85.35	88.35	87.22
	(N-m)	75.95	88.31	85.78
FORCE APPLIED ON THE ANKLE $\phi = 30^\circ$	FORCE	105.71	130.57	100.31
	(N)	102.58	124.07	93.17
	MOMENT	69.02	94.35	57.44
	(N-m)	68.49	81.98	54.95
FORCE APPLIED ON THE KNEE $\phi = 60^\circ$	FORCE	225.16	175.74	228.90
	(N)	186.81	174.25	228.40
	MOMENT	103.07	68.47	103.51
	(N-m)	85.45	62.68	101.71
FORCE APPLIED ON THE ANKLE $\phi = 60^\circ$	FORCE	92.49	119.73	121.16
	(N)	92.22	116.03	110.63
	MOMENT	62.72	86.29	72.39
	(N-m)	58.34	84.27	64.10
FORCE APPLIED ON THE KNEE $\phi = \text{LIMIT}$	FORCE	237.39	147.70	217.49
	(N)	229.24	146.74	214.87
	MOMENT	108.24	59.85	97.13
	(N-m)	104.88	50.65	96.18
FORCE APPLIED ON THE ANKLE $\phi = \text{LIMIT}$	FORCE	115.53	95.89	146.48
	(N)	112.21	91.63	127.15
	MOMENT	79.57	65.11	88.64
	(N-m)	76.89	65.01	73.77

TABLE XXI
MAXIMUM MAGNITUDES OF THE ACTIVE MUSCLE FORCE AND MOMENT VECTORS
AT THE HIP JOINTS OF THREE MALE SUBJECTS FOR THE INDICATED
POSITIONS OF THE LEG WITH $\theta = 90^\circ$, KNEE LOCKED.

LEG POSITION	MAGNITUDE	SUBJECT MS 1	SUBJECT MS 2	SUBJECT MS 3
FORCE APPLIED ON THE KNEE $\phi = 0$	FORCE	179.58	104.88	156.93
	(N)	171.00	100.85	144.48
	MOMENT	76.36	47.17	76.97
	(N-m)	74.22	45.35	72.06
FORCE APPLIED ON THE ANKLE $\phi = 0$	FORCE	122.76	108.63	68.70
	(N)	113.25	103.95	65.53
	MOMENT	97.03	81.76	65.35
	(N-m)	89.35	78.51	61.85
FORCE APPLIED ON THE KNEE $\phi = 30^\circ$	FORCE	258.43	278.49	216.60
	(N)	255.37	259.65	204.70
	MOMENT	123.37	141.21	100.90
	(N-m)	121.42	130.89	94.23
FORCE APPLIED ON THE ANKLE $\phi = 30^\circ$	FORCE	206.81	219.08	120.17
	(N)	199.42	212.99	114.86
	MOMENT	158.40	164.78	104.78
	(N-m)	153.42	159.56	100.19
FORCE APPLIED ON THE KNEE $\phi = 60^\circ$	FORCE	241.66	293.26	262.80
	(N)	209.29	264.13	257.43
	MOMENT	111.01	143.70	128.19
	(N-m)	100.19	130.06	125.37
FORCE APPLIED ON THE ANKLE $\phi = 60^\circ$	FORCE	193.13	235.41	143.23
	(N)	191.78	172.72	122.51
	MOMENT	153.58	138.85	110.64
	(N-m)	152.41	107.27	98.22
FORCE APPLIED ON THE KNEE $\phi = \text{LIMIT}$	FORCE	363.81	404.89	240.94
	(N)	340.15	366.06	217.99
	MOMENT	151.83	196.25	118.43
	(N-m)	141.75	178.22	107.12
FORCE APPLIED ON THE ANKLE $\phi = \text{LIMIT}$	FORCE	216.89	214.93	97.62
	(N)	202.71	188.56	86.39
	MOMENT	152.56	170.00	82.52
	(N-m)	142.40	142.70	75.08

TABLE XXII
MAXIMUM MAGNITUDES OF THE ACTIVE MUSCLE FORCE AND MOMENT VECTORS
AT THE HIP JOINTS OF THREE MALE SUBJECTS FOR THE INDICATED
POSITIONS OF THE LEG WITH $\theta = 90^\circ$, KNEE FLEXED.

LEG POSITION	MAGNITUDE	SUBJECT MS 1	SUBJECT MS 2	SUBJECT MS 3
FORCE APPLIED ON THE KNEE $\phi = 0$	FORCE (N)	267.13 265.47	225.98 219.46	137.94 122.20
	MOMENT (N-m)	126.33 125.96	112.07 110.62	65.03 57.13
FORCE APPLIED ON THE ANKLE $\phi = 0$	FORCE (N)	246.51 235.51	174.45 139.92	73.48 69.44
	MOMENT (N-m)	149.44 146.99	108.59 92.42	49.43 47.89
FORCE APPLIED ON THE KNEE $\phi = 30^\circ$	FORCE (N)	301.30 287.74	262.33 231.63	182.97 174.16
	MOMENT (N-m)	141.86 134.09	135.88 125.28	83.35 78.26
FORCE APPLIED ON THE ANKLE $\phi = 30^\circ$	FORCE (N)	242.00 241.29	194.50 174.54	93.01 80.29
	MOMENT (N-m)	138.08 137.19	124.76 113.05	55.12 44.41
FORCE APPLIED ON THE KNEE $\phi = 60^\circ$	FORCE (N)	274.83 261.89	326.92 312.84	224.62 219.62
	MOMENT (N-m)	117.67 112.03	159.67 151.90	122.04 113.92
FORCE APPLIED ON THE ANKLE $\phi = 60^\circ$	FORCE (N)	341.40 317.56	206.43 196.64	110.16 105.27
	MOMENT (N-m)	132.69 125.01	115.72 109.67	66.65 63.88
FORCE APPLIED ON THE KNEE $\phi = \text{LIMIT}$	FORCE (N)	269.76 255.58	281.39 276.75	252.14 232.98
	MOMENT (N-m)	122.66 117.02	139.54 138.47	126.32 111.52
FORCE APPLIED ON THE ANKLE $\phi = \text{LIMIT}$	FORCE (N)	212.60 204.01	227.62 220.20	86.18 85.76
	MOMENT (N-m)	108.11 102.94	130.84 124.47	56.45 55.39

TABLE XXIII
MAXIMUM MAGNITUDES OF THE ACTIVE MUSCLE FORCE AND MOMENT VECTORS
AT THE HIP JOINTS OF THREE FEMALE SUBJECTS FOR THE INDICATED
POSITIONS OF THE LEG WITH $\theta = 90^\circ$, KNEE LOCKED.

LEG POSITION	MAGNITUDE	SUBJECT FS 1	SUBJECT FS 2	SUBJECT FS 3
FORCE APPLIED ON THE KNEE $\phi = 0$	FORCE	86.78	118.69	81.30
	(N)	86.70	113.95	80.98
	MOMENT	37.36	55.71	35.29
	(N-m)	37.23	54.06	34.82
FORCE APPLIED ON THE ANKLE $\phi = 0$	FORCE	53.37	49.31	48.04
	(N)	51.38	48.39	44.04
	MOMENT	42.28	40.02	38.35
	(N-m)	40.59	39.26	35.49
FORCE APPLIED ON THE KNEE $\phi = 30^\circ$	FORCE	158.80	173.84	182.28
	(N)	149.29	172.29	181.51
	MOMENT	69.35	82.32	83.30
	(N-m)	64.69	81.42	79.89
FORCE APPLIED ON THE ANKLE $\phi = 30^\circ$	FORCE	84.34	78.35	103.24
	(N)	68.08	72.15	97.51
	MOMENT	72.76	67.72	83.75
	(N-m)	59.13	62.19	79.66
FORCE APPLIED ON THE KNEE $\phi = 60^\circ$	FORCE	157.12	143.48	251.60
	(N)	153.24	132.43	241.19
	MOMENT	63.69	69.67	114.94
	(N-m)	61.91	67.03	109.64
FORCE APPLIED ON THE ANKLE $\phi = 60^\circ$	FORCE	70.02	89.32	118.93
	(N)	68.02	83.98	102.39
	MOMENT	53.57	74.39	99.27
	(N-m)	52.49	70.45	84.42
FORCE APPLIED ON THE KNEE $\phi = \text{LIMIT}$	FORCE	194.25	156.35	298.85
	(N)	187.30	153.27	278.59
	MOMENT	88.25	71.83	143.99
	(N-m)	84.68	71.46	131.10
FORCE APPLIED ON THE ANKLE $\phi = \text{LIMIT}$	FORCE	122.73	77.48	150.75
	(N)	118.21	71.58	148.18
	MOMENT	81.24	58.69	115.65
	(N-m)	80.27	55.74	114.77

TABLE XXIV
MAXIMUM MAGNITUDES OF THE ACTIVE MUSCLE FORCE AND MOMENT VECTORS
AT THE HIP JOINTS OF THREE FEMALE SUBJECTS FOR THE INDICATED
POSITIONS OF THE LEG WITH $\theta = 90^\circ$, KNEE FLEXED.

LEG POSITION	MAGNITUDE	SUBJECT FS 1	SUBJECT FS 2	SUBJECT FS 3
FORCE APPLIED ON THE KNEE $\phi = 0$	FORCE (N)	152.27 148.94	152.48 137.03	89.66 85.70
	MOMENT (N-m)	65.22 63.35	74.04 64.12	38.21 32.84
FORCE APPLIED ON THE ANKLE $\phi = 0$	FORCE (N)	85.31 75.21	103.33 94.27	74.29 60.87
	MOMENT (N-m)	46.72 38.77	67.30 61.47	43.99 36.20
FORCE APPLIED ON THE KNEE $\phi = 30^\circ$	FORCE (N)	162.03 159.67	120.55 120.37	157.50 152.97
	MOMENT (N-m)	87.01 84.58	56.02 55.50	73.13 70.08
FORCE APPLIED ON THE ANKLE $\phi = 30^\circ$	FORCE (N)	104.54 103.65	81.15 78.83	132.52 122.08
	MOMENT (N-m)	67.25 67.41	64.62 62.59	78.08 68.17
FORCE APPLIED ON THE KNEE $\phi = 60^\circ$	FORCE (N)	248.47 242.56	160.26 156.69	209.12 196.52
	MOMENT (N-m)	109.61 105.34	75.37 73.06	95.97 90.52
FORCE APPLIED ON THE ANKLE $\phi = 60^\circ$	FORCE (N)	132.46 128.06	86.49 84.67	150.92 144.33
	MOMENT (N-m)	79.41 76.88	62.12 60.97	99.27 94.45
FORCE APPLIED ON THE KNEE $\phi = \text{LIMIT}$	FORCE (N)	185.25 183.18	150.59 149.47	256.72 234.51
	MOMENT (N-m)	84.90 83.31	71.08 71.14	117.89 112.69
FORCE APPLIED ON THE ANKLE $\phi = \text{LIMIT}$	FORCE (N)	160.47 149.07	94.34 78.24	185.65 174.91
	MOMENT (N-m)	90.90 83.66	57.21 43.79	113.45 103.65

TABLE XXV

MAXIMUM MAGNITUDES OF THE ACTIVE MUSCLE FORCE AND MOMENT VECTORS
AT THE HIP JOINTS OF THREE MALE SUBJECTS FOR THE INDICATED
POSITIONS OF THE LEG WITH $\theta = 120^\circ$, KNEE LOCKED.

LEG POSITION	MAGNITUDE	SUBJECT MS 1	SUBJECT MS 2	SUBJECT MS 3
FORCE APPLIED ON THE KNEE $\phi = 0$	FORCE (N)	95.27	119.22	90.25
		62.76	113.54	86.82
	MOMENT (N-m)	43.24	56.50	37.54
		28.24	54.22	37.24
FORCE APPLIED ON THE ANKLE $\phi = 0$	FORCE (N)	70.30	73.67	30.15
		66.54	70.27	29.86
	MOMENT (N-m)	54.58	54.97	26.13
		51.71	51.58	25.86
FORCE APPLIED ON THE KNEE $\phi = 30^\circ$	FORCE (N)	211.95	256.31	145.24
		207.65	238.03	119.63
	MOMENT (N-m)	97.90	122.13	65.94
		94.76	97.47	54.85
FORCE APPLIED ON THE ANKLE $\phi = 30^\circ$	FORCE (N)	80.23	166.02	92.29
		75.92	151.33	90.18
	MOMENT (N-m)	62.18	131.79	78.81
		58.54	109.71	76.91
FORCE APPLIED ON THE KNEE $\phi = \text{LIMIT}$	FORCE (N)	238.81	388.21	229.76
		231.80	343.50	219.12
	MOMENT (N-m)	112.32	171.84	91.09
		109.51	148.21	87.01
FORCE APPLIED ON THE ANKLE $\phi = \text{LIMIT}$	FORCE (N)	157.92	177.56	101.06
		155.16	175.97	92.83
	MOMENT (N-m)	124.91	138.69	75.50
		122.65	137.08	69.53

TABLE XXVI

MAXIMUM MAGNITUDES OF THE ACTIVE MUSCLE FORCE AND MOMENT VECTORS
AT THE HIP JOINTS OF THREE MALE SUBJECTS FOR THE INDICATED
POSITIONS OF THE LEG WITH $\theta = 120^\circ$, KNEE FLEXED.

LEG POSITION	MAGNITUDE	SUBJECTS MS 1	SUBJECTS MS 2	SUBJECTS MS 3
FORCE APPLIED ON THE KNEE $\phi = 0$	FORCE	125.05	111.30	88.23
	(N)	118.38	100.73	86.67
	MOMENT	59.72	51.45	39.14
	(N-m)	57.10	45.72	38.30
FORCE APPLIED ON THE ANKLE $\phi = 0$	FORCE	79.23	95.84	63.49
	(N)	75.34	77.50	60.42
	MOMENT	47.00	51.11	34.88
	(N-m)	45.89	47.13	33.94
FORCE APPLIED ON THE KNEE $\phi = 30^\circ$	FORCE	168.79	214.14	153.79
	(N)	164.55	211.56	149.71
	MOMENT	77.20	92.18	61.31
	(N-m)	77.38	89.05	60.42
FORCE APPLIED ON THE ANKLE $\phi = 30^\circ$	FORCE	106.08	127.08	226.19
	(N)	98.62	118.62	218.82
	MOMENT	66.65	53.62	97.45
	(N-m)	61.97	49.98	92.64
FORCE APPLIED ON THE KNEE $\phi = 60^\circ$	FORCE	278.13	363.66	122.97
	(N)	275.60	348.63	112.15
	MOMENT	127.30	159.34	74.84
	(N-m)	126.00	156.51	66.94
FORCE APPLIED ON THE ANKLE $\phi = 60^\circ$	FORCE	158.36	129.91	76.15
	(N)	151.98	123.21	69.57
	MOMENT	97.88	87.30	52.87
	(N-m)	93.00	80.78	47.41
FORCE APPLIED ON THE KNEE $\phi = \text{LIMIT}$	FORCE	282.46	373.14	246.03
	(N)	229.10	333.97	241.98
	MOMENT	128.14	170.30	129.97
	(N-m)	104.48	151.44	121.63
FORCE APPLIED ON THE ANKLE $\phi = \text{LIMIT}$	FORCE	183.64	199.53	99.50
	(N)	158.55	186.21	95.45
	MOMENT	118.56	127.55	70.00
	(N-m)	101.99	118.86	67.86

TABLE XXVII

MAXIMUM MAGNITUDES OF THE ACTIVE MUSCLE FORCE AND MOMENT VECTORS
AT THE HIP JOINTS OF THREE FEMALE SUBJECTS FOR THE INDICATED
POSITIONS OF THE LEG WITH $\theta = 120^\circ$, KNEE LOCKED.

LEG POSITION	MAGNITUDE	SUBJECT FS 1	SUBJECT FS 2	SUBJECT FS 3
FORCE APPLIED ON THE KNEE $\phi = 0$	FORCE	90.29	124.89	102.98
	(N)	83.41	107.25	94.30
	MOMENT	38.28	51.14	43.49
	(N-m)	37.58	43.39	38.30
FORCE APPLIED ON THE ANKLE $\phi = 0$	FORCE	38.74	31.38	48.66
	(N)	32.15	29.53	41.14
	MOMENT	29.46	25.28	35.55
	(N-m)	24.33	22.92	30.03
FORCE APPLIED ON THE KNEE $\phi = 30^\circ$	FORCE	158.86	175.54	176.50
	(N)	152.75	166.62	158.17
	MOMENT	69.85	75.97	63.98
	(N-m)	64.97	71.84	56.21
FORCE APPLIED ON THE ANKLE $\phi = 30^\circ$	FORCE	67.08	79.88	81.36
	(N)	63.18	77.37	76.66
	MOMENT	50.91	62.75	64.57
	(N-m)	47.82	61.18	58.85
FORCE APPLIED ON THE KNEE $\phi = 60^\circ$	FORCE	194.23	164.48	300.22
	(N)	183.88	159.48	290.35
	MOMENT	65.68	79.70	132.96
	(N-m)	63.92	78.51	130.13
FORCE APPLIED ON THE ANKLE $\phi = 60^\circ$	FORCE	107.63	85.54	216.26
	(N)	106.79	84.10	198.01
	MOMENT	67.16	69.20	131.19
	(N-m)	65.62	67.79	123.01
FORCE APPLIED ON THE KNEE $\phi = \text{LIMIT}$	FORCE	237.61	192.01	328.22
	(N)	220.53	191.53	318.57
	MOMENT	80.38	90.85	109.14
	(N-m)	74.56	88.44	111.03
FORCE APPLIED ON THE ANKLE $\phi = \text{LIMIT}$	FORCE	136.84	94.45	196.53
	(N)	134.97	91.99	185.14
	MOMENT	107.59	78.67	121.08
	(N-m)	105.50	76.92	120.42

TABLE XXVIII

MAXIMUM MAGNITUDES OF THE ACTIVE MUSCLE FORCE AND MOMENT VECTORS
AT THE HIP JOINTS OF THREE FEMALE SUBJECTS FOR THE INDICATED
POSITIONS OF THE LEG WITH $\theta = 120^\circ$, KNEE FLEXED.

LEG POSITION	MAGNITUDE	SUBJECT FS 1	SUBJECT FS 2	SUBJECT FS 3
FORCE APPLIED ON THE KNEE $\phi = 0$	FORCE	73.04	128.22	118.36
	(N)	69.44	121.21	105.76
	MOMENT	26.83	48.71	44.83
	(N-m)	23.82	47.27	38.11
FORCE APPLIED ON THE ANKLE $\phi = 0$	FORCE	65.91	85.04	67.72
	(N)	64.64	76.72	63.20
	MOMENT	43.00	26.13	22.29
	(N-m)	42.14	23.62	21.49
FORCE APPLIED ON THE KNEE $\phi = 30^\circ$	FORCE	148.41	168.18	166.79
	(N)	142.21	163.47	164.85
	MOMENT	62.48	81.61	53.31
	(N-m)	59.89	79.10	51.46
FORCE APPLIED ON THE ANKLE $\phi = 30^\circ$	FORCE	86.63	92.87	159.17
	(N)	80.48	87.28	139.16
	MOMENT	29.76	55.34	88.94
	(N-m)	28.72	52.83	79.16
FORCE APPLIED ON THE KNEE $\phi = 60^\circ$	FORCE	208.35	161.91	219.02
	(N)	195.93	155.49	215.78
	MOMENT	92.03	68.73	64.00
	(N-m)	86.96	65.66	64.38
FORCE APPLIED ON THE ANKLE $\phi = 60^\circ$	FORCE	133.83	85.62	209.98
	(N)	122.38	84.89	170.52
	MOMENT	74.55	52.75	84.09
	(N-m)	72.80	51.65	62.67
FORCE APPLIED ON THE KNEE $\phi = \text{LIMIT}$	FORCE	237.32	194.45	250.91
	(N)	218.11	187.26	249.38
	MOMENT	107.06	86.77	111.87
	(N-m)	98.91	85.28	114.84
FORCE APPLIED ON THE ANKLE $\phi = \text{LIMIT}$	FORCE	146.90	81.03	216.37
	(N)	146.00	73.25	196.18
	MOMENT	99.37	41.14	127.11
	(N-m)	99.00	40.78	114.03

REFERENCES

1. Payne, P.R. and Hawker, F.W., "USAF Experience of Flail Injury for Noncombat Ejections in the Period 1964-1970," AMRL Report, No. AMRL-TR-72-111, 1973.
2. Payne, P., "On Pushing Back the Frontiers of Flail Injury," in: Glaister, D.H., Ed., Biodynamic Response to Windblast, Advisory Group for Aerospace Research and Development, AGARD Conference Proceedings, No. 170 (AGARD-CP-170), Paper B9, July, 1975.
3. Brinkley, J.W. and Payne, P.R., "An Assessment of Aerodynamic Forces Acting on the Crewman During Escape," Advisory Group for Aerospace Research and Development, AGARD Conference Proceedings, No. CP-134, Paper A4, February, 1974.
4. Hawker, F.W. and Euler, A.J., "Experimental Evaluation of Limb Flail Initiation and Ejection Seat Stability," in Glaister, D.H., Ed., Biodynamic Response to Windblast, Advisory Group for Aerospace Research and Development, AGARD Conference Proceedings, No. 170, (AGARD-CP-170), Paper B10, July, 1975.
5. Hawker, F.W. and Euler, A.J., "Wind Tunnel Measurements of Vertical Acting Limb Flail Forces and Torso/Seat Back Forces in an ACES-II Ejection Seat," Technical Report No. AMRL-TR-76-3, June 1976.
6. Schneck, D.J., "Aerodynamic Forces Exerted on an Articulated Body Subjected to Windblast," AMRL Report, No. AMRL-TR-76-109, 1976.
7. Engin, A.E., "Measurement of Resistive Torques in Major Human Joints," AMRL Report, No. AMRL-TR-79-4, 1979a.
8. Engin, A.E., "Passive Resistive Torques About Long Bone Axes of Major Human Joints," Aviation, Space, and Environmental Medicine, Vol. 50, No. 10, pp. 1052-1057, 1979b.
9. Engin, A.E., I. Kaleps, R.D. Peindl, and M.H. Moeinzadeh, "Passive Resistive Force and Moments in Human Shoulder," Proceedings of the 32nd ACEMB, Vol. 21, p. 25, 1979c.
10. Engin, A.E., "On the Biomechanics of Major Articulating Human Joints," an INVITED CHAPTER in NATO ASI-Progress in Biomechanics, edited by N. Akkas, Sijthoff & Noordhoff Publishers, Netherlands, pp. 157-188, 1979d.
11. Engin, A.E. and I. Kaleps, "Active Muscle Torques About Long-Bone Axes of Major Human Joints," Aviation, Space and Environmental Medicine, Vol. 51, No. 6, pp. 551-555, 1980a.

12. Engin, A.E., "On the Biomechanics of the Shoulder Complex," Journal of Biomechanics, Vol. 13, No. 7, pp. 575-590, 1980b.
13. Engin, A.E. and R.D. Peindl, "Two Devices Developed for Kinematic and Force Data Collection in Biomechanics--Application to Human Shoulder Complex," Developments in Theoretical and Applied Mechanics, edited by J.E. Stoneking, Vol. 10, pp. 33-50, The University of Tennessee Press, 1980c.
14. Engin, A.E., N. Akkas, and I. Kaleps, "Passive Resistive Force and Moments in Human Elbow Joint," 1980 Advances in Bioengineering, ASME Publication, pp. 229-232, 1980d.
15. Engin, A.E., "Resistive Force and Moments in Major Human Joints," an INVITED LECTURE in Proceedings of the Eighth Canadian Congress of Applied Mechanics, pp. 181-200, 1981a.
16. Engin, A.E., and M.H. Moeinzadeh, "Dynamic Modeling of Human Articulating Joints," Proceedings of the Third International Conference on Mathematical Modeling, University of Southern California, Los Angeles, p. 58, 1981b.
17. Engin, A.E., and M.H. Moeinzadeh, "Modeling of Human Joint Structures," AMRL Report, No. AMRL-TR-81-117, 1981c.
18. Skreiner, M., "Study of the Geometry and the Kinematics of Instantaneous Spatial Motion," Journal of Mechanisms 1, pp. 115, 1966.
19. Bocher, M., Introduction to Higher Algebra No. S1238, Dover Publications, Inc., New York, N.Y., 1964.
20. Hertzberg, H.T.E., Engineering anthropology, In: Human Engineering Guide to Equipment Design (Revised Edition), H.P. Van Cott and R.G. Kinkade (Eds.), U.S. Government Printing Office, Washington, D.C., 1972.

PUBLICATIONS ARISING FROM THIS RESEARCH CONTRACT

1. Engin, A.E., "Major Articulating Joint Response to Mechanical Loading," Review of Air Force Sponsored Basic Research in Environmental Physiology and Biomechanics, Proceedings of a Conference held at the University of Kentucky, September 23-25, 1980, Paper No: 28.
2. Engin, A.E., "Response of Human Shoulder to External Forces," Proceedings of the VIIIth International Congress of Biomechanics, p. 189, 1981 (The full length paper will be published in BIOMECHANICS VIII).
3. Engin, A.E. and Kazarian, L., "Active Muscle Force and Moment Response of the Human Arm and Shoulder," Aviation, Space and Environmental Medicine, Vol. 52, No. 9, pp. 523-530, 1981.
4. Engin, A.E., Peindl, R.D., and N. Berme, "Kinematic and Force Data Collection in Biomechanics by Means of Sonic Emitters - I: Theory," (Manuscript is in preparation).
5. Engin, A.E., Peindl, R.D., and N. Berme, "Kinematic and Force Data Collection in Biomechanics by Means of Sonic Emitters - II: Application to the Shoulder Complex," (Manuscript is in preparation).

DATE
ILME